

**THE UNIVERSITY OF MICHIGAN**  
**DEPARTMENT OF ATMOSPHERIC, OCEANIC, AND SPACE SCIENCE**  
Space Physics Research Laboratory  
2245 Hayward Street  
Ann Arbor, Michigan 48109-2143

**Contract/Grant Number** NAGW 4388

**Project Name** Composition and Evolution of the Atmosphere of Venus

**Report Author(s)** Thomas Donahue  
**Author(s) Phone** 313/763-2390

**Report Date** July 17, 1996

**Report Type** Annual Report

**Period Covered** 1 /1/96-12/31/96

**Project Director:** Thomas M. Donahue

**Principal Investigator(s)** Thomas M. Donahue

**Program Technical Officer** Jay T. Berhstralh  
**Address** NASA, Office of Space Science  
300 E. Street SW  
Two Independence Square  
Washington, DC 20546-0001

**UM Authorization**  
**(when required)**

---



July 16, 1996

Dr. Jay T. Bergstralh  
NASA, Office of Space Science  
300 E Street SW  
Two Independence Square  
Washington, D.C. 20546-0001

Dr. Dennis Bogan  
NASA, Office of Space Science  
300 E. Street SW  
Two Independence Square  
Washington, D.C. 20546-0001

RE: Renewal of NASA NAGW-4388, January, 1997-December, 1997

Dear Jay and Dennis:

Much of my time during the first five months of 1996 were perforce devoted to analyzing data acquired by the Galileo Probe Mass Spectrometer (GPMS) and writing the GPMS team's Science paper. Because of my 18 years of experience analyzing mass spectrometer data from the Pioneer Venus Probe Mission (LNMS), and my emeritus status I found myself uniquely prepared to make rapid progress in analyzing and interpreting the GPMS results and with time to do so. I enclose a copy of the Science paper that resulted. Since that paper was written, post flight calibration is proceeding methodically and we have had a careful look at the data obtained between 14.5 bar and 21 bar which was barely discussed in the Science paper. (See the COSPAR paper, also enclosed) The most interesting result here is that in this altitude range the water vapor mixing ratio gets up to 1.6 times solar, compared to the 0.2 times solar below 11 bar that was quoted in our preliminary report. Like H<sub>2</sub>S and HCl, H<sub>2</sub>O increases in mixing ratio with decreasing altitude (or perhaps horizontal displacement). We are inclined to attribute this effect to the probe's finding itself in the descending volatile poor arm of a circulation system. We are awaiting calibration of the instrument for NH<sub>3</sub> for further enlightenment.

In the meanwhile, I have been able to get started on a couple of Venus hydrogen projects. One of these should be finished and on the way to publication by the time this letter would have been written in the past. I have been trying to understand how to reconcile the standard treatment of the evolution of the H<sub>2</sub>O and HDO reservoirs on the planet over 4.5 Gyr in the presence of H and D escape and injection by comets. The simple relations

$$\frac{d[H]}{dt} = -\phi_1 + P_1 \quad (1)$$



$$\frac{d[D]}{dt} = -\phi_2 + P_2 \quad (2)$$

govern this evolution.

Where the fractionation factor  $f$  is given by

$$f = \frac{\phi_2/[D]}{\phi_1/[H]} , \quad (3)$$

and, if we take

$$\phi_1 = -K[H] , \quad (4)$$

with  $K$  constant (big assumptions) and let

$$R_s = (D/H)_s \quad (5)$$

in the cometary source, the solutions to (1) and (2) are

$$[H]/[H_0] = e^{-Kt} + \frac{P_1}{\phi_1} \left( \frac{[H]}{H_0} \right)_{4.5} (1 - e^{-Kt}) \quad (6)$$

$$[D]/[D_0] = e^{-fKt} + \frac{R_s}{f} \frac{P_1}{\phi_1} \left( \frac{[H]}{H_0} \right)_{4.5} (1 - e^{-fKt}) \quad (7)$$

or

$$R = \frac{[D]}{[H]} = \frac{(1 - e^{-fKt})/f + (R_s/R_0)(P_1/\phi_1[H/H_0])^{-1}e^{-fKt}}{1 - e^{-Kt} + (P_1/\phi_1[H]/[H_0])^{-1}e^{-Kt}} \quad (8)$$

These relations are discussed in detail in a chapter for Venus II I have written (copy enclosed).

Early this year my GSFC PV colleagues and I published a paper in JGR, Planets (Hartle et al, enclosed) showing how analysis of PVO data over several solar cycles allowed us to determine H and D escape fluxes  $\phi_1$  and  $\phi_2$  averaged over the planet and the solar cycle:

$$\phi_1 = 7 \times 10^6 \text{ cm}^{-2} \text{ s}^{-1} ,$$



$$f = 0.44.$$

This is close to the Charge Separation Electric Field  $H^+$  flux obtained by Hartle and Grebowski and generalized by Hartle and myself for solar cycle effects

$$\phi_1(E) = 9 \times 10^6 \text{ cm}^{-2} \text{ s}^{-1}$$

$$f = 0.17$$

It is not a good representation of my "best guess" for the combined electric field, charge exchange flux (E + CE) (See Hartle et al, Donahue and Hartle, Donahue et al, all enclosed).

$$\phi_1(E + CE) = 16 \times 10^6 \text{ cm}^{-2} \text{ s}^{-1},$$

$$f = 0.10.$$

We can put these values for  $\phi_1$  and  $f$  in (6) and (8), along with the measured value of

$$R = D/H = 150 \pm 30$$

and

$$P_1 = 7 \times 10^5 - 4.2 \times 10^6 \text{ cm}^{-2} \text{ s}^{-1}$$

(see Donahue et al, Venus II),

where

$$1 \leq R_s/R_o \leq 2$$

The funny thing is that the problem is over determined if we have  $[H]$ ,  $\phi_1$ ,  $R$ ,  $f$ ,  $P_1$ ,  $R_s/R_o$  given by experiment. This is because the measurement of  $R$  at 4.5 Gyr and

$$K = \{\phi_1/[H]\}_{4.5}$$

means, for any assumed  $R_s/R_o$

$$\left( \frac{P_1}{\phi_1} \frac{[H]}{[H_o]} \right)_{4.5}$$

is determined. Then in (6)



$$\left( \frac{[H]}{[H_0]} \right)_{4.5} = e^{-Kt} + \left( \frac{P_1}{\phi_1} \frac{[H]}{[H_0]} \right)_{4.5} (1 - e^{-Kt_1})$$

and  $[H_0/H]$  which gives the ratio of the original water inventory to the present on is set.

There is no freedom in setting  $P_1/\phi_1$  !

I am now in the process of investigating the implications.

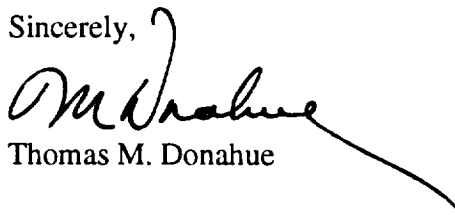
I am also preparing to have a go at calculating the charge exchange contribution to hydrogen loss rates, using realistic models for exospheric H,  $H^+$ , D,  $D^+$ , and ion temperature from PV data. This has never been done properly. Hodges and I have proposed doing this a couple of times, but Hodges has not been funded for his part. I hope to get his "unfunded" help in closing this embarrassing gap in our knowledge.

I have presented papers on Cytherean and Martian Water at the European Geological Society Meeting at the Hague and at the Pale Blue Dot workshop recently at NASA ARC.

During the final year of this grant I propose:

- a) to finish the calculation of charge exchange loss rates of H and D from Venus;
- b) to continue to analyze Galileo Probe Neutral Mass Spectrometer data after MODA support terminates on April 30, 1997.
- c) To begin work on the sulfur chemistry and redox state of the atmosphere of Venus.

Sincerely,



Thomas M. Donahue



## REPORTS

Science

# The Galileo Probe Mass Spectrometer: Composition of Jupiter's Atmosphere

Hasso B. Niemann, Sushil K. Atreya, George R. Carignan,  
Thomas M. Donahue, John A. Haberman, Dan N. Harpold,  
Richard E. Hartle, Donald M. Hunten, Wayne T. Kasprzak,  
Paul R. Mahaffy, Tobias C. Owen, Nelson W. Spencer,  
Stanley H. Way

The composition of the Jovian atmosphere from an altitude marked by an atmospheric pressure of 0.5 to 21 bars was determined by a quadrupole mass spectrometer on the Galileo probe. The mixing ratio of He (helium) to  $H_2$  (hydrogen), 0.156, is close to the solar ratio. The abundances of methane, water, argon, neon, and dihydrogen sulfide were measured; krypton and xenon were detected. As measured in the Jovian atmosphere, the amount of carbon is 8.9 times the solar abundance relative to  $H_2$ , the amount of sulfur is greater than the solar abundance, and the amount of oxygen is much less than the solar abundance. The neon abundance compared with that of hydrogen is about an order of magnitude less than the solar abundance. Isotopic ratios of carbon and the noble gases are consistent with solar values. The measured ratio of deuterium to hydrogen (D/H) of  $(5 \pm 2) \times 10^{-6}$  indicates that this ratio is greater in solar-system hydrogen than in local interstellar hydrogen, and the  $^3He/^4He$  ratio of  $(1.1 \pm 0.2) \times 10^{-6}$  provides a new value for protosolar (solar nebula) helium isotopes. Together, the D/H and  $^3He/^4He$  ratios are consistent with conversion in the sun of protosolar deuterium to present-day  $^3He$ .

Determination of the composition of Jupiter's atmosphere should constrain the relative importance of direct contributions to the atmosphere from the solar nebula itself, on the one hand, and from large icy or rocky objects present in the early outer solar system, on the other. The contribution of these "planetesimals" could have been in the form of an early atmosphere around Jupiter's primitive solid core or in the form of volatiles they carried to the planet after it began to acquire its atmosphere of  $H$  and  $He$  from the solar nebula (1, 2). The degree of resemblance between the sun's atmosphere and that of Jupiter in the abundances relative to  $H$  of elements such as  $C$ ,  $N$ , and  $O$  should be decisive in providing the required constraints.

Before the direct, in situ measurements reported here, remote spectroscopic sensing from Earth and from spacecraft had indicated that the relative abundances of  $C$  (in  $CH_4$ ) and  $N$  (in  $NH_3$ ) were greater than the solar abundances (3, 4). Phosphine and water vapor had been detected, but their abundances below the clouds were uncertain, and  $H_2S$  and the noble gases other than  $He$  had not been detected at all. De-

finite data to replace these tantalizing clues to the sources of volatile compounds in Jupiter's atmosphere were not available before this descent of the probe.

An accurate direct measurement of the abundances of  $He$  and the other noble gases is important for understanding how Jupiter has processed its constituents. Abundances less than those of the solar values would signal the formation, in the metallic interior of the planet, of a separate  $He$  phase, some of which has precipitated deeper into the interior. Remote sensing had indicated a modest depletion of  $He$ , but this indirect result is much less satisfactory than the direct sensing by two of the Galileo instruments reported here.

The Galileo probe mass spectrometer (GPMS) was designed to measure the mixing ratios of major and minor species while

determining the isotopic ratios of their constituent elements (5). Signals were recorded from over 6000 individual values of mass-to-charge ratio ( $m/z$ ). The data returned by the instrument have led to the discovery of six new atmospheric constituents and the measurement of numerous abundances and isotopic ratios. The gas sampling system admitted the Jovian atmosphere through low-conductance leaks to the ion source of a quadrupole mass analyzer. The ion source was pumped by a getter and the analyzer volume pumped to a much lower pressure by a getter backed by a sputter-ion pump. One inlet (direct leak 1; DL1) was open from 0.52 to 3.78 bars; the other inlet (DL2) functioned from 8.21 bars to the end at about 21 bars (6).

Figure 1 shows a sample mass spectrum from the 3-bar region at 228 K, before any significant water cloud was expected, and another one from the 11-bar region, where the 350 K temperature assures that the probe was far below any water condensation level. Comparison of the two spectra shows a large increase in the second direct leak of  $H_2O$  and  $NH_3$ . In fact, the design of the leak 1 sampling system, with a relatively long vacuum path to the ion source, precludes a sensitive detection of the surface active species  $H_2O$  and  $NH_3$  in the atmospheric region sampled by this leak. Raw counts shown in these spectra must be corrected for the counting system dead time. The efficiencies of the ion source and the pumping system vary from species to species, and the sensitivity factors, which are different for the two direct leaks, must be individually determined. In most cases, we used preflight calibrations, but for the most important species we were able to do some recalibrations on the spare instrument. With the direct leaks, the background level was typically between 0 and 3 counts. Two background measurements demonstrated that the instrument arrived at Jupiter in a very clean state and quickly lost its memory of almost all gases contributed by DL1.

Table 1. Mixing ratios to  $H_2$  and isotopic ratios in the Jovian atmosphere. Blank spaces indicate zero.

Species	Jovian atmosphere	Ratio to solar value	Prior results	References
$^4He$	$0.156 \pm 0.008$	0.80	0.11	(12, 13)
$^{20}Ne$	$(2.3 \pm 0.25) \times 10^{-6}$	0.10		
$^{36}Ar$	$(1.0 \pm 0.4) \times 10^{-6}$	1.8		
$^{84}Kr$	$(8.5 \pm 4) \times 10^{-9}$	$\leq 5$		
$^{136}Xe$	$(8 \pm 2.5) \times 10^{-9}$	$\leq 50$		
$CH_4$	$(2.1 \pm 0.15) \times 10^{-5}$	3	$2.2 \times 10^{-5}$	(3, 4)
$H_2O$	$(3.7 \pm 0.35) \times 10^{-4}$	$\leq 0.2$		
$NH_3$	$(3.5 \pm 0.3) \times 10^{-5}$	$\leq 10$	$2.5 \times 10^{-4}$	(10)
$H_2S$	$(7.7 \pm 0.5) \times 10^{-6}$	2.2		
D/H	$(5 \pm 2) \times 10^{-6}$		$(2.0, 3.6) \times 10^{-6}$	(17-19)
$^3He/^4He$	$(1.1 \pm 0.1) \times 10^{-6}$			
$^{12}C/^{13}C$	$0.0108 \pm 0.0005$	1.0		

H. B. Niemann, J. A. Haberman, D. N. Harpold, R. C. Hartle, W. T. Kasprzak, P. R. Mahaffy, S. H. Way, Goddard Space Flight Center, Greenbelt, MD 20771, USA.  
S. K. Atreya, G. R. Carignan, T. M. Donahue, University of Michigan, 2455 Hayward Street, Ann Arbor, MI 48106, USA.  
D. M. Hunten, University of Arizona, Tucson, AZ 85721, USA.  
T. C. Owen, University of Hawaii, 2680 Woodlawn Drive, Honolulu, HI 96822, USA.  
N. W. Spencer, 14013 Remington Drive, Silver Spring, MD 20902, USA.



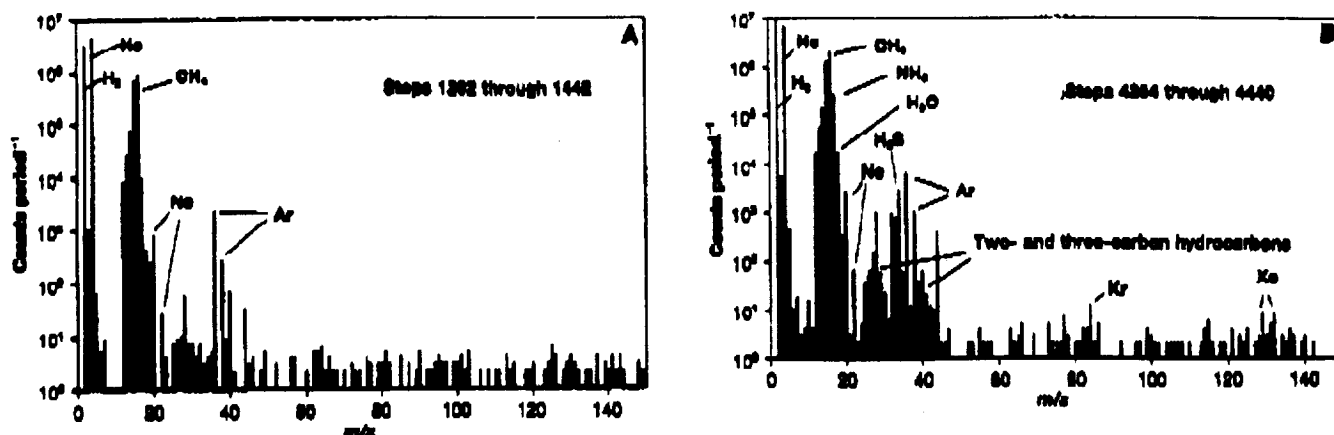


Fig. 1. Sample mass spectra. The spectra in (A) were obtained through DL1 between pressures of 2.72 and 3.06 bar, with ambient temperature at 226 K. The spectra in (B) were obtained through DL2 between pressures of 10.6 and 11.3 bar, with ambient temperature at 260 K. No corrections have been made for dead time or for different efficiencies at different masses.

Table 1 shows the mixing ratios (number densities relative to  $H_2$ ) of species that were detected and for which reliable measurements could be made. Error estimates are roughly 1 $\sigma$  and represent the data scatter about the average value. Some of the observed mixing ratios can be compared with those for the solar system as compiled by Anders and Grevesse (7), commonly referred to as the solar abundances. Also shown are results of earlier analyses based on Voyager or Earth-based spectra.

The jovian  $He/H_2$  ratio,  $0.156 \pm 0.006$ , is the average of 14 individual measurements from DL1 ( $0.157 \pm 0.006$ ) and 4 from DL2 ( $0.151 \pm 0.004$ ). All the other noble gases were detected, and they are elementally fractionated. The Ne ratio to  $H_2$  is about an order of magnitude less than the solar ratio, whereas for Ar the ratio is slightly greater. Kr and Xe were clearly detected; upper limits on the mixing ratios are respectively 5 and 50 times the solar values. For all four of the heavier noble gases, the isotopic ratios are close to the solar values.

The  $^3He/^4He$  and the D/H ratios were determined from an analysis of the 3 amu (atomic mass unit) data. This analysis is complicated by the need to correct for  $H_3^+$  produced in the ion source and to distinguish between the contributions of HD and  $^3He$ .  $H_3^+$  is generated in one of two ways: by dissociative ionization of  $CH_4$ , or by a two-body ion-molecule reaction between  $H_2^+$  and  $H_2$ . The efficiency of  $H_3^+$  production could be determined during the second background study when little  $H_2$  and He, but a considerable amount of  $CH_4$ , existed in the ion source and  $CH_4$  was the only important source of 3-amu ions. During pre-flight calibration, when the  $H_2$  pressure in the GPMS was varied over a large range, the  $HD/H_2$  ratio for the laboratory  $H_2$  sample and the efficiency of  $H_3^+$  production in

DL1 and DL2 were separately determined. During probe descent, the  $^3He/^4He$  ratio was determined from 3-amu and 4-amu data obtained with the noble gas cell (NGC) sample (6). Hydrogen was effectively absent from this gas sample. The result,  $1.1 \times 10^{-4}$  (Table 1), indicates that He in the jovian atmosphere has a smaller proportion of  $^3He$  than the protosolar He found in meteorites, where  $^3He/^4He = (1.5 \pm 0.3) \times 10^{-4}$  (8). Evidently, the "protosolar" He isotopes in meteorites do not, in fact, reflect the values that existed in the solar nebula.

With the He mixing ratio and  $H_3^+$  production efficiencies in hand, the  $HD/H_2$  ratio was determined from the DL1 and DL2 data at 3 amu and 2 amu. During DL2 sampling, the electron energy in the ion source was reduced at times from 75 eV to 25 eV or 15 eV. Few and no He ions, respectively, were produced under these conditions, and the ratios of the 3-amu rate to the 2-amu rate provided an upper limit to  $HD/H_2$  (assuming no  $H_3^+$  production) of  $(1.1 \pm 0.3) \times 10^{-4}$ . The average value of  $HD/H_2$ , measured from inlet 2 data, was just at this limit. The ratios measured in inlets 1 and 2 were almost precisely the same. The  $^{12}C/^{13}C$  isotopic ratio was determined with high precision in DL1 data where the contribution of  $NH_3$  at 17 amu was negligible. The ratio is exactly that of the solar values.

Reasonably good agreement was found for  $CH_4$  mixing ratios in DL1 and DL2, within the calibration uncertainty of  $\pm 20\%$ . This determination indicates that atmospheric  $^{12}C$  is more abundant by a factor of 3 relative to  $H_2$  than in solar system material. The measured mixing ratio of  $H_2S$  in the well-mixed atmosphere between 8 and 11 bars increased by a factor of 4 with depth. There was a tentative detection of HCl. Water vapor and  $NH_3$  were readily adsorbed on metal surfaces, and

their densities in the ion source may lag behind those in the gas stream. The measurements made while DL2 was open should be the most reliable, but they were made just after enrichment cell 1 (BC1) was closed. Some of the  $NH_3$  and  $H_2O$  detected in DL2 may therefore have been contributed by outgassing of this adsorbed gas in the presence of abundant  $H_2$  and He (9). Hence, for the present, only upper limits can be set for these molecules. The constraint for  $NH_3$ , 16 times the solar value, is weaker than the existing estimate, 1 to 1.3 times the solar value, from analysis of Jupiter's microwave emission spectrum (10). The limit on water vapor, 0.2 times the solar value, is significant in view of the solar or greater values found for the other volatiles C, N, and S.

Two- and three-hydrocarbon species appeared to be present. The direct leaks showed no sign of any heavier hydrocarbons. Upper limits for the mixing ratios of these heavy hydrocarbon species are  $\sim 1$  ppb.

Our  $He/H_2$  ratio (0.156) agrees almost exactly with the ratio of 0.157 obtained by the helium abundance detector (HAD) on the Galileo probe (11); some of the implications of this measurement are discussed elsewhere (11). This value is considerably larger than the value of 0.11 obtained from Voyager data (12), but is little (if any) less than the value for the present sun. The protosolar value, deduced from evolutionary models of the sun, is probably a more relevant standard and is 18% greater (11). It is widely believed that Saturn's atmosphere, with a  $He/H_2$  ratio about one-fifth of the protosolar value, has been depleted of He by rain-out of He droplets in the interior (13, 14). The GPMS and HAD results agree with the Voyager data in suggesting that the same process must operate at Jupiter,



though not to the same extent. This loss of He is a likely explanation of the Ne depletion observed by the GPMS, if the solubility of Ne in He is as large as has been suggested (15).

The value of  $(5 \pm 2) \times 10^{-3}$  deduced for D/H from HD/H<sub>2</sub> is higher than the ratios derived from Earth-based spectroscopic observations (16, 17):  $(2 \pm 1) \times 10^{-3}$  from CH<sub>3</sub>D/CH<sub>4</sub> and  $(2 \pm 1) \times 10^{-3}$  from HD/H<sub>2</sub>. It agrees well with the value found in a recent analysis of Voyager infrared spectra (18):  $(3.8 \pm 0.5) \times 10^{-3}$ . The jovian D/H ratio should be the same as the protoplanar or solar-nebular value because the nebula was the source of Jupiter's hydrogen. [The terrestrial ratio is  $1.6 \times 10^{-4}$ .] The sun converted all its D to <sup>3</sup>He early in its history; thus, Uels (8) argued that the original D/H in the solar nebula should be equal to the difference between the <sup>3</sup>He/<sup>4</sup>He ratios in the solar wind and in meteorites, which should contain nebular He (19). Geise's value for protoplanar D/H is  $(2.6 \pm 1.0) \times 10^{-3}$ , and this overlaps the GPMS value. Substituting the new determination of protosolar <sup>3</sup>He/<sup>4</sup>He =  $(1.1 \pm 0.2) \times 10^{-6}$  for the meteoritic one, the same argument would yield D/H =  $(3 \pm 1) \times 10^{-3}$ , a value that is closer to that derived directly from HD. It is clear that D/H on Jupiter is distinctly higher than the value of  $(1.6 \pm 0.1) \times 10^{-3}$  found in local interstellar H (20), as expected from the steady destruction of D in the galaxy by stellar nucleosynthesis during the last  $4.5 \times 10^9$  years.

Earth-based imaging (21) and the remarkably small number of cloud particles detected by the nephelometer experiment (22) indicate that the probe may have descended into an unusually clear part of the jovian atmosphere. An obvious explanation is that the region was one of subsidence, like most clear regions on Earth. Our H<sub>2</sub>O abundance value, then, may be less than the planetary average, although this result is unlikely. In a cloud, the relative humidity should be just over 100%, and this is consistent with the comprehensive analysis of Voyager spectra by Carlson et al. (18). The corresponding profile of water vapor has a scale height of about 3 km. If, for example, the relative humidity is reduced by a downdraft from 100% to 90%, the amount of subsidence required is  $3 \ln(90/100)$  km, or a mere 0.3 km. Our measurements were made at far greater depths than the expected condensation level (5 or 6 bars); to perturb the humidity at such a deep level would require a downdraft extending over a range of well over a scale height, far more than needed simply to clear out the clouds. There remains the possibility of a global-scale circulation, perhaps upward at high latitudes and downward at low.

The large atmospheric abundance of C

suggests that sources other than the gas of the solar nebula contributed a significant share of the volatiles in the envelope of Jupiter. These elements and water should have been in the condensed phase in the neighborhood of the accreting Jupiter. One possible explanation for a deficiency of water was proposed by Gautier and Owen (3, 4): most of the planetesimals accreted to the rocky, icy core of the embryo planet rather than being collected after the planet began to amass its gaseous envelope from the neighboring solar nebula. Water vapor, being the least volatile, remained close to the core, whereas gases like CO, CH<sub>4</sub>, and N<sub>2</sub> could mix with the nebula-derived envelope, enriching it in C and N. Although this scenario could reproduce the observed abundances, it must be tested by rigorous modeling. If there was a large mass of late-accreting planetesimals, the low relative abundance of atmospheric H<sub>2</sub>O requires them to have been rich in carbonaceous materials and deficient in O. It has been customary to assume that outer solar-system planetesimals resemble the least-altered carbonaceous chondrites that fall to Earth, which contain more O than C (23), but there are many that are much drier. The mean densities observed for many satellites in the outer solar system have been explained by assuming a rock: ice ratio of order unity, but perhaps much of the low-density material is carbonaceous rather than icy.

If our results are representative of the entire planet (24), they preclude models in which several Earth masses of late-accreting, water-rich planetesimals deliver volatiles to the jovian envelope (1). There is no sign of the dense water cloud, or the corresponding vapor, invoked to explain waves spreading from the Shoemaker-Levy 9 impacts (25). Water vapor observed in the impact plumes probably came from the impactors, not Jupiter, as suggested (26).

## REFERENCES AND NOTES

1. D. J. Stevenson, *Annu. Rev. Earth Planet. Sci.* 10, 287 (1982); J. B. Pollack and P. Bodenheimer, in *Origin and Evolution of Planetary and Satellite Atmospheres*, S. K. Atreya, J. B. Pollack, M. S. Matthews, Eds. (Univ. of Arizona Press, Tucson, 1989), p. 584; W. B. Hubbard, *ibid.*, p. 599.
2. J. I. Lunine and D. J. Stevenson, *Astrophys. J. Suppl.* 88, 493 (1989); T. Owen and A. Bar-Nir, *Icarus* 116, 218 (1986).
3. D. Gautier and T. Owen, in *Origin and Evolution of Planetary and Satellite Atmospheres*, S. K. Atreya, J. B. Pollack, M. S. Matthews, Eds. (Univ. of Arizona Press, Tucson, 1989), p. 487.
4. K. S. Noll and H. P. Larson, *Icarus* 89, 18A (1991).
5. H. B. Niemann et al., *Space Sci. Rev.* 60, 111 (1992).
6. Each inlet also fed a gas sample to an enrichment chamber, in which a porous carbon material absorbed complex hydrocarbons and heavy noble gases. The noble gases not adsorbed by EC1 were captured and fed to the analyzer in an NGC from which H<sub>2</sub> was eliminated by a getter pump. This procedure lowered the threshold of detectability by a factor of 10 (to 0.1 part per billion by volume). The gases not adsorbed in EC1 were also pumped away, and the adsorbed ones were later released by heating the coil and analyzer. These measurements, and two measurements of background, were carried out after inlet 1 was closed and before inlet 2 was opened. EC2 was filled from inlet 2 when the pressure was 8.4 to 9 bars. The two enrichment coils raised the sensitivity to stable hydrocarbons and the heavier noble gases by as much as a factor of 500. The system was controlled by a read-only memory, incremented each 1/2 s through 8192 steps. Many scans were made at integral masses through the range of 2 to 180 amu, resulting 75 s; other sequences covered only selected masses. The dynamic range was 10<sup>4</sup>.
7. E. Anders and N. Greessen, *Gemm. Cosmochim. Acta* 58, 157 (1994). These abundances, commonly referred to as "solar" or "solar-system" abundances, are based on a combination of evidence from the sun itself and from primitive meteorites.
8. J. Geise, in *Origin and Evolution of the Elements*, N. Prantzos, E. Vangioni-Flam, M. Cassé, Eds. (Cambridge Univ. Press, Cambridge, 1993), p. 89.
9. The enrichment coils were heated and the evolved gases measured between 6.5 and 7 bar and 11.8 and 14.8 bar.
10. A. Marini, R. Courth, D. Gautier, A. Lacomba, *Icarus* 41, 410 (1990); I. de Pater and S. T. Massie, *ibid.* 82, 143 (1993).
11. U. von Zahn and D. M. Hunten, *Science* 200, 200 (1990).
12. B. J. Conrath, D. Gautier, R. A. Menel, J. S. Himmstein, *Astrophys. J.* 388, 807 (1994).
13. R. Smoluchowski, *Nature* 215, 981 (1967).
14. D. J. Stevenson and E. S. Salpeter, *Astrophys. J. Suppl.* 26, 221 (1977); *ibid.*, p. 239.
15. M. S. Roush and D. J. Stevenson, *EOS (Spring suppl.)* 78, 040 (1989).
16. D. Gautier and T. Owen, in (3), p. 504.
17. W. H. Smith, W. V. Schamp, K. H. Baines, *Astrophys. J.* 88, 907 (1988).
18. B. E. Carlson, A. A. Lada, W. B. Rossow, *J. Geophys. Res.* 98, 5851 (1993). The D/H ratio quoted in this report has been adjusted to reflect our slightly larger measurement of CH<sub>3</sub>D abundance.
19. The solar wind value is  $(4.5 \pm 0.4) \times 10^{-4}$ , and the meteoritic one is  $(1.1 \pm 0.3) \times 10^{-4}$ .
20. J. L. Linde et al., *Astrophys. J.* 402, 694 (1993); see also X. Lindey et al., in *Light Element Abundances*, P. Crane, Ed. (Springer-Verlag, Berlin, 1993), p. 216.
21. G. Orton et al., *Science* 261, 261 (1993).
22. B. Rapant, D. B. Colburn, P. Avin, K. A. Pages, *ibid.*, p. 261.
23. H. B. Wilk, *Gemm. Cosmochim. Acta* 5, 879 (1954); S. Mason, *Meteoritics* (Wiley, New York, 1962), *Fourth*.
24. A good interpretation of the observed variations in abundances could involve relatively small differences in the solubility of volatiles in metallic H. Approximately 50% of Jupiter's H is in the metallic phase. For instance, if the mixing ratio of a minor constituent in the molecular part of the planet is much larger than the solar value, then this mixing ratio in the metallic interior may be slightly smaller than the solar value or vice versa.
25. A. P. Ingersoll and H. Kanamaru, *Nature* 374, 708 (1993).
26. A. L. Soroush et al., *Icarus*, in press.
27. We thank J. Cooley for his efforts as instrument manager, R. Lutz and T. Tyler for the mechanical design contributions, A. Ogan for his help in the enrichment coil design, R. Abell, H. Powers, and H. Mende for the precision assembly welding and machining, and R. Arvey and H. Benton for the electronics assembly and testing at Goddard Space Flight Center. The contributions to the electronics system design of B. Block, J. Carls, J. Elder, J. Meurer, and W. Pirklis at the University of Michigan are gratefully acknowledged. The hybrid electronic circuits were fabricated at the General Electric Avionics Division at Valley Forge, PA, and the microchips for the gas sampling system were designed and fabricated by Alar Industries in Oceanside, CA. The chemical getter material was provided by the BASF Center of Milan, Italy. M. Wong of the University of Michigan participated in



the data analysis. We also thank the Galileo Probe Project personnel at NASA Ames Research Center, and we particularly acknowledge the contributions of

A. Wilhelm, C. Soback, and P. Mella for their efforts during the development, spacecraft integration, and

testing phases. 16 March 1996; accepted 17 April 1996



COSPAR 1996

## Chemical Composition Measurements of the Atmosphere of Jupiter with the Galileo Probe Mass Spectrometer

H. B. Niemann<sup>1</sup>, S. K. Atreya<sup>2</sup>, G. R. Carignan<sup>3</sup>, T. M. Donahue<sup>3</sup>, J. A. Haberman<sup>1</sup>, D. N. Harpold<sup>1</sup>, R. E. Harle<sup>1</sup>, D. M. Hunten<sup>3</sup>, W. T. Kasprzak<sup>1</sup>, P. R. Mahaffy<sup>1</sup>, T. C. Owen<sup>4</sup>, N. W. Spencer<sup>5</sup>

1. *Goddard Space Flight Center, Greenbelt, MD 20771 USA*
2. *Department of Atmospheric, Oceanic and Space Sciences, University of Michigan, 2455 Hayward Street, Ann Arbor, MI 48109 USA*
3. *Lunar and Planetary Laboratory, University of Arizona, Tucson, AZ 85721 USA*
4. *University of Hawaii, Institute for Astronomy, 2680 Woodlawn Drive, Honolulu, HI 96822 USA*
5. *12013 Remington Drive, Silver Spring, MD 20902 USA*

### ABSTRACT

The Galileo Probe entered the atmosphere of Jupiter on December 7, 1995. Measurements of the chemical and isotopic composition of the Jovian atmosphere were obtained by the mass spectrometer during the descent over the 0.5 to 20 bar pressure region over a time period of approximately 1 hour. The sampling was either of atmospheric gases directly introduced into the ion source of the mass spectrometer through capillary leaks or of gas which had been chemically processed to enhance the sensitivity of the measurement to trace species or noble gases. The analysis of this data set continues to be refined based on supporting laboratory studies on an engineering unit. The mixing ratios of the major constituents of the atmosphere hydrogen and helium have been determined as well as mixing ratios or upper limits for several less abundant species including: methane, water, ammonia, ethane, ethylene, propane, hydrogen sulfide, neon, argon, krypton, and xenon. Analysis also suggests the presence of trace levels of other 3 and 4 carbon hydrocarbons, of propane nitrile, phosphine, hydrogen chloride, and of benzene. The data set also allows upper limits to be set for many species of interest which were not detected. Isotope ratios were measured for  $^3\text{He}/^4\text{He}$ ,  $\text{D}/\text{H}$ ,  $^{13}\text{C}/^{12}\text{C}$ ,  $^{20}\text{Ne}/^{22}\text{Ne}$ ,  $^{36}\text{Ar}/^{40}\text{Ar}$  and for isotopes of both Kr and Xe.



## INTRODUCTION

The determination of the composition of Jupiter's atmosphere and the comparison with solar abundances is of interest from the point of view of understanding both the nature of the formation of this planet through mechanisms such as direct capture of nebular gas or infusion of icy planetesimals and the subsequent evolution of its atmosphere by precipitation of constituents into the interior. Although remote sensing from Voyager and other spacecraft and from ground based observations had constrained the relative abundance to hydrogen of helium, methane, water, ammonia, phosphine, and other species prior to the Galileo Probe entry, sampling below the cloud layers was only possible for many species with the insitu measurements enabled by the Probe. Isotopic determinations which had been obtained by earth based spectroscopy for some species such as deuterium [Smith, et al., 1989, Carlson et al., 1993] could be measured for a broad range of species with an insitu mass spectrometer measurement.

Preliminary analysis of the Galileo Probe Neutral Mass Spectrometer (GPMS) data [Niemann et al., 1996] gave isotope ratios for the noble gases, D/H, and  $^{13}\text{C}/^{12}\text{C}$ , and abundance ratios to hydrogen for helium, methane, neon, argon, and hydrogen sulfide as well as upper limits to the mixing ratio for water, ammonia, krypton, and xenon in the 9 to 12 bar region of the atmosphere. Continuing analysis of the GPMS data since this preliminary report has established the presence of the additional species ethane, ethylene, and propane, suggested the presence of hydrogen-chloride, benzene, and propane nitrile, and demonstrated an unexpected and substantial increase in the abundance of water, hydrogen sulfide, ethane and other species with increasing depth into the atmosphere over the 11 bar to 23 bar pressure regime. It has been suggested [Atreya ??, 1996, Owen et al., 1996] that this increase may be due to the probe entry into the downwelling side of a large scale vertical atmospheric circulation structure which has an atypical abundance of many species compared to the global average. This depletion is attributed to precipitation of gases moving upward through the cold region of the adjacent member of the circulation cell.

*Detection of  
HCl and  
one and two  
carbon  
hydrocarbon  
was also  
reported.*

*Niemann et al  
1996*

## EXPERIMENT DESCRIPTION

### Instrument Description

The instrument has been described [Niemann et al., 1992]. The instrument consists of a quadrupole analyzer mass spectrometer with a mass range 2 to 150 amu. The ion source had a magnetically confined electron beam emitted from a hot filament. The electron energy was nominally 75 eV with occasional 25 eV and 15 eV measurements. The ion detector was an electron multiplier operated in a pulse counting mode. The ion source and analyzer volumes were continuously pumped by a miniature sputter ion pump and by chemical getters. The gas sampling system allowed gas from one of two direct leaks (DL1 or DL2) or from enrichment cells (EC1 or EC2) to be introduced into the ionization region of the mass spectrometer. The operation of one of the enrichment cells was optimized for the detection of rare gases (RG). Several background spectra were taken. The gas sampling system and other instrument elements are shown schematically in Figure 1. Figure 2 illustrates the time sequencing of the direct atmospheric



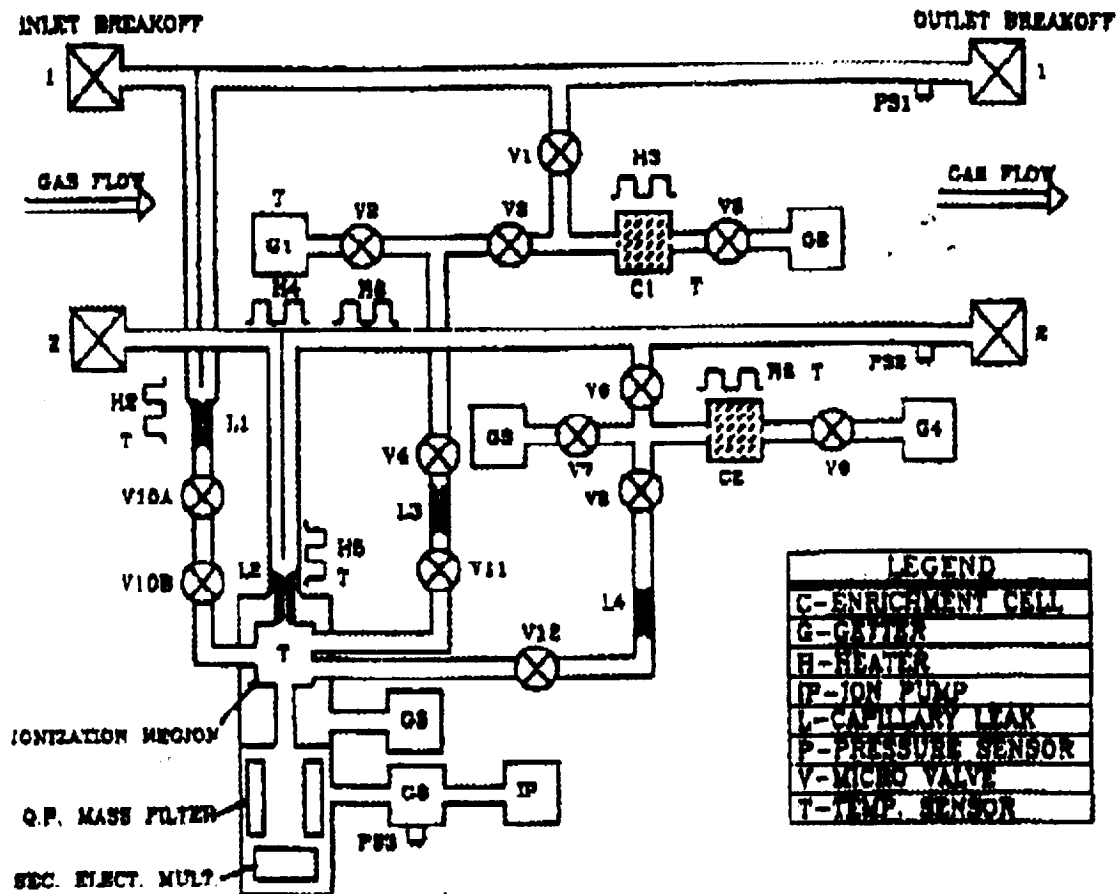


Figure 1. The GPMS inlet lines, enrichment cells, capillary leaks, micro valves and other instrument elements are schematically illustrated. From [Niemann et al., 1992].

measurements, the first background measurement, and the sampling of the atmosphere by the enrichment cells over the pressure and temperature ranges encountered by the probe.

The gas sampling system allowed atmospheric gas flowing through one of two inlet lines to be sampled directly or after chemical processing by one of two enrichment cells. The later measurements were designed to provide a cleaner noble gas

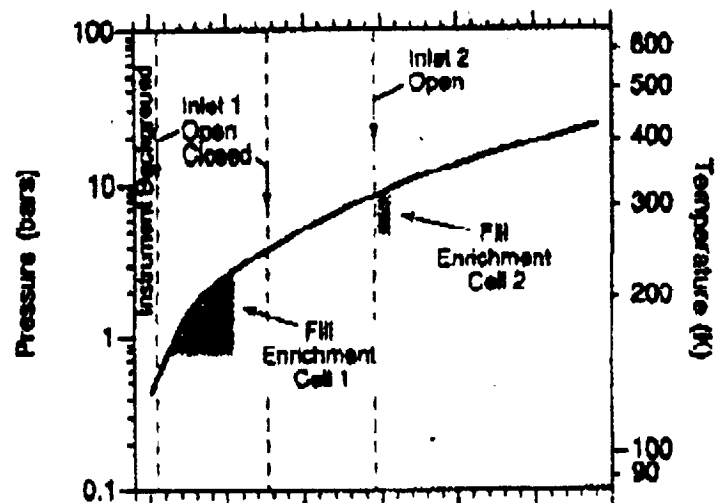


Figure 2. The sequencing of the 2 separate inlets and the enrichment cell sampling times are illustrated.



measurement and an increased signal to noise level for trace species. In addition background measurements were taken at 3 intervals during the descent sequence. The measurement sequence over the 6863 integration steps during which data was transmitted and the estimated effect on the pressure in the mass spectrometer ion source is illustrated in Figure 3. The detailed step number and the time at which each sequence was initiated is summarized in Table 1 together with the approximate temperature and pressure at the start of the sequence as derived from the Atmospheric Structure Experiment [Sief, et al., 1996].

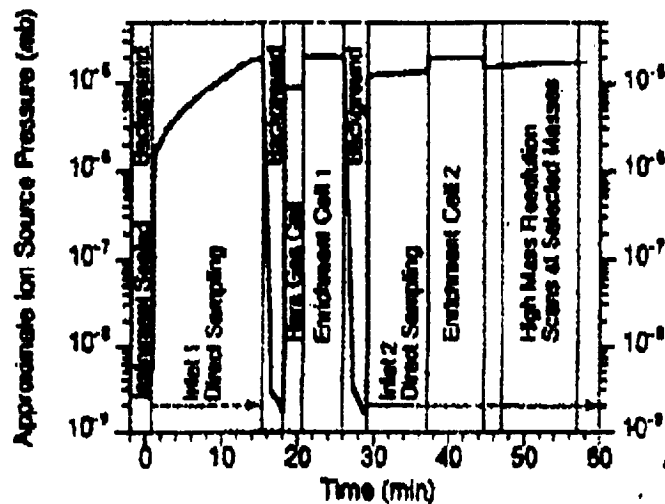


Figure 3. The descent sequence is illustrated by showing the approximate ion source pressure at various periods during the descent. Background measurement periods and enrichment cell periods are also illustrated.

Table 1. Galileo Probe Mass Spectrometer Descent Sequence					
measurement period	step	time (sec)	T (K)	P (bar)	notes on instrument state
DL1 (direct leak 1)	0	0	130	0.4	V10A and V10B open
B1 (background 1)	1811	917	251	3.8	all source inlet valves closed
RG (rare gas)	2161	1092	268	4.6	V2, V3 closed, V4 open
EC1 (enrichment cell 1)	2452	1238	281	5.4	V1, V2, V5 closed, H3 on, V3, V4 open
B2 (background 2)	3097	1561	306	7.3	all source inlet valves closed
DL 2a (direct leak 2a)	3482	1753	321	8.6	inlet 2 open, all other source inlet valves closed
EC2 (enrichment cell 2)	4442	2233	353	12.1	V8, V12 open, V7, V9 closed, C2 heated by H6, signal through L4 is added to that from L2 which has no shut off valve
DL2b (direct leak 2b)	5331	2677	381	15.7	V8 closed



### Instrument Performance

Although several of the probe experiments were affected by the greater than expected thermal coupling to the probe interior of the Jovian atmosphere [Young et al., 1996], the data set from the mass spectrometer was relatively little impacted. This was due, in part, to the protection of thermal inertia of the internal pressurized housing which had been implemented to avoid electrical discharge at certain pressure levels during the descent. Temperatures in the instrument electronics varied from approximately -10 C several minutes into the descent to approximately 70 C near the end of the probe mission.

The response of the detector to changes in the sampling system for several selected masses over the course of the descent is illustrated in Figure 2. The signal levels during the background measurement periods and the enrichment cell periods indicated that valves and heaters performed as expected

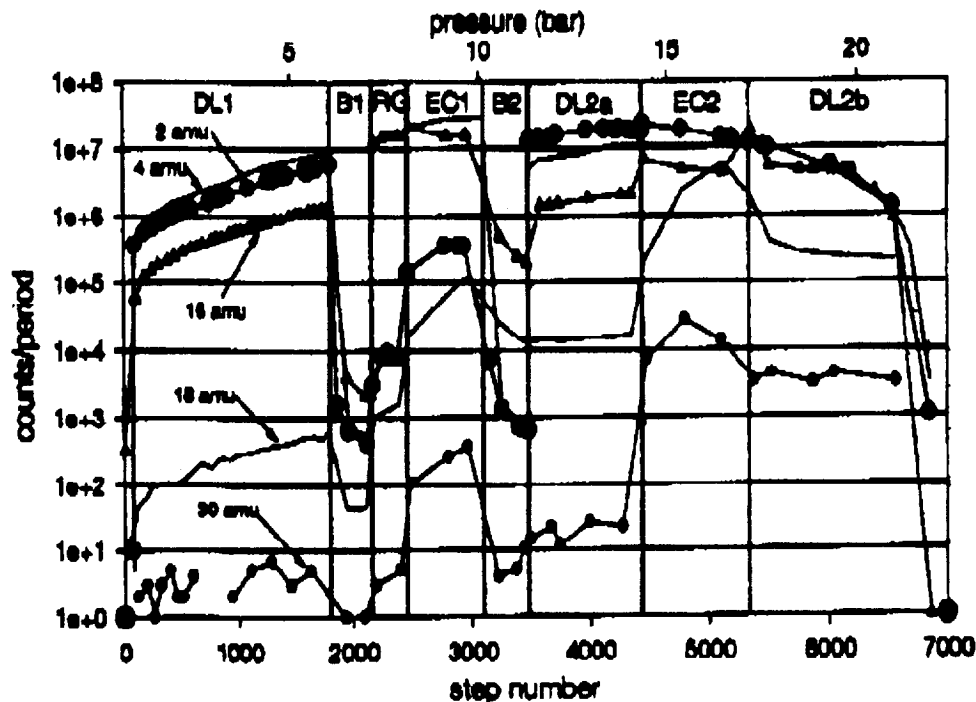


Figure 2. Detector counts for selected mass values are shown over the entire descent sequence. Relatively large increases in the count rate at masses 18 and 30 after EC2 are evident. The counts have been corrected for detector dead time effects. These corrections are valid over the entire descent for the counts shown at 30 amu, 18 amu, and 16 amu. However, in the later portion of the DL2a region, the EC2 region and the DL2b region the detector is



nearly saturated at 2 and 4 amu and for these measurements the form of this correction is not valid.

The variation in ratios of the counts/period in the DL1 and the DL2 region for the different masses illustrate the need for independent calibrations for the two capillary leaks. This is true, in general, for each separate species. DL2 introduces the gas into the ionization region in a direct beam path from the end of the capillary leak and a portion of this gas is ionized before it thermalizes with the walls of the chamber. The path to the ionization region from DL1 is more indirect because of the requirement to close valves V10a and V10b after the first segment of the measurement is complete.

## COMPOSITIONAL ANALYSIS

### Summary of Previous Results and New Findings

We have previously reported abundances of  $0.156 \pm 0.006$  for  $^4\text{He}$ ,  $(2.1 + 0.15) \times 10^3$  for  $\text{CH}_4$ ,  $(7.7 + 0.5) \times 10^5$  for  $\text{H}_2\text{S}$  and upper limits of  $(3.7 + 0.35) \times 10^4$  for  $\text{H}_2\text{O}$ ,  $(3.5 + 0.3) \times 10^4$  for  $\text{NH}_3$ ,  $(8.5 + 0.4) \times 10^5$  for  $\text{Kr}$ , and  $(5 + 2.5) \times 10^5$  for  $\text{Xe}$ . The helium to hydrogen ratio is in excellent agreement with the value derived from another Probe instrument the Helium Abundance Detector [Von Zahn, et al., 1996]. Methane abundances were derived from measurements in both the DL1 and DL2a region. The minimal interference at mass 17 in the DL1 region allow the  $^{13}\text{C}/^{12}\text{C}$  ratio to be established at 0.011 [Niemann et al., 1996], identical to the solar value.

The upper limit of  $3.7 \times 10^4$  for water previously reported [Niemann, et al., 1996] was derived from the region just below 12 bar (prior to step 4442 where the enrichment cell measurement was initiated). This value represents a limit of 0.2 times the solar value. However, the data shown in Figure 2 shows that the water abundance increased by the time the enrichment cell experiment EC2 had been completed and direct sampling of the atmosphere resumed at 15.6 bar. This rapid increase in mixing ratio is also observed for several other species and is consistent with the view that atmospheric circulation effects created a large region substantially depleted in condensable species at the higher altitude regions of the probe entry site. Another example is the variation in mass 30 counts with step number, also shown in Figure 2.

The DL2b sequence provides data from the deepest part of the atmosphere sampled before the instrument began to degrade due to the extreme conditions. High quality data was obtained during the DL2b sequence over the pressure range from 15.6 bar to approximately 21 bar. This region shows the greatest number of chemical species in the spectra. In addition to the species listed above we have identified ethane, ethylene, and propane in the spectra. Our preliminary analysis also suggests the presence of trace levels of other 3 and 4 carbon hydrocarbons, of propane nitrile, phosphine, hydrogen chloride, and of benzene.

### Post Encounter Laboratory Calibration

The calibration of the flight unit in 1985 sampled a variety of chemical species postulated to be present in Jupiter's atmosphere. Several of the species identified in the GPMS data were not included in these calibration experiments and we are presently continuing these experiments with a spare GPMS unit. This calibration is necessary for quantification of



mixing ratios since the sensitivity of the instrument to different gases varies considerably from species to species due to the gas inlet and pumping systems.

## REFERENCES

Atreya, S. K., reference to be supplied

Carlson, B. E., A. A. Lacis, W. B. Rossow, Tropospheric Gas Composition and Cloud Structure of the Jovian North Equatorial Belt, *J. Geophys. Res.* 98, 5251 (1993).

Niemann, H. B., S. K. Atreya, G. R. Carignan, T. M. Donahue, J. A. Haberman, D. N. Harpold, R. E. Harle, D. M. Hunten, W. T. Kasprzak, P. R. Mahaffy, T. C. Owen, N. W. Spencer, S. H. Way, The Galileo Probe Mass Spectrometer: Composition of Jupiter's Atmosphere, *Science* 272, 781 (1996).

Niemann, H. B., D. N. Harpold, S. K. Atreya, G. R. Carignan, D. M. Hunten, and T. C. Owen, *Space Science Review*, 60, 168 (1992).

Owen, T. C., H. B. Niemann, S. K. Atreya, G. R. Carignan, T. M. Donahue, D. N. Harpold, R. E. Harle, D. M. Hunten, W. T. Kasprzak, P. R. Mahaffy, T. C. Owen, N. W. Spencer, S. H. Way, The GPMs Determination of the Composition of Jupiter's Atmosphere: Implications for Origin and Evolution, EOS, American Geophysical Union 77, s171 (1996).

Self, A., *Science* 272, 849 (1996).

Smith, W. H., W. V. Schempp, K. H. Baines, *Astrophys. J.* 336, 967 (1989).

Von Zahn, U., and D. M. Hunten, The Helium Mass Fraction in Jupiter's Atmosphere, *Science* 272, 849 (1996).

Young, R. E., M. A. Smith, C. K. Sobeck, Galileo Probe: In Situ Observations of Jupiter's Atmosphere, *Science* 272, 837 (1996).



272,781 1996

485

## REPORTS

# The Galileo Probe Mass Spectrometer: Composition of Jupiter's Atmosphere

Hasso B. Niemann, Sushil K. Atreya, George R. Carignan,  
Thomas M. Donahue, John A. Haberman, Dan N. Harpold,  
Richard E. Hartle, Donald M. Hunten, Wayne T. Kasprzak,  
Paul R. Mahaffy, Tobias C. Owen, Nelson W. Spencer,  
Stanley H. Way

The composition of the jovian atmosphere from an altitude marked by an atmospheric pressure of 0.5 to 21 bars was determined by a quadrupole mass spectrometer on the Galileo probe. The mixing ratio of He (helium) to  $H_2$  (hydrogen), 0.158, is close to the solar ratio. The abundances of methane, water, argon, neon, and dihydrogen sulfide were measured; krypton and xenon were detected. As measured in the jovian atmosphere, the amount of carbon is 2.9 times the solar abundance relative to  $H_2$ , the amount of sulfur is greater than the solar abundance, and the amount of oxygen is much less than the solar abundance. The neon abundance compared with that of hydrogen is about an order of magnitude less than the solar abundance. Isotopic ratios of carbon and the noble gases are consistent with solar values. The measured ratio of deuterium to hydrogen (D/H) of  $(5 \pm 2) \times 10^{-6}$  indicates that this ratio is greater in solar-system hydrogen than in local interstellar hydrogen, and the  $^3He/^4He$  ratio of  $(1.1 \pm 0.2) \times 10^{-4}$  provides a new value for protosolar (solar nebula) helium isotopes. Together, the D/H and  $^3He/^4He$  ratios are consistent with conversion in the sun of protosolar deuterium to present-day  $^3He$ .

Determination of the composition of Jupiter's atmosphere should constrain the relative importance of direct contributions to the atmosphere from the solar nebula itself, on the one hand, and from large icy or rocky objects present in the early outer solar system, on the other. The contribution of these "planetesimals" could have been in the form of an early atmosphere around Jupiter's primitive solid core or in the form of volatiles they carried to the planet after it began to acquire its atmosphere of  $H$  and  $He$  from the solar nebula (1, 2). The degree of resemblance between the sun's atmosphere and that of Jupiter in the abundances relative to  $H$  of elements such as  $C$ ,  $N$ , and  $O$  should be decisive in providing the required constraints.

Before the direct, in situ measurements reported here, remote spectroscopic sensing from Earth and from spacecraft had indicated that the relative abundances of  $C$  (in  $CH_4$ ) and  $N$  (in  $NH_3$ ) were greater than the solar abundances (3, 4). Phosphine and water vapor had been detected, but their abundances below the clouds were uncertain, and  $H_2S$  and the noble gases other than  $He$  had not been detected at all. De-

finite data to replace these tantalizing clues to the sources of volatile compounds in Jupiter's atmosphere were not available before this descent of the probe.

An accurate direct measurement of the abundances of  $He$  and the other noble gases is important for understanding how Jupiter has processed its constituents. Abundances less than those of the solar values would signal the formation, in the metallic interior of the planet, of a separate  $He$  phase, some of which has precipitated deeper into the interior. Remote sensing had indicated a modest depletion of  $He$ , but this indirect result is much less satisfactory than the direct sensing by two of the Galileo instruments reported here.

The Galileo probe mass spectrometer (GPMS) was designed to measure the mixing ratios of major and minor species while

determining the isotopic ratios of their constituent elements (5). Signals were recorded from over 6000 individual values of mass-to-charge ratio ( $m/z$ ). The data returned by the instrument have led to the discovery of six new atmospheric constituents and the measurement of numerous abundances and isotopic ratios. The gas sampling system admirably the jovian atmosphere through low-conductance leaks to the ion source of a quadrupole mass analyzer. The ion source was pumped by a getter and the analyzer volume pumped to a much lower pressure by a getter backed by a sputter-ion pump. One inlet (direct leak 1; DL1) was open from 0.52 to 3.78 bars; the other inlet (DL2) functioned from 8.21 bars to the end at about 21 bars (6).

Figure 1 shows a sample mass spectrum from the 3-bar region at 228 K, before any significant water cloud was expected, and another one from the 11-bar region, where the 350 K temperature assures that the probe was far below any water condensation level. Comparison of the two spectra shows a large increase in the second direct leak of  $H_2O$  and  $NH_3$ . In fact, the design of the leak 1 sampling system, with a relatively long vacuum path to the ion source, precludes a sensitive detection of the surface active species  $H_2O$  and  $NH_3$  in the atmospheric region sampled by this leak. Raw counts shown in these spectra must be corrected for the counting system dead time. The efficiencies of the ion source and the pumping system vary from species to species, and the sensitivity factors, which are different for the two direct leaks, must be individually determined. In most cases, we used preflight calibrations, but for the most important species we were able to do some recalibrations on the spare instrument. With the direct leaks, the background level was typically between 0 and 3 counts. Two background measurements demonstrated that the instrument arrived at Jupiter in a very clean state and quickly lost its memory of almost all gases contributed by DL1.

Table 1. Mixing ratios to  $H_2$  and isotopic ratios in the jovian atmosphere. Blank spaces indicate zero.

Species	Jovian atmosphere	Ratio to solar value	Prior results	References
$^4He$	$0.158 \pm 0.008$	CAD	0.11	(12, 13)
$^{20}Ne$	$(2.3 \pm 0.25) \times 10^{-6}$	0.10		
$^{36}Ar$	$(1.0 \pm 0.4) \times 10^{-6}$	1.8		
$^{34}S$	$\approx (8.5 \pm 4) \times 10^{-6}$	$\approx 5$		
$^{136}Xe$	$\approx (8 \pm 2.6) \times 10^{-8}$	$\approx 60$		
$CH_4$	$(2.1 \pm 0.15) \times 10^{-6}$	3	$2.2 \times 10^{-6}$	(3, 4)
$H_2O$	$\approx (3.7 \pm 0.35) \times 10^{-4}$	$\approx 3.2$		
$NH_3$	$\approx (3.5 \pm 0.3) \times 10^{-6}$	$\approx 10$	$2.5 \times 10^{-4}$	(10)
$H_2S$	$(7.7 \pm 0.8) \times 10^{-6}$	2.2		
D/H	$(5 \pm 2) \times 10^{-6}$		$(2.0, 3.6) \times 10^{-6}$	(17-19)
$^3He/^4He$	$(1.1 \pm 0.1) \times 10^{-4}$			
$^{12}C/^{13}C$	$0.0108 \pm 0.0006$	1.0		

H. B. Niemann, J. A. Haberman, D. N. Harpold, R. E. Hartle, W. T. Kasprzak, P. R. Mahaffy, S. H. Way, Goddard Space Flight Center, Greenbelt, MD 20771, USA.  
S. K. Atreya, G. R. Carignan, T. M. Donahue, University of Michigan, 2455 Hayward Street, Ann Arbor, MI 48106, USA.  
D. M. Hunten, University of Arizona, Tucson, AZ 85721, USA.  
T. C. Owen, University of Hawaii, 2880 Woodlawn Drive, Honolulu, HI 96822, USA.  
N. W. Spencer, 13013 Remington Drive, Silver Spring, MD 20902, USA.



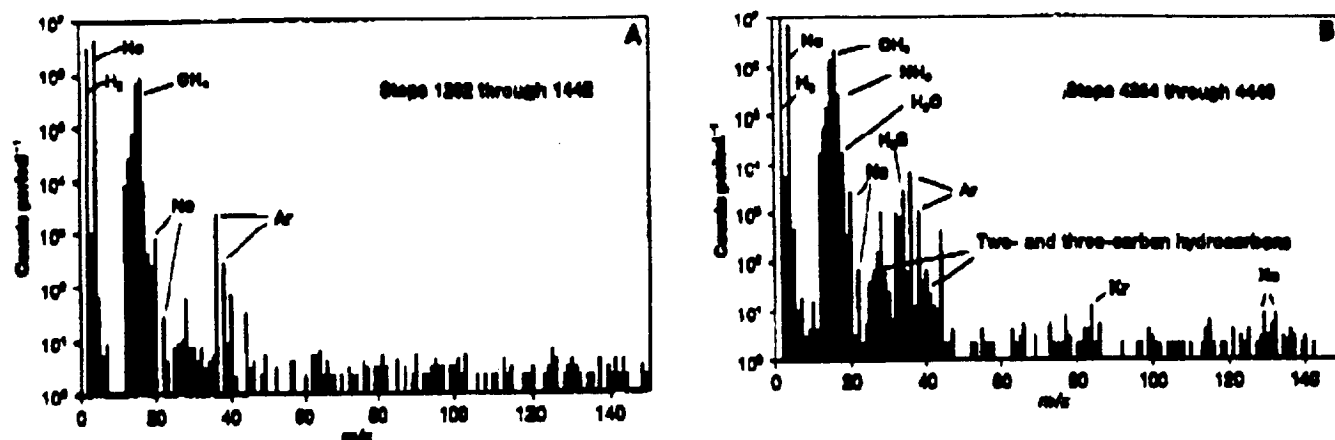


Fig. 1. Sample mass spectra. The spectra in (A) were obtained through DL1 between pressures of 2.72 and 3.06 bar, with ambient temperature at 220 K. The spectra in (B) were obtained through DL2 between pressures of 10.6 and 11.3 bar, with ambient temperature at 380 K. No corrections have been made for dead time or for different efficiencies at different masses.

Table 1 shows the mixing ratios (number densities relative to  $H_2$ ) of species that were detected and for which reliable measurements could be made. Error estimates are roughly 1σ and represent the data scatter about the average value. Some of the observed mixing ratios can be compared with those for the solar system as compiled by Anders and Grevesse (7), commonly referred to as the solar abundances. Also shown are results of earlier analyses based on Voyager or Earth-based spectra.

The Jovian  $He/H_2$  ratio,  $0.156 \pm 0.006$ , is the average of 14 individual measurements from DL1 ( $0.157 \pm 0.006$ ) and 4 from DL2 ( $0.151 \pm 0.004$ ). All the other noble gases were detected, and they are chemically fractionated. The Ne ratio to  $H_2$  is about an order of magnitude less than the solar ratio, whereas for Ar the ratio is slightly greater. Kr and Xe were clearly detected; upper limits on the mixing ratios are respectively 5 and 50 times the solar values. For all four of the heavier noble gases, the isotopic ratios are close to the solar values.

The  $^3He/^4He$  and the D/H ratios were determined from an analysis of the 3 amu (atomic mass unit) data. This analysis is complicated by the need to correct for  $H_3^+$  produced in the ion source and to distinguish between the contributions of HD and  $^3He$ .  $H_3^+$  is generated in one of two ways: by dissociative ionization of  $CH_4$  or by a two-body ion-molecule reaction between  $H_2^+$  and  $H_2$ . The efficiency of  $H_3^+$  production could be determined during the second background study when little  $H_2$  and He, but a considerable amount of  $CH_4$ , existed in the ion source and  $CH_4$  was the only important source of 3-amu ions. During pre-flight calibration, when the  $H_2$  pressure in the GPMS was varied over a large range, the HD/ $H_2$  ratio for the laboratory  $H_2$  sample and the efficiency of  $H_3^+$  production in

DL1 and DL2 were separately determined. During probe descent, the  $^3He/^4He$  ratio was determined from 3-amu and 4-amu data obtained with the noble gas cell (NGC) sample (6). Hydrogen was effectively absent from this gas sample. The result,  $1.1 \times 10^{-4}$  (Table 1), indicates that He in the jovian atmosphere has a smaller proportion of  $^3He$  than the protosolar He found in meteorites, where  $^3He/^4He = (1.5 \pm 0.3) \times 10^{-4}$  (8). Evidently, the "protosolar" He isotopes in meteorites do not, in fact, reflect the values that existed in the solar nebula.

With the He mixing ratio and  $H_3^+$  production efficiencies in hand, the HD/ $H_2$  ratio was determined from the DL1 and DL2 data at 3 amu and 2 amu. During DL2 sampling, the electron energy in the ion source was reduced at times from 75 eV to 25 eV or 15 eV. Few and no He ions, respectively, were produced under these conditions, and the ratios of the 3-amu rate to the 2-amu rate provided an upper limit to HD/ $H_2$  (assuming no  $H_3^+$  production) of  $(1.1 \pm 0.3) \times 10^{-4}$ . The average value of  $HD/H_2$ , measured from mixer 2 data, was just at this limit. The ratios measured in Inlets 1 and 2 were almost precisely the same. The  $^{12}C/^{13}C$  isotopic ratio was determined with high precision in DL1 data where the contribution of  $NH_3$  at 17 amu was negligible. The ratio is exactly that of the solar values.

Reasonably good agreement was found for  $CH_4$  mixing ratios in DL1 and DL2, within the calibration uncertainty of  $\pm 20\%$ . This determination indicates that atmospheric  $^{13}C$  is more abundant by a factor of 3 relative to  $H_2$  than in solar system material. The measured mixing ratio of  $H_2S$  in the well-mixed atmosphere between 8 and 11 bars increased by a factor of 4 with depth. There was a tentative detection of HCl. Water vapor and  $NH_3$  were readily adsorbed on metal surfaces, and

their densities in the ion source may lag behind those in the gas stream. The measurements made while DL2 was open should be the most reliable, but they were made just after enrichment cell 1 (BC1) was closed. Some of the  $NH_3$  and  $H_2O$  detected in DL2 may therefore have been contributed by outgassing of this adsorbed gas in the presence of abundant  $H_2$  and He (9). Hence, for the present, only upper limits can be set for these molecules. The constraint for  $NH_3$ , 16 times the solar value, is weaker than the existing estimate, 1 to 1.3 times the solar value, from analysis of Jupiter's microwave emission spectrum (10). The limit on water vapor, 0.2 times the solar value, is significant in view of the solar or greater values found for the other volatiles C, N, and S.

Two- and three-hydrocarbon species appeared to be present. The direct scans showed no sign of any heavier hydrocarbons. Upper limits for the mixing ratios of these heavy hydrocarbon species are  $\sim 1$  ppb.

Our  $He/H_2$  ratio (0.156) agrees almost exactly with the ratio of 0.157 obtained by the helium abundance detector (HAD) on the Galileo probe (11); some of the implications of this measurement are discussed elsewhere (11). This value is considerably larger than the value of 0.11 obtained from Voyager data (12), but is little (if any) less than the value for the present sun. The protosolar value, deduced from evolutionary models of the sun, is probably a more relevant standard and is 18% greater (11). It is widely believed that Saturn's atmosphere, with a  $He/H_2$  ratio about one-fifth of the protosolar value, has been depleted of He by rain-out of He droplets in the interior (13, 14). The GPMS and HAD results agree with the Voyager data in suggesting that the same process must operate at Jupiter,



though not to the same extent. This loss of He is a likely explanation of the Ne depletion observed by the GPMS, if the solubility of Ne in He is as large as has been suggested (15).

The value of  $(5 \pm 2) \times 10^{-5}$  deduced for D/H from HD/H<sub>2</sub> is higher than the ratios derived from Earth-based spectroscopic observations (16, 17):  $(2 \pm 1) \times 10^{-5}$  from CH<sub>4</sub>/DCH<sub>4</sub> and  $(2 \pm 1) \times 10^{-5}$  from HD/H<sub>2</sub>. It agrees well with the value found in a recent analysis of Voyager infrared spectra (18):  $(3.8 \pm 0.5) \times 10^{-5}$ . The jovian D/H ratio should be the same as the protomolar or solar-nebular value because the nebula was the source of Jupiter's hydrogen. [The terrestrial ratio is  $1.6 \times 10^{-4}$ .] The sun converted all its D to <sup>3</sup>He early in its history; thus, Geiss (8) argued that the original D/H in the solar nebula should be equal to the difference between the <sup>3</sup>He/<sup>4</sup>He ratios in the solar wind and in meteorites, which should contain nebular He (19). Geiss's value for protomolar D/H is  $(2.6 \pm 1.0) \times 10^{-5}$ , and this overlaps the GPMS value. Substituting the new determination of protosolar <sup>3</sup>He/<sup>4</sup>He =  $(1.1 \pm 0.2) \times 10^{-8}$  for the meteoritic one, the same argument would yield D/H =  $(3 \pm 1) \times 10^{-5}$ , a value that is closer to that derived directly from HD. It is clear that D/H on Jupiter is distinctly higher than the value of  $(1.6 \pm 0.1) \times 10^{-5}$  found in local interstellar H (20), as expected from the steady destruction of D in the galaxy by stellar nucleosynthesis during the last  $4.5 \times 10^9$  years.

Earth-based imaging (21) and the remarkably small number of cloud particles detected by the nephelometer experiment (22) indicate that the probe may have descended into an unusually clear part of the jovian atmosphere. An obvious explanation is that the region was one of subsidence, like most clear regions on Earth. Our H<sub>2</sub>O abundance value, then, may be less than the planetary average, although this result is unlikely. In a cloud, the relative humidity should be just over 100%, and this is consistent with the comprehensive analysis of Voyager spectra by Carlson et al. (18). The corresponding profile of water vapor has a scale height of about 3 km. If, for example, the relative humidity is reduced by a downdraft from 100% to 90%, the amount of subsidence required is  $3 \ln(90/100)$  km, or a mere 0.3 km. Our measurements were made at far greater depths than the expected condensation level (5 or 6 bars); to perturb the humidity at such a deep level would require a downdraft extending over a range of well over a scale height, far more than needed simply to clear out the clouds. There remains the possibility of a global-scale circulation, perhaps upward at high latitudes and downward at low.

The large atmospheric abundance of C

suggests that sources other than the gas of the solar nebula contributed a significant share of the volatiles in the envelope of Jupiter. These elements and water should have been in the condensed phase in the neighborhood of the accreting Jupiter. One possible explanation for a deficiency of water was proposed by Gautier and Owen (3, 4): most of the planetesimals accreted to the rocky, icy core of the embryo planet rather than being collected after the planet began to amass its gaseous envelope from the neighboring solar nebula. Water vapor, being the least volatile, remained close to the core, whereas gases like CO, CH<sub>4</sub>, and N<sub>2</sub> could mix with the nebula-derived envelope, enriching it in C and N. Although this scenario could reproduce the observed abundances, it must be tested by rigorous modeling. If there was a large mass of late-accreting planetesimals, the low relative abundance of atmospheric H<sub>2</sub>O requires them to have been rich in carbonaceous materials and deficient in O. It has been customary to assume that outer solar-system planetesimals resemble the least-altered carbonaceous chondrites that fall to Earth, which contain more O than C (23), but there are many that are much drier. The mean densities observed for many satellites in the outer solar system have been explained by assuming a rock: ice ratio of order unity, but perhaps much of the low-density material is carbonaceous rather than icy.

If our results are representative of the entire planet (24), they preclude models in which several Earth masses of late-accreting, water-rich planetesimals deliver volatiles to the jovian envelope (1). There is no sign of the dense water cloud, or the corresponding vapor, invoked to explain waves spreading from the Shoemaker-Levy 9 impacts (25). Water vapor observed in the impact plumes probably came from the impactors, not Jupiter, as suggested (26).

## REFERENCES AND NOTES

1. D. J. Stevenson, *Annu. Rev. Earth Planet. Sci.* 10, 257 (1982); J. B. Pollack and P. Bodenheimer, in *Origin and Evolution of Planetary and Satellite Atmospheres*, S. K. Atreya, J. B. Pollack, M. S. Matthews, Eds. (Univ. of Arizona Press, Tucson, 1989), p. 664; W. B. Hubbard, *ibid.*, p. 689.
2. J. I. Lunine and D. J. Stevenson, *Astrophys. J. Suppl.* 69, 493 (1989); T. Owen and A. Bar-Nir, *ibid.* 118, 215 (1989).
3. D. Gautier and T. Owen, in *Origin and Evolution of Planetary and Satellite Atmospheres*, S. K. Atreya, J. B. Pollack, M. S. Matthews, Eds. (Univ. of Arizona Press, Tucson, 1989), p. 467.
4. K. B. Noll and H. P. Larson, *Science* 89, 199 (1981).
5. H. B. Niemann et al., *Space Sci. Rev.* 60, 111 (1982).
6. Each inlet also fed a gas sample to an enrichment chamber, in which a porous carbon material adsorbed complex hydrocarbons and heavy noble gases. The noble gases not adsorbed by EC1 were captured and fed to the analyzer in an NGC from which H<sub>2</sub> was eliminated by a getter pump. This procedure lowered the threshold of detectability by a factor of 10 (to 0.1 part per billion by volume). The gases not adsorbed by EC1 were also pumped away, and the adsorbed ones were later released by heating the cell and analyzed. These measurements, and two measurements of background, were carried out after inlet 1 was closed and before inlet 2 was opened. EC2 was filled from inlet 2 when the pressure was 8.4 to 9 bars. The two enrichment cells raised the sensitivity to stable hydrocarbons and the heavier noble gases by as much as a factor of 500. The system was controlled by a read-only memory, reprogrammed each 1/2 s through 8192 steps. Many scans were made at integral masses through the range of 2 to 180 amu, requiring 75 s; other sequences covered only selected masses. The dynamic range was 10<sup>5</sup>.
7. E. Anders and N. Greessen, *Geochim. Cosmochim. Acta* 58, 187 (1994). These abundances, commonly referred to as "solar" or "solar-system" abundances, are based on a combination of evidence from the sun itself and from primitive meteorites.
8. J. Geiss, in *Origin and Evolution of the Elements*, N. Prantzos, E. Vangioni-Flam, M. Cassé, Eds. (Cambridge Univ. Press, Cambridge, 1993), p. 88.
9. The enrichment cells were heated and the evolved gases measured between 6.5 and 7 bar and 11.8 and 14.5 bar.
10. A. Martin, R. Courtin, D. Gautier, A. Lacomba, *Science* 251, 410 (1993); L. de Pater and S. T. Mousis, *ibid.* 262, 143 (1993).
11. U. von Zahn and D. M. Hunten, *Science* 200, 100 (1990).
12. B. J. Conrath, D. Gautier, R. A. Hanel, J. B. Hrynshaw, *Astrophys. J.* 392, 307 (1994).
13. R. Smoluchowski, *Nature* 215, 981 (1967).
14. D. J. Stevenson and E. S. Salpeter, *Astrophys. J. Suppl.* 26, 221 (1977); *ibid.*, p. 238.
15. M. S. Rousson and D. J. Stevenson, *ICB (Spring Suppl.)* 78, 040 (1988).
16. D. Gautier and T. Owen, in 53, p. 504.
17. W. H. Smith, W. V. Schampo, K. H. Sannes, *Astrophys. J.* 35, 907 (1988).
18. B. E. Carlson, A. A. Lada, W. B. Rossow, *J. Geophys. Res.* 88, 2851 (1983). The D/H ratio quoted in this report has been adjusted to reflect our slightly larger measurement of CH<sub>4</sub> abundance.
19. The solar wind value is  $(4.5 \pm 0.4) \times 10^{-5}$ , and the meteoritic one is  $(1.5 \pm 0.3) \times 10^{-5}$ .
20. J. L. Lunine et al., *Astrophys. J.* 402, 684 (1993); see also X. Luny et al., in *Light Element Abundances*, P. Crane, Ed. (Springer-Verlag, Berlin, 1993), p. 216.
21. G. Orton et al., *Science* 250, 1000 (1992).
22. B. Reppert, D. S. Colburn, P. Avin, K. A. Pagan, *ibid.*, p. 1001.
23. H. B. Noll, *Geochim. Cosmochim. Acta* 5, 879 (1982); E. Mason, *Meteorites* (Wiley, New York, 1963).
24. A good interpretation of the observed variations in abundances could involve relatively small differences in the solubility of volatiles in metallic H. Approximately 90% of Jupiter's H is in the metallic phase. For instance, if the solubility of a minor constituent in the molecular part of the planet is much larger than the solar value, then this raising ratio in the metallic interior may be slightly smaller than the solar value or vice versa.
25. A. P. Ingersoll and M. Kanamaru, *Nature* 374, 708 (1990).
26. A. L. Sprague et al., *ibid.*, in press.
27. We thank J. Cooley for his efforts as instrument manager, R. Lutz and T. Tyler for the mechanical design contributions, A. Doan for his help in the enrichment cell design, R. Abell, H. Powers, and H. Menda for the precision assembly welding and machining, and R. Arvey and H. Barton for the electronics assembly and testing at Goddard Space Flight Center. The contributions to the electronics system design of B. Block, J. Carlisle, J. Eiler, J. Maurer, and W. Prikus at the University of Michigan are gratefully acknowledged. The hybrid electronic circuits were fabricated at the General Planets Aeronautics Division at Valley Forge, PA, and the microscopes for the gas sampling system were designed and fabricated by Aker Industries in Oakland, CA. The chemical getter material was provided by the SAES Getter of Milan, Italy. M. Wong of the University of Michigan participated in



THE UNIVERSITY OF TEXAS AT AUSTIN

the data analysis. We also thank the Galileo Probe  
Project personnel at NASA Ames Research Center  
and we particularly acknowledge the contributions of

A. Wilhelm, C. Soback, and P. Mela for their efforts  
during the development, spacecraft integration, and

testing phases. 16 March 1996; accepted 17 April  
1996



# ION/NEUTRAL ESCAPE OF HYDROGEN AND DEUTERIUM: EVOLUTION OF WATER

T.M. DONAHUE  
*University of Michigan, Ann Arbor*

D.H. GRINSPOON  
*University of Colorado, Boulder*

R.E. HARTLE  
*NASA Goddard Space Flight Center*

R.R. HODGES, JR.  
*University of Texas at Dallas*

Venus II.  
Ugayona  
J. P...  
Els. Boyler,  
Hunt...  
Phillips

Infrared remote soundings and *in situ* mass spectrometric measurements place the present water vapor abundance in the lower atmosphere of Venus at  $30 \pm 10$  ppm, and there is some evidence of spatial and temporal variability. These measurements also agree that the D/H ratio in this water vapor is  $150 \pm 30$  times that of terrestrial water. No other hydrogen compounds are present with mixing ratios as large as 5 ppm v/v. The significance of these measurements for the evolution of water in the planet depends on the history of escape of hydrogen and deuterium and their replenishment by exogenous and endogenous sources - such as comets and volcanoes. A charge separation electric field driven upward flow from the night side bulge region produces escape fluxes averaged over the entire planet of  $(1.5 \pm 0.2) \times 10^7 \text{ cm}^{-2} \text{ s}^{-1}$  in  $\text{H}^+$  and  $(5.6 \pm 1) \times 10^4 \text{ cm}^{-2} \text{ s}^{-1}$  in  $\text{D}^+$  during solar maximum (fractionation factor - 0.15). Very serious depletion of  $\text{H}^+$  and  $\text{D}^+$  in the bulge during periods of low solar activity reduces the escape to 0.15 these rates. The solar cycle average loss rates are  $(9 \pm 1.0) \times 10^6 \text{ cm}^{-2} \text{ s}^{-1}$  for H and  $(3.2 \pm 0.6) \times 10^4 \text{ cm}^{-2} \text{ s}^{-1}$  for D. Until charge exchange loss rates are calculated for atmospheric models that conform to Pioneer Venus observations they can only be estimated. The best guess is that H escapes at rates between  $9$  and  $7 \times 10^6 \text{ cm}^{-2} \text{ s}^{-1}$  during the solar cycle so that the solar cycle average is  $8 \times 10^6 \text{ cm}^{-2} \text{ s}^{-1}$ . The fractionation factor should be small - about 0.02. The total flux could be as large as  $1.7 \times 10^7 \text{ cm}^{-2} \text{ s}^{-1}$  and as small as  $9 \times 10^6 \text{ cm}^{-2} \text{ s}^{-1}$ , depending on the actual charge exchange contribution. The loss rates can also be calculated from the solar cycle modulation of bulge densities. For hydrogen, a solar cycle planet-wide average of  $(6 - 7.5) \times 10^6 \text{ cm}^{-2} \text{ s}^{-1}$  is deduced.  $f$  is very large - 0.44. This result suggests that the electric field driven flow in the thermosphere is responsible for the entire escape flux of about  $8 \times 10^6 \text{ cm}^{-2} \text{ s}^{-1}$ ,  $0.15 \leq f \leq 0.44$ . If today's water vapor is predominantly a remnant of an ancient supply of water and the fractionation factor has not changed, Venus has lost the equivalent of at least 4 meters of liquid water spread uniformly over its surface - 0.12 percent of a full terrestrial ocean (fto). This lower limit would be 30 times larger if  $f$  is 0.44. If there is a source of water with  $\text{D}/\text{H} = 1.6 \times 10^{-4}$ , the amount of early water required to account for today's large D/H ratio increases to something between 0.6 to 16% of a fto. It is also possible that the water present today has been supplied by outgassing of highly fractionated water from the mantle, perhaps during a massive resurfacing event.

## 1. INTRODUCTION

Today, the surface and atmosphere of Venus are very dry. How dry is a question that this chapter will address. How dry the interior may be is a question much more difficult to answer and thus one this chapter will consider only in passing. The planet is losing water because



hydrogen escapes into space after water molecules have been dissociated in the upper atmosphere. Observations made by instruments on the Pioneer Venus Orbiter (PVO) have greatly improved our understanding of escape processes and their magnitude. This chapter will examine these findings in considerable detail. The planet's atmosphere may also be acquiring water at a rate comparable to the loss rate because of encounters with comets and contemporaneous outgassing of the interior. Thus, in principle, an appreciable component of the water vapor in the atmosphere today may have been contributed by one or both of these sources. On the other hand, much of the water vapor, and particularly the deuterated water vapor, may be the residue of water Venus acquired as it was being created. It is also possible that the provenance of much of the deuterated water vapor (HDO) is very different than that of ordinary vapor ( $\text{H}_2\text{O}$ ) since the light isotope of hydrogen might be in a virtual steady state balancing escape and injection of deuterium-poor water while the heavy isotope is mostly a still decaying remnant of the primordial planetary water inventory. In such a case most of the light isotope in the atmosphere today could have arrived there relatively recently. This chapter will devote much of its attention to a discussion of the degree to which the source of today's water can be determined. In this regard explaining the remarkably high value of the deuterium to hydrogen ratio in the water vapor will be the principal objective of the chapter. This review will elaborate on developments since the last major reviews on this topic were published (Hunten *et al.*, 1989, Kasting and Toon, 1989).

## **2. PLANETOGENESIS: INITIAL VOLATILE INVENTORY**

There is almost a consensus today that the terrestrial planets were formed by collisions among planetesimals that grew by accreting gases and dust from the solar nebula during several tens of million years after the sun itself developed. Models of the latter stages of this process, after  $10^{25} - 10^{26}$  gm embryos had been formed, place the maturing planetesimals on very eccentric orbits that would have thoroughly mixed the material out of which the four planets were made (Wetherill, 1991). Some or most of the volatile inventory of the planets, including water, may have been acquired during this phase of accretion. In this case, Venus and Earth, in particular, should have started with about the same endowment of volatiles, although they may have had very divergent experiences with outgassing and release of volatiles from their interiors after they reached their present size. Another very important source of volatiles for these planets may have been a heavy bombardment by volatile-rich comet-like objects arriving from the outer solar system toward the end of the accretionary period. The crater record clearly shows that such a bombardment occurred. How rich the intruders were in volatiles is less evident, but it is plausible to postulate that they were an important source of volatiles. Again, it is difficult to understand how they would have contributed very different amounts of volatiles to Earth and



Venus. On the other hand, singular events such as giant impacts by Mars-sized objects that caused large scale atmospheric erosion may well have affected one planet and not another. A recent attempt to explain the great difference in the rare gas abundances in the atmospheres of Earth and Venus (Pepin, 1991) invokes such a giant impact to power an atmospheric blow off event on Earth that did not occur on Venus, destroying an initial balance in the two rare gas planetary abundances. This model also invokes early blow off of a dense hydrogen atmosphere driven by strong extreme ultraviolet radiation from the young sun to explain the elemental and isotopic rare gas fractionation patterns.

An alternative to fractionation by hydrodynamic escape to explain volatile abundances is that the terrestrial planets received their argon, krypton and xenon, already fractionated, from impacting icy planetesimals (Owen, Bar-Nun and Kleinfeld, 1992). To account for the large abundance of argon on Venus, a late impact by a massive comet would be invoked. This proposal has been criticized on the ground that the gases would be eroded in the very impact that is meant to supply them (Kaula, 1994). A criterion is needed to determine whether impactors are to be sources or eroders of planetary volatiles.

Further support for the "twin planet" model is the near equality of the nitrogen and oxidized carbon inventory. This balance is attained by comparing the  $\text{CO}_2$  converted to carbonate on Earth with atmospheric  $\text{CO}_2$  on Venus. The conversion on Earth depends on water for the weathering of silicate rocks and on an ocean in which the carbonate can precipitate. Thus, the absence of liquid water on Venus is crucial for the difference in presentation of carbon but begs the question of whether there was ever abundant water on that planet. Among the volatiles whose abundances have been assessed water is the odd one out.

On the other hand, Lewis (1972) has shown that, during the time when dust and gas were condensing to form the primitive solar system condensates, the temperature in the planetary disk at 0.7 AU was so high that minerals containing water of hydration would not have been formed there. If the terrestrial planets accreted most of their components from material that condensed near their present orbits, primitive Earth might have contained much more water than primitive Venus did. Indeed, Lewis (1972) argues that the density differences among the terrestrial planets can be explained if this is the case, whereas it is difficult to understand the apparently systematic density variation otherwise. Prinn and Fegley (1989), however, have pointed out that gas-solid reactions are kinetically inhibited at typical nebula temperatures, so that neither Venus nor Earth or Mars could have obtained their water this way.

If, on the other hand, Earth received an appreciable contribution of water from a bombardment of volatile-rich objects at the end of accretion, it is hard to understand why Venus would not. However, volatiles acquired as a late accreting veneer and those stored in the interior



of the planet may well have undergone very different evolutionary paths (Pepin, 1995). In particular, the late arriving volatiles may have been severely eroded by planetesimal impact and enhanced euv heating not long after their arrival, while those in the interior had to wait for their release by outgassing processes. Thus, if for some reason the orbits of large planetesimals did not commonly cross each other in the later stages of accretion, the volatile endowment of Earth and Venus might have been very different.

### 3. EVOLUTION OF ESCAPING D AND H

The measurement long considered diagnostic to the determination of whether or not Venus once had abundant water interacting with its atmosphere is that of the ratio of deuterium to hydrogen (D/H ratio) in its water today. Most processes by which hydrogen isotopes escape from a planet discriminate strongly against loss of deuterium, leading to enrichment of deuterium. If the relative efficiency of deuterium and hydrogen loss -- the fractionation factor -- is known, the ratio of the hydrogen content of a reservoir supplying the escaping hydrogen at two arbitrary times can be determined from the ratio of the D to H ratios. This is irrespective of the absolute magnitudes of the content of the reservoirs or the escape flux (unless the *net* loss of hydrogen has a zero rate). Thus, if the abundance of hydrogen in the atmosphere of Venus today (probably in the form of H<sub>2</sub>O and perhaps some H<sub>2</sub>) can also be determined, the present D to H ratio measured and the D to H ratio in primitive planetary water measured or plausibly estimated, the size of the early reservoir can be fixed.

If the amount of atomic hydrogen in a vertical column of hydrogen compounds is [H] and that of deuterium [D], the respective escape fluxes  $\phi_1$  and  $\phi_2$ , and source strengths  $P_1$  and  $P_2$ .

$$\frac{d[H]}{dt} = P_1 - \phi_1, \quad (1)$$

$$\frac{d[D]}{dt} = P_2 - \phi_2. \quad (2)$$

The fractionation factor is normally defined as

$$f = \frac{\phi_2/[D]}{\phi_1/[H]} \quad (3)$$

$$= \frac{\phi_2}{\phi_1} \left( \frac{1}{R} \right) \quad (4)$$

where



$$R = [D]/[H], \quad (5)$$

and, in case water is the dominant hydrogen component,

$$R = \frac{[HDO]}{2[H_2O]}. \quad (5)$$

Integration of (4) gives the Rayleigh distillation relationship for the ratio of the size of the reservoir at some time  $t_2$  to a later time  $t_1$ ,

$$r(t_1, t_2) = \frac{[H(t_2)]}{[H(t_1)]} = \left( \frac{R(t_1)}{R(t_2)} \right)^{\frac{1}{1-f}}, \quad (6)$$

independent of  $\phi_1$  and  $P_1$ , if  $f$  is constant. If, at  $t_1$ ,  $[H]$  is indistinguishable experimentally from the hydrogen steady state,  $[H_{ss}]$ , that is if  $\phi_1 = P_1$ ,  $f$  would be undefined. Eq. 6 then could not be used to relate  $[H]$  at a very early time,  $t_2$ , to  $[H]$  at  $t_1$ .

If the effective D to H ratio in the sources is  $R_s$ , Eq (2) becomes

$$\frac{d[D]}{dt} = R_s P_1 - R f \phi_1. \quad (7)$$

Eqs. (1) and (7) can be integrated, numerically if necessary, provided there is a way to get a handle on the escape rates and source strengths and how they evolve. An analytical solution can be found if the hydrogen loss rate is a linear function of the total amount of hydrogen in the system,

$$\phi_1 = K[H]. \quad (8)$$

and both  $P_1$  and  $P_2$  are time independent. In that case,

$$[H] = [H_{ss}] + [H_0 - H_{ss}] e^{-Kt}, \quad (9)$$

$$[D] = [D_{ss}] + [D_0 - D_{ss}] e^{-fKt}, \quad (10)$$

where

$$[H_{ss}] = P_1/K = \phi_{1ss}/K, \quad (11)$$

with a similar definition for  $[D_{ss}]$ .  $[H_0]$  and  $[D_0]$  are the initial abundances. The ratio of (10) and (9) (Gurwell, 1995) gives



$$R(t) = \frac{R_0([H_0]/H_{ss}) e^{-t/\tau_H} + (R_s/f)(1 - e^{-t/\tau_H})}{([H_0]/[H_{ss}])e^{-t/\tau_H} + (1 - e^{-t/\tau_H})}. \quad (12)$$

where

$$\tau_H = H_{ss}/\phi_{ss}. \quad (13)$$

In a typical case a hydrogen inventory of  $8 \times 10^{22}$  atoms per  $\text{cm}^2$  is being evacuated at a rate of  $10^7$  atoms per  $\text{cm}^2\text{s}$  so that  $\tau_H$  is about 0.25 Gyr.  $R(t)$  is a function which increases with time to a maximum if  $R_s$  is small. It then decreases with time to a limit

$$R_{ss} = R_s/f. \quad (14)$$

This will be the approximate value of  $R$  in the extreme or "mature" steady state where neither  $[H]$  nor  $[D]$  is any longer varying appreciably with time.

$[H]$ , of course, reaches an approximate steady state long before  $[D]$  does. During the time when  $[H]$  is virtually in a steady state there is a useful approximation to (12), obtained by setting the denominator in (12) equal to unity, or setting

$$P = K[H] \quad (15)$$

$$\frac{d[H]}{dt} = 0 \quad (16)$$

$$[H] = [H_{ss}] \quad (17)$$

in (9). Then

$$R_1(t) = R_s/f + [r_0 R_0 - (R_s/f)] e^{-t/\tau_H} \quad (18)$$

where

$$r_0 = r(0, \infty) = [H_0]/[H_{ss}]. \quad (19)$$

This approximation has appeared several times in the literature with  $[H_{ss}]$  set equal to  $[H_0]$ . Sometimes this has not been appropriate, particularly in the late stages of Rayleigh fractionation of an early reservoir  $[H_0]$ , where the hydrogen escape flux and the hydrogen source strengths are approximately in balance and  $R_s$  very different from  $R_i(t)$ .

The behavior of  $R_i(t)$  in the approximation (18) is strongly dependent on  $r_0$ . Long after  $[H]$  has reached a virtual steady state,  $[D]$  can be much larger than  $[D_{ss}]$  and  $R_i$  very large



compared to  $R_s/f$ , its steady state limit. Thus, long after hydrogen has lost all memory of the original deuterium may retain it. The expression (18) seems to have appeared in the literature first in a paper dealing with oxygen fractionation on Mars (McElroy and Yung, 1976). The conditions specified in that paper were that loss of oxygen was balanced with its production from water at all times so that from the very beginning oxygen was in the steady state. Enrichment of  $^{18}\text{O}$  occurred because of a fractionation factor effectively determined by diffusive separation of  $^{16}\text{O}$  and  $^{18}\text{O}$  above the homopause. The counterpart of Eq. (18) was appropriate to that situation as it is to the application of Eq. (18) to hydrogen when water is taken always to be in a steady state between cometary impacts and escape of hydrogen (Grinspoon, 1987; Grinspoon and Lewis, 1988). But it was not to others in which its hydrogen analog with  $[\text{H}_0]$  set equal to  $[\text{H}_{ss}]$  has been applied to Martian and Cytherean hydrogen.

In (12) two characteristic times appear. One is the time constant associated with establishment of a steady state for hydrogen  $\tau_H$ , the other, for the establishment of a steady state for deuterium and, thus, for R is

$$\tau_D = \tau_H/f. \quad (20)$$

or 1.7 Gyr if  $f$  is 0.15 and  $\tau_H$  is 0.25 Gyr. In Figure 1  $R(t/\tau_H)$  is plotted for several values of  $r_0$  and  $f$ , with  $R_s = R_0 = 1.6 \times 10^{-4}$ . The approximation (18) fits the curves in Fig. 1 for  $R(t/\tau_H)$  well if  $t/\tau_H$  is greater than 15. In the case of Venus, with a hydrogen escape flux of  $10^7 \text{ cm}^{-2} \text{ s}^{-1}$  and  $\text{H}_{ss}$  equal to  $8.3 \times 10^{23} \text{ atoms cm}^{-2}$  (corresponding to 30 ppm of  $\text{H}_2\text{O}$ ),  $t/\tau$  would be 15 or larger for all times after 4 Gyr. In Figure 1 curves are also plotted for the case  $r_0 e^{-t/\tau_H} \gg (1 - e^{-t/\tau_H})$  corresponding to Rayleigh fractionation of a primitive ocean and  $r_0 = 1$ , which is a pure steady state. Practical application of these relationships to the atmosphere of Venus will be made in Section 6.

A useful approximation for  $r_0$  can be obtained by rearranging (12), setting  $R_s = R_0$  and  $\rho = R(t)/R_0$ , noting that in all practical cases

$$t/\tau_H > \frac{5.05}{1-f} \quad (21)$$

$$e^{-(t/\tau_H)} \ll 1 \quad (22)$$

and

$$\rho e^{-(t/\tau_H)} \ll e^{-f(t/\tau_H)} \quad (23)$$

for



$$t/\tau_H \geq 8 \quad (24)$$

and any reasonable value of  $f$ . Thus,

$$r_0 \equiv \rho e^{t/\tau_H} - (e^{t/\tau_H} - 1)/f. \quad (25)$$

In most cases,

$$r_0 \equiv (\rho - f^{-1})e^{t/\tau_H}, \quad (26)$$

since usually

$$e^{t/\tau_H} \gg 1. \quad (27)$$

$r_0$  is plotted in Fig. 2 along with the approximation (26) for a large range of fractionation factors and for  $\rho = 150$ . Such a large fractionation factor cannot be achieved at times

$$t < 5.05\tau_H/(1-f) \quad (28)$$

because Eq. (25) becomes singular at this time. But as  $t$  increases above the limit set by Eq. (16) the value of  $r_0$  required to achieve  $\rho$  equal to 150 in the presence of a source with  $R_s = 1.6 \times 10^{-4}$  decreases rapidly to a minimum. It then increases exponentially for values of  $t/\tau_H$  larger than 6 to 8 depending on  $f$ . For times much greater than  $\tau_H$ , large values of  $r_0$  are required if an enhancement of D/H as large as 150 is still realized after a long period of quasi-steady state between escape and a source of low  $R_s$ . It is most interesting that, for  $f \geq 0.02$ , an enhancement,  $R$ , of 150 cannot be obtained at any time unless  $r_0$  is larger than about 180. The signature of a massive loss of hydrogen will have persisted, no matter what the hydrogen steady state lifetime, if  $R$  is large.

On the other hand, if the planet never had a large amount of water exposed to its atmosphere and the sources always have been balanced with escaping hydrogen, so that  $r_0$  is identically unity,  $R(t)$  would have risen from  $R_s$  to  $R_s/f$  monotonically. An enrichment of 150 times  $r_0$  would have been attainable with a source  $R_s$  of  $1.6 \times 10^{-4}$  only if  $f$  is less than  $6.4 \times 10^{-3}$ .  $\tau_{ss}$  would then be 50 Gyr. If  $f$  is as large as 0.15,  $R_s$  would have to be  $3.75 \times 10^{-3}$ , 22 times  $r_0$ , to produce a steady state of 150 times  $R_0$  if  $R_0 = 1.6 \times 10^{-4}$ .

Unfortunately, it is not clear that the ideal case in which  $\phi_1$  varies linearly with  $[H]$  is often attained on any planet including Venus. One practical problem is that the tropospheric hydrogen may be mostly bound in condensables such as water vapor, which is prevented by a cold trap from passing freely through the tropopause. This is certainly the case on Earth, where stratospheric  $CH_4$  and  $H_2$  are the sources of much of the hydrogen above the tropopause. Only



if the  $\text{CH}_4$  and  $\text{H}_2$  abundances can be shown to vary linearly with the water vapor content of the troposphere will  $\phi_1$  be proportional to  $[\text{H}]$ . This discussion neglects the water in liquid form, which provides a source for atmospheric hydrogen that surely will balance escape until the oceans run dry.

On Venus the clouds constitute a barrier between the lower atmosphere and the upper atmosphere. The hydrogen mixing ratio is much less above them than it is below them. It remains to be determined how the mixing ratio in the upper atmosphere determining the escape flux, would be affected if the amount of water vapor in the lower atmosphere were very much -- say orders of magnitude -- larger than it is today.

In the case of Mars,  $\text{H}_2\text{O}$  is optically thick to the solar ultraviolet radiation which photolyzes it. Increasing the  $\text{H}_2\text{O}$  mixing ratio in the troposphere merely increases the altitude at which H is produced from  $\text{H}_2\text{O}$ . The consequence is that stratospheric H and  $\text{H}_2$ , which are generated by a complex of chemical reactions involving odd hydrogen and odd oxygen, change only slightly, even when  $\text{H}_2\text{O}$  changes by very large amounts. Consequently, the hydrogen escape flux changes non-linearly with the total amount of hydrogen below the diffusion bottleneck near the homopause.

#### **4. DIAGNOSTICS: REQUIRED**

The properties of the atmosphere to be determined if the problem of the evolution of water is to be addressed effectively include 1) the D/H ratio in water or some suitable substance such as atomic hydrogen, molecular hydrogen,  $\text{H}_2\text{S}$  or their ions, 2) the abundance of water and other hydrogen constituents of the mixed atmosphere, with their temporal and spatial variations, if any, understood and 3) the escape fluxes of hydrogen and deuterium suitably averaged globally, diurnally, and over the solar cycle. Also required, but more difficult to obtain, are the average rates for infection of H and D by comets and by outgassing of the interior. Thanks mostly to the Pioneer Venus mission and remote spectrographic sensing from Earth and the Galileo spacecraft, most of the items on the first of these shopping lists by this time have been acquired. It is also possible to set reasonable bounds to the rate at which comets inject water, and the D/H ratio for water on one comet, P. Halley, is now known with good precision (Balsinger *et al.*, 1995, Eberhardt *et al.*, 1995). Magellan has provided enough information about volcanism on Venus to allow speculation about the outgassing history of the planet to be at least informed.

#### **5. DIAGNOSTICS: MEASUREMENTS**

##### **A) D/H Ratio**

By this time the D/H ratio is one of the most thoroughly measured properties of the planet. These measurements, all concordant, fall into several classes.



- 1) Measurement of the HDO/H<sub>2</sub>O ratio in the clouds by mass spectroscopy;
- 2) measurement of the HDO/H<sub>2</sub>O ratio in the mixed atmosphere spectrographically from Earth;
- 3) measurements of the 1 amu and 2 amu ions in the ionosphere and the interpretation of the measurements in terms of ion chemistry;
- 4) calculation of the H and D densities in the upper atmosphere from measurements of H<sup>+</sup>, D<sup>+</sup>, O<sup>+</sup> and O densities at altitudes where these ions and neutrals are in a chemical steady state.

The first of these measurements was made by the neutral mass spectrometer (LNMS) on the Large Pioneer Venus Probe as the probe descended. In the clouds, between about 50 km and 25 km, the inlet leaks to the LNMS were sealed by sulfuric acid droplets. Very large signals in several mass channels near 18 amu and 19 amu appeared at this time. The spectrometer was then sampling H<sub>2</sub>O and HDO from the sulfuric acid drops. There were also greatly enhanced signals from CH<sub>3</sub>D and HD, apparently created by transfer of deuterium from Cytherean HDO to artifact CH<sub>4</sub> and H<sub>2</sub> in the LNMS (Donahue and Hodges, 1992). Taking account of all the D and H represented in HDO, CH<sub>3</sub>D, HD and H<sub>2</sub>O gave a D/H ratio of  $(2.5 \pm 0.5) \times 10^{-2}$  for Venus water,  $157 \pm 30$  times the D/H ratio in SMOW.

McElroy et al. (1982) first pointed out that the ion of mass 2 in the ionosphere could not be H<sub>2</sub><sup>+</sup> and must, therefore, be D<sup>+</sup>. They concluded that the measurements implied a hundredfold enrichment of deuterium in the atmosphere of Venus, measurement of the densities ions at 2 amu and 1 amu by the PVO ion mass spectrometer were analyzed with the help of data from the neutral mass spectrometer. The assumption was made on the one hand that the 2 amu species was H<sub>2</sub><sup>+</sup> and on the other hand that it was D<sup>+</sup>. The reactions removing H<sub>2</sub><sup>+</sup> and D<sup>+</sup> are quite different, the first being an ion molecule reaction with CO<sub>2</sub> forming CO<sub>2</sub>H<sup>+</sup> and H, and the second a charge exchange reaction with O forming O<sup>+</sup> and D. The alternatives lead to very different height profiles for the 2 amu ions. Clearly the D<sup>+</sup> option was favored. One set of analyses by Hartle and Taylor (1983) gave  $(2.2 \pm 0.6) \times 10^{-2}$  for the D/H ratio after extrapolation to the homopause. The other set by Kumar and Taylor (1984) gave  $1.4 \times 10^{-2}$  and  $2.5 \times 10^{-2}$  for the ratio when corrected for diffusive separation.

Neutral mass spectrometers have serious problems in measuring the density of neutral atomic hydrogen because of its extreme reactivity. Fortunately, the atomic hydrogen and deuterium densities in the lower thermosphere may be calculated from measurements of the densities of O<sup>+</sup>, H<sup>+</sup>, D<sup>+</sup> and O with ion and neutral mass spectrometers in the region where the lifetimes of these species for ion molecule reactions are short compared to diffusion times. Because the resonant reactions





and the H<sup>+</sup> removal reaction



determine the densities of H<sup>+</sup>, O and H; in this region the H density may be calculated from the relationship

$$n(\text{H}) = \{n(\text{H}^+)/n(\text{O}^+)\} \{k_{29}n(\text{O})(T_i/T)^{\frac{1}{2}} + k_{30}n(\text{CO}_2)\}, \quad (31)$$

where  $n$  are number densities,  $k_{29,30}$  are the reaction rate coefficient for reactions 29 and 30 and  $T_i$  and  $T$  are the ion and neutral temperatures (Brinton, et al., 1980). An analogous expression holds for  $n(\text{D})$ . The measurements of these quantities will be discussed in detail in section (5f). H and D densities were obtained in the night time bulge region of the thermosphere during the first three Cytherean years that PVO was in orbit and during its reentry during 1992. When extrapolated to the homopause the ratio of deuterium to hydrogen densities obtained was  $2.17 \times 10^{-2}$ . Considering the uncertainty introduced by the need to extrapolate the thermospheric ratios, the agreement among all these determinations must be considered excellent.

Near infrared spectral bands of H<sub>2</sub>O and HDO emitted deep in the atmosphere of Venus in a window near 2.3  $\mu\text{m}$  have been analyzed to determine the mixing ratios of H<sub>2</sub>O and HDO by two groups. One working from Mauna Kea (de Bergh *et al.*, 1991) analyzed their observations to derive a D/H ratio of  $(1.9 \pm 0.6) \times 10^{-2}$  ( $120 \pm 40$  times SMOW) in the mixed atmosphere. The other, observing from the Kuiper Observatory Aircraft (Bjoraker, 1992) obtained  $(2.5 \pm 0.3) \times 10^{-2}$  ( $157 \pm 18$  times SMOW).

All of these measurements are in good agreement with each other. The ionospheric measurement tends to be a little lower than those effectively obtained by observing the mixed atmosphere. This may be because of the need to extrapolate measured densities to the homopause in the case of the measurements made in the upper atmosphere. Because of the possibility of error in this procedure, we shall prefer the “tropospheric” measurements and use a value of  $2.4 \times 10^{-2}$  ( $150 \times \text{SMOW}$ ) in this chapter.

## B) Water Vapor Abundance

There is no shortage of measurements of the water vapor mixing ratio in the atmosphere of Venus. Unfortunately, they lack the concordance of the D/H measurement. The measurements reported before April, 1992 are recorded in Figure 3. Those obtained by gas chromatographs and humidity sensors on Venera 13 and 14 and the Pioneer Venus Large Probe are orders of magnitude higher than the rest. Given the difficulties with contamination confronting in situ measurements such as these and their gross disagreement with other measurements free of these



problems we regard these data as unreliable. Analysis of near infrared spectra of the day sky obtained by the Venera 11 and 12 spectrophotometer yields a mixing ratio that decreases monotonically from 200 ppm at 50 km to 20 ppm at the surface. This result is perplexing because such a profile has been obtained by no other instrument, including other infrared soundings on the nightside. Most of the near infrared soundings in the 1.7 and 2.3  $\mu\text{m}$   $\text{H}_2\text{O}$  bands radiated on the nightside of Venus and reported before 1992 gave results that clustered around 40 ppm from 50 km to low altitudes. There is one exception reported by Bell *et al.*, (1991) where one observation gave a mixing ratio of 200 ppm among others much lower. A large latitude dependence in water vapor was invoked to account for the variation of infrared net fluxes measured by the four Pioneer Venus entry probes (Revercomb *et al.*, 1985). These refer to heights above 40 km. The values shown in Fig. 3 decrease with latitude. The lowest are near  $60^\circ$ , the next near  $30^\circ$  and the very high measurement near the equator.

The LNMS data at 18 and 19 amu have been analyzed by Donahue and Hodges (1992 and 1993). Their results are plotted in Fig. 4. The mixing ratio obtained by fitting the  $\text{H}_2\text{O}$  counting rate profile to the counting rate profile for  $^{36}\text{Ar}$  was  $28^{+18}_{-5}$  ppm, between 10 and 26 km,  $6.3^{+4}_{-3}$  ppm at 51.3 km,  $4.2^{+3}_{-2}$  ppm at 55.3 km, and an apparent decrease below 10 km to  $7 \pm 3$  ppm at 0.9 km. These mixing ratios are normalized to the  $^{36}\text{Ar}$  abundances of 30 ppm obtained by the LNMS. The decrease in  $\text{H}_2\text{O}$  mixing ratio below 10 km may only be apparent. It is a consequence of a failure of the HDO counting rate, which is due mostly to Cytherean water, to rise below 10 km as rapidly as the  $^{36}\text{Ar}$  counting rate. The  $\text{H}_2\text{O}$  signal is dominated by the terrestrial contaminant and could easily mask a variety of profiles for Venus  $\text{H}_2\text{O}$ . It is quite possible that deuterium atoms are being transferred to the very abundant deuterium-poor methane in the mass spectrometer. If there is really a decrease in the  $\text{H}_2\text{O}$  mixing ratio, there should be another hydrogen compound created to take the place of water vapor. There is no evidence for a hydrogenic compound in the LNMS spectrum into which the  $\text{H}_2\text{O}$  has been transformed by a gas phase reaction. At no mass channel belonging to a candidate reaction product can there be found evidence for a count rate sufficiently large at 0.9 km to make up the deficiency in  $\text{H}_2\text{O}$  there and which then decreases to zero at 10 km.

Since 1992 the near-infrared spectra of emissions from the dark side of Venus, obtained by Crisp *et al.*, (1991) and Bezard *et al.*, (1990), have been simulated by Pollack *et al.*, (1993). These data are fit best by a water vapor mixing ratio that is constant at  $30 \pm 10$  ppm from 40 km to about 10 km, but may decrease between 10 km and the surface. The case for the decrease below 10 km is by no means robust. The profile obtained by the LNMS (Fig. 4) well represents their reconstruction. High-resolution spectra obtained by Bezard *et al.*, (1991) and deBergh *et al.*, (1992) in the 1.18  $\mu\text{m}$ , 1.7  $\mu\text{m}$  and 2.3  $\mu\text{m}$  windows are also well fit by a constant mixing ratio profile of  $30 \pm 15$  ppm. Galileo NIMS measurements also gave  $30 \pm 15$  ppm with no



horizontal variations exceeding 20% over a wide latitude range (Drossart *et al.*, 1993). Water vapor measurements are also discussed by Esposito *et al.* (this book).

### C) Methane and H<sub>2</sub>

The PVLNMS registered very large signals at 2, 3, 15, 16 and 17 amu (Donahue and Hodges, 1993). All of the 2 and 3 amu detected can be accounted for by terrestrial H<sub>2</sub> emanating from instrument surfaces, probably in the getter pumps and, except when the leaks were plugged, from H<sub>2</sub><sup>+</sup> produced in the ion source by electron bombardment of CH<sub>4</sub>. A contribution of H<sub>2</sub> from the Venus atmosphere with an appropriately high HD/H<sub>2</sub> ratio associated with more than about 2 ppm of H<sub>2</sub> can be excluded, and the data are consistent with no H<sub>2</sub> at all. The CH<sub>4</sub>, in addition to that introduced into the LNMS deliberately to help in mass peak deconvolution, can be accounted for by methanation, probably occurring on getter surfaces and involving instrumental H<sub>2</sub> and CO from the atmosphere. Thus, this CH<sub>4</sub> component mimics an atmospheric gas (Donahue and Hodges, 1993). The feature at 17 amu, except when the leaks were plugged, and below 10 km, appears to consist of a mixture of <sup>13</sup>CH<sub>4</sub>, and CH<sub>3</sub><sup>+</sup> generated in the ion source by an ion-molecule reaction involving CH<sub>3</sub><sup>+</sup> and CH<sub>4</sub>.

### D) Hydrogen in the thermosphere: Lyman- $\alpha$ Scattering

Ultraviolet Spectrometer (OUVS) (Lyman- $\alpha$  spectra from 20 orbits spanning the first three Venus years have been analyzed by Paxton *et al.* (1988). By fitting emission rates to theoretical models for resonantly scattered solar Lyman- $\alpha$  they have determined the atomic hydrogen number density and vertical flux at the base of the exosphere (200 km). Both remained remarkably constant at  $(6.0 \pm 1.5) \times 10^4 \text{ cm}^{-3}$  and  $(7.5 \pm 1.5) \times 10^7 \text{ cm}^{-2} \text{ s}^{-1}$  in the subsolar region as solar activity varied. The integrated vertical column of hydrogen above 110 km was found to be  $(3.6 \pm 1) \times 10^{13} \text{ cm}^{-2}$ . Recently, reanalysis of these measurements by Hartle *et al.* (1995) has revised these values to  $(7.5 \pm 2) \times 10^4 \text{ cm}^{-3}$  at 200 km and  $(2.9 \pm 0.6) \times 10^7 \text{ cm}^{-2} \text{ s}^{-1}$ . The large flux in a region where the escape flux is much smaller than  $10^7 \text{ cm}^{-2} \text{ s}^{-1}$ , supplies lateral flow of hydrogen to the nightside, where the hydrogen eventually escapes to space or descends below 100 km and returns to the dayside. Light atoms participate in the planetary-wide circulation of winds to the nightside in the thermosphere and back to the dayside in the middle atmosphere. Consequently, the densities of the light species H, D and H<sub>2</sub> display a prominent bulge in the post-midnight sector of the nighttime hemisphere. The circulation of the high mass major atmospheric species is divergence-free. Because of their much greater scale height, this results in a net loss of light gases on the dayside in the thermosphere and a net gain on the nightside. The consequent nightside bulge in abundance is shifted into the dawn sector by the superrotation



of the atmosphere. For further discussion of the effects of superrotation in the upper atmosphere is contained in the chapter by Bougher *et al* (this book).

### **E) Escape of Hydrogen and Deuterium**

Until recently, two processes were thought to make important contribution to hydrogen escape. Exospheric temperatures are only 300 K on the dayside and 123 K on the nightside. At such temperatures, the planet-wide average Jeans escape flux is about  $5 \times 10^5 \text{ cm}^{-2} \text{ s}^{-1}$ , utterly negligible compared to non-thermal loss processes. Collision of energetic oxygen atoms produced by dissociative recombination of  $\text{O}_2^+$  ions with thermal hydrogen was once considered a major source, contributing a planet-wide average flux of  $1.2 \times 10^6 \text{ cm}^{-2} \text{ s}^{-1}$ , with zero fractionation factor (Rodriguez *et al.*, 1984) or  $3.5 \times 10^7 \text{ cm}^{-2} \text{ s}^{-1}$  with a large fractionation factor of 0.31 according to Gurwell and Yung (1992). However, Hodges (1993) has pointed out that these calculations neglected the effect of collisions by the initially hot atoms with thermal oxygen that degrade their velocities before they can collide with hydrogen in the exosphere. After the effect of these collisions has been accounted for, the hydrogen loss rate following such collisions is reduced to insignificance, compared to the dominant processes involving hydrogen ions. The first of these is charge exchange in the exosphere between  $\text{H}^+$  ions with greater escape velocity in the tail of the hot ion distribution and thermal hydrogen atoms. Two calculation of the loss rate due to these collisions gave discordant results. Most of the loss occurs in the 20% of the exosphere comprising the bulge on the nightside. The Monte Carlo model of Hodges and Tinsley (1986) predicted a planet-wide average loss rate of  $2.8 \times 10^7 \text{ cm}^{-2} \text{ s}^{-1}$  for this process. A treatment by Rodriguez *et al.*, (1984) gave  $3.2 \times 10^6 \text{ cm}^{-2} \text{ s}^{-1}$ . Donahue and Hartle (1992) have criticized both models for using unrealistic H and  $\text{H}^+$  distributions. They also pointed out that the calculations consider only solar maximum conditions whereas  $\text{H}^+$  ion densities are reduced to at most 0.15 their solar maximum values during solar minimum (Figure 5). When solar activity is high the ionopause is far from the planet.  $\text{O}^+$  ions created in the daytime ionosphere are transported in great numbers to the nightside, where they create  $\text{H}^+$  ions in the bulge region by charge transfer collisions with neutral hydrogen. As solar activity decreases the density of ions in the ionosphere decreases and the ionopause closes in. Transport of  $\text{O}^+$  to the nightside is reduced and production of  $\text{H}^+$  with the bulge consequently decreases considerably. Another theoretical effort to recalculate the charge exchange loss rate using the densities measured by PVO for a complete range of solar activity is required. In the meanwhile, Donahue and Hartle (1992) recommend a rate of  $9 \times 10^6 \text{ cm}^{-2} \text{ s}^{-1}$  for the planet-wide average escape flux during Solar Maximum. This recommendation is based on an estimate of the effect of adjusting the properties of the two exospheric models in question to realistic ones. Deuterium also is lost by charge



exchange. The fractionation factor for the process has been estimated to be 0.02 (Krasnopol'sky, 1985).

Recently, another important escape mechanism for light ions has been identified. It is the analog of the terrestrial polar wind in which light ions are accelerated to escape velocity in the charge separation electric field that maintains the major ions and electrons of the ionosphere in a stable vertical distribution despite their mass difference. Hartle and Grebowsky (1993, 1995) have shown that hydrogen and deuterium ions are flowing upward in these fields with more than enough velocity to escape. The outward flux of  $H^+$  in the bulge during solar maximum is  $7.5 \times 10^7 \text{ cm}^{-2} \text{ s}^{-1}$ , for this mechanism (E) giving a planet-wide average flux of  $H^+$  during solar maximum of  $1.5 \times 10^7 \text{ cm}^{-2} \text{ s}^{-1}$ . The  $D^+$  planet-wide rate was measured to be  $5.6 \times 10^4 \text{ cm}^{-2} \text{ s}^{-1}$ . The fractionation factor for the process is, thus, 0.15.

These escape fluxes will vary with solar activity. During the reentry phase of PVO in the fall of 1992 the 10.7 cm radio flux was at a level of  $125 \times 10^{22} \text{ W cm}^{-2} \text{ Hz}^{-1}$ . In 1978 and 1979 when the orbiter was exploring the solar-maximum, the 11.7 cm flux was between 200 and  $250 \times 10^{22} \text{ W cm}^{-2} \text{ Hz}^{-1}$  (Figure 6). Since the  $H^+$  ion densities in 1992 were reduced by a factor of 0.15 and the electric field loss is proportional to the ion densities, the planet-wide average (E) flux of  $H^+$  was reduced to  $2.3 \times 10^6 \text{ cm}^{-2} \text{ s}^{-1}$ .  $f$  remained at 0.15. Thus, the solar cycle average electric field driven flux  $\phi_{IE}$  is  $9 \times 10^6 \text{ cm}^{-2} \text{ s}^{-1}$  with a fractionation factor of 0.15. Because the charge exchange loss rate (CE) is proportional to the product of the ion and neutral densities it should be reduced from  $9 \times 10^6 \text{ cm}^{-2} \text{ s}^{-1}$  to only  $7 \times 10^6 \text{ cm}^{-2} \text{ s}^{-1}$  in 1992. If the electric field escape flux and the charge exchange flux are additive and independent, the solar maximum planet-wide hydrogen escape flux (E + CE) would be  $2.4 \times 10^7 \text{ cm}^{-2} \text{ s}^{-1}$  with a fractionation factor of 0.10. The low solar activity flux (E + CE) in 1992 would be  $8.9 \times 10^6 \text{ cm}^{-2} \text{ s}^{-1}$  with  $f$  equal to 0.06. The solar cycle average escape flux would be 0.9 and  $0.8 \times 10^7 \text{ cm}^{-2} \text{ s}^{-1}$  for the (E) and (CE) respectively making the solar cycle average flux (EC + CE)  $1.7 \times 10^7 \text{ cm}^{-2} \text{ s}^{-1}$  and 0.1 the effective fractionation factor. These measured and estimated fluxes are listed in Table 1.

#### **F) Transition from Solar Maximum to Solar Minimum: Flux Calculations**

The Pioneer Venus Orbiter reentered the atmosphere in the autumn of 1992. As it did so its instruments, including the neutral and ion mass spectrometer, determined ion and neutral densities in the nighttime ionosphere. As solar activity declined the hydrogen escape flow out of the bulge diminished, but the horizontal inflow from the dayside hemisphere continued undiminished. Consequently, the hydrogen and deuterium content of the bulge grew until the downward flux had increased sufficiently to balance the inflow. The densities of hydrogen and deuterium during the first three years of the mission and in 1992 have been calculated from the orbiter data following the technique discussed (Hartle *et al.*, 1996) and in Section 5a. The results



are shown in Fig. 7 and 8. The average hydrogen density in the bulge increased by a factor of 6.7 and that of deuterium by a factor of 4. That this increase is due to the reduced escape flux and not to a change in the circulation from the night to daytime hemispheres suggested by the smaller deuterium effect and the absence of any modulation for helium (Fig. 8). (In Fig. 9 we show the thermospheric D/H ratios during the four years for which data are available. These are the basis for the discussion in Section 5a.)

The number of hydrogen atoms in the thermosphere and exosphere  $\psi$  is governed by the simple relationship

$$\frac{d\psi}{dt} = \varphi_s A / 2 - (\varphi_D + \varphi_e) A_B \quad (32)$$

where  $\varphi_s$  is the upward flux into the thermosphere on the dayside (area  $A/2$ ),  $\varphi_D$  is the return flux into the mesosphere at the base of the bulge (area  $A_B$ , which is about 20% of the planetary area  $A$ ), and  $\varphi_e$  is the escape flux from the bulge. It is possible to calculate the escape flux  $\Phi_e$  during solar maximum and  $\phi_e$  from the bulge during solar minimum in the steady state when  $d\psi/dt \equiv 0$  in (30).

$$2.5\Phi_s = \Phi_D + \Phi_1, \quad (33a)$$

$$2.5\phi_s = \phi_D + \phi_1. \quad (33b)$$

$\Phi_D$  and  $\phi_D$  are proportional to the density in the bulge during solar maximum and solar minimum respectively, therefore

$$\Phi_D = 0.15\phi_D \quad (34)$$

As was noted in 5A,  $\Phi_s$  is known from PVUUVS data (Paxton et al., 1987), as revisited by Hartle et al. (1996), to be  $2.9 \times 10^7 \text{ cm}^{-2} \text{ s}^{-1}$ . Unfortunately the same is not true of  $\phi_s$ , but there is no apparent reason that atmospheric circulation which is responsible for the flow of hydrogen should depend on solar activity. Thus, it is probably safe to assume that  $\phi_s$  and  $\Phi_s$  are the same. In any event diffusion limitation prevents  $\phi_s$  from exceeding 1.5



where  $\epsilon$  is the appropriate ratio  $\phi_1 / \Phi_1$ . In Table 1 the escape fluxes called for by this relationship are contained with the measured electric field flux and estimated charge exchange flux discussed in Section 5E.

Table 1				
$\Phi_1$ in $10^7 \text{ cm}^{-2} \text{ s}^{-1}$				
Process	$\epsilon$	Eq 33	Section 5E	$\langle \bar{\phi}_e \rangle$
E	0.15	6.3-5.7	7.5	0.9
<del>E</del> CD	0.73	7-6.3	4.5	0.8
E + CE	0.37	6.6-5.9	12	1.7

Even <sup>after</sup> paying due respect to all the uncertainties in the measurements on which these estimates are based, the electric field escape process alone appears to give reasonable agreement between the measured observed value and the one that explains the solar cycle variations in bulge densities. It is difficult to reconcile a very large contribution from  $\text{H}^+$ , H charge exchange with these results. In any event a very small planetary average flux of about  $1.5 \times 10^7 \text{ cm}^{-2} \text{ s}^{-1}$  during solar maximum and  $2 \times 10^6 \text{ cm}^{-2} \text{ s}^{-1}$  during times of low solar activity ~~in minimum~~ is indicated.

The effective H and D escape fluxes  $\langle \bar{\phi} \rangle$  resulting from this analysis of the bulge are also tabulated in Table 2. The "synthesis" flux in the table captures both the measured E flux and the flux determined from bulge properties in the case of hydrogen.  $\epsilon$  is assumed to be 0.15. No such synthesis is possible for deuterium.



Table 2					
$\langle \bar{\phi}_1 \rangle$ Hydrogen in $10^7 \text{ cm}^{-2} \text{ s}^{-1}$					
	E	CE	E + CE	Bulge	Synthesis
	0.15	0.73	0.37	0.15	0.15
$\langle \bar{\phi}_1 \rangle$	$0.9 \pm 0.1$	0.8	1.6	0.6-0.75	$0.8 \pm 0.2$
f	0.15	0.02	0.10	0.44	0.15-0.44
$\langle \bar{\phi}_2 \rangle$ Deuterium in $10^4 \text{ cm}^{-2} \text{ s}^{-1}$					
$\langle \bar{\phi}_2 \rangle$	$3.2 \pm 0.6$	0.5	3.7	8-10	NA

A similar analysis for deuterium calls for a solar maximum steady state flux, of about  $1.4 - 1.7 \times 10^5 \text{ cm}^{-2} \text{ s}^{-1}$  planet wide, ( $8 - 10 \times 10^4 \text{ cm}^{-2} \text{ s}^{-1}$  solar cycle average) with only electric field acceleration important. Combined, these fluxes result in a very large fractionation factor of 0.44. It is difficult to conceive of a loss mechanism so highly fractionating in the modern atmosphere of Venus. The "observed" loss rate for deuterium ions (Hartle and Grebowsky, 1993) was only one third as large --  $5.6 \times 10^4 \text{ cm}^{-2} \text{ s}^{-1}$ . This discrepancy could be removed if  $\Phi_e$  for deuterium were reduced by a factor of about 3, which can be accomplished only by reducing D/H to about  $1.0 \times 10^{-2}$ , given the observed density at 220 km during solar maximum Years 1, 2 and 3. This would be an unacceptably large correction in the HDO / H<sub>2</sub>O ratio.

## 6. EVOLUTION OF WATER

We shall first consider two cases based on the fluxes discussed in Section 5E. In one the measured charge exchange flux will be added to the electric field flux. In the other it will not. In the first case, the average escape flux is  $1.7 \times 10^7 \text{ cm}^{-2} \text{ s}^{-1}$  with a fractionation factor of 0.10. In the second, it is  $(9 \pm 1.0) \times 10^6 \text{ cm}^{-2} \text{ s}^{-1}$  and f is 0.15. If the present hydrogen abundance [H] is set by the 30 ppm of water vapor in the lower atmosphere, the characteristic time required to establish a steady state in hydrogen is

$$\tau_H = (160 - 300) \text{ Myr.} \quad (36)$$



$\tau_D$ , to establish a steady state in deuterium and in R, becomes

$$\tau_D = (1.6 - 2.1) \text{ Gyr.} \quad (37)$$

Finally, the relationship of  $R_{ss}$  to  $R_s$  is

$$R_{ss} = (6.7 - 10) R_s. \quad (38)$$

Such large values of  $f$  do not allow a highly differentiated "mature" steady state if the source is not rich in deuterium.

One end member scenario for evolutions of water on Venus has the hydrogen and deuterium today as remnants of an early larger supply of water. In the case of Rayleigh fractionation, the factor  $r$  in equation (6) for  $[H_2O]/[H]$  is either 262 or 363, depending on choice of  $f$ . Originally the water on Venus would have been between 3.9 and 5.4 meters deep if spread uniformly over the planet's surface as a liquid. This is between 0.12 and 0.17 percent of a full terrestrial ocean (fto). The mixing ratio of this water in the vapor phase would have been between 1.0 and 1.4 percent if Venus then had the same dense atmosphere it has now. According to Watson *et al.*, (1982), vigorous hydrodynamic escape or "blowoff" of hydrogen, driven by solar extreme ultraviolet radiation (euv) heating, would have occurred if the mixing ratio of  $H_2$  in the upper atmosphere exceeded 2 percent. Because euv from the early sun was almost surely enhanced, this coincidence led Donahue *et al.*, (1982) to suggest that Venus may have started with the equivalent of a full terrestrial ocean, either in steam or liquid form. Blowoff, for which the fractionation factor was close to zero, would have exhausted all but a trace of this water in 280 Myr, without changing the D/H ratio appreciably. This concept was elaborated by Kasting and Pollack (1983) and Kasting, *et al.* (1984) who calculated the blowoff escape rate that would have been reached in a runaway greenhouse induced when Venus developed an atmosphere in which an ocean had been converted to steam. They assumed a radiatively equilibrated atmosphere in which there were 90 bars of  $CO_2$  and showed that before the sun reached its present luminosity, surface temperatures on Venus would become so high that all the water in an ocean would have been converted to steam with a surface pressure of 270 bars. Blowoff would then follow. This model was superseded by one in which the effect of convection and condensation was taken into account. Initial conditions called for a surface pressure of 1 Bar of an  $N_2$ ,  $O_2$  mixture, one bar of  $H_2O$  and a ocean, liquid because the moist convection left the surface temperature below  $100^\circ C$ .  $CO_2$  was presumed to be converted to carbonate as on Earth. The stratosphere was wet in this "moist greenhouse". Hydrogen was rapidly lost as in the "runaway greenhouse". A cold trap developed only after nearly all of the water was lost, because of the low pressure of the non-condensable gases. Thus, a serious defect of the previous model, in which the development of a



cold trap in the presence of 90 bars of CO<sub>2</sub> stopped blowoff with 20 bars of water left was avoided. In both models, atomic oxygen was presumed to have been lost, swept along in the flood of rapidly flowing hydrogen, and also oxidizing the crust. After the blowoff stopped, the remaining oxygen could have been reduced to its present insignificant level by reaction with CO. This gas should have accompanied outgassing CO<sub>2</sub> in a much larger relative abundance than prevails today. After the water had gone, no medium in which carbonate could form would have remained, and CO<sub>2</sub> would have accumulated in the atmosphere to its present level.

As was discussed in Section 2, the simple Rayleigh fractionation relationship (6) cannot be used to determine the initial hydrogen inventory if hydrogen is in or near a steady state, that is, if  $P_1 \equiv \phi_1$  and  $d[H]/dt \equiv 0$ . It is not the amount of hydrogen remaining in the atmosphere  $[H]$  that is decisive in establishing this situation. It is the size of  $\phi_1$  compared to  $P_1$ . The fact that  $\phi_1$  is so small makes the possibility that it is balanced by a source of hydrogen, particularly from comets, very great (Grinspoon, 1987; Grinspoon and Lewis, 1988). The Venus D/H ratio is much larger than it would be if there were a mature steady state between escape and a source of incoming cometary water. The D/H ratio in Comet P. Halley is  $3.16 \times 10^{-4}$  (Balsinger, *et al.*, 1995; Eberhardt, *et al.*, 1995). So, if  $f$  is 0.15, the steady state D/H ratio on Venus when cometary water having such a D/H ratio is injected, becomes  $2 \times 10^{-3}$  – less than a tenth of its present value. As Gurwell has pointed out, if there is a source with  $R_s$  equal to  $1.6 \times 10^{-4}$ , balancing escape of H, a ratio  $\rho$  of 150 today, when  $t/\tau_H$  is between 14.5 and 28 can be attained only if  $r_0$  is between 1300 and 2300 (Figures 1 and 2). Thus, even more early water would be needed than if the cometary source were absent. 19.5 to 34.5 meters of water, 5 to 6.3 times as much as needed in the case of simple Rayleigh fractionation, would be required. On the other hand, an outgassing source, such as suggested by Grinspoon (1993) involving a very depleted mantle, would be sufficient to balance the current escape flux. The challenge is to demonstrate how it can be sufficiently fractionated.

A similar analysis based on the fluxes deduced in Section 5H –  $\langle \bar{\phi}_1 \rangle \equiv 7.5 \times 10^6 \text{ cm}^{-2} \text{ s}^{-1}$ ,  $f = 0.44$  – calls for the ratio of the primeval reservoir to the present one,  $r$  in Eq. 6, to be very large -- 7700, if there are no sources. This would require 115 meters of water, 3.5 percent of a terrestrial ocean. In the case of a hydrogen steady state based on Eq. (25), with  $\tau/\tau_H$  equal to 12.5,  $r$  becomes  $3.5 \times 10^4$ . The required early reservoir would grow to 520 m of water, 16% of a full terrestrial ocean.  $\tau_{ss}$  would be only 830 Myr, but the  $R_s$  required for a steady state with  $R = 2.4 \times 10^{-2}$  would grow to  $1.1 \times 10^{-3}$ . (Some quantities determined here differ slightly from those quoted by Hartle et al. (1990) because it is assumed to be 150 in this chapter but 157 in that paper).

In fact, the influx of cometary water on Venus probably fails to balance the loss of hydrogen to space by about an order of magnitude. Shoemaker and colleagues (Shoemaker and Wolfe,



1982, Shoemaker et al. 1990) estimate the fluence of active cometary mass on Earth, and consequently also Venus, <sup>at</sup>  $5 \times 10^{17}$  gm/yr for the past 100 Myr and  $1.6 \times 10^{17}$  gm/yr for the past Gyr. Shoemaker et al (1994) also argue that the flux of extinct periodic comets may be comparable to the flux of active comets. If so and if 30% of the cometary mass is water, the effective or average source of cometary water  $P_1$  on Venus is presently between 0.7 and  $1.4 \times 10^6 \text{ cm}^{-2} \text{ s}^{-1}$ . The average value of  $P_1$  over the past billion years would have been a factor of 3 larger. If the hydrogen source from comets is that small the estimates of  $H_0/H$  from Eq(12), based on steady state assumptions, are too large. Those based on simple Rayleigh fractionation (Eq6) should be valid unless they are important endogenous sources of highly fractionated water, such as those Grinspoon (1993), has discussed. A constant ratio  $K$  between the escape flux  $\phi_1$  and the hydrogen burden of the atmosphere  $H$ , now in the neighborhood of  $0.3 \text{ Gyr}^{-1}$  is obviously incompatible with an amplification factor  $H_0/H$  of approximately 400 given by Eq(6). To obtain such a "small" loss of hydrogen,  $\tau_H$  must be about 0.75 Gyr. Alternatively, the present state of the atmosphere would need to be very close to a steady state

$$H_{ss} = 0.9996H \quad (39)$$

This would require that

$$P_1 = 0.9996 \phi_1 \quad (40)$$

It is much easier to accommodate a constant value of  $\tau_H$  to obtain the amplification ratio  $H_0/H$  of 7700 called for by the Rayleigh fractionation relationship (6) if  $f$  is as large as 0.44:

$$\left(1 - \frac{P_1}{\phi_1}\right) = 7700^{-\frac{\phi_{11}}{H}} \approx \phi_1^{\tau_H} \quad (41)$$

This condition would be satisfied if  $\phi_1$  is  $7.2 \times 10^6$ , as given by the bulge study,  $P_1$  is  $1.4 \times 10^6 \text{ cm}^{-2} \text{ s}^{-1}$  and the mixing ratio of water vapor is 40ppm instead of 30ppm. Alternatively, for example, it can be satisfied with 30ppm of water vapor,  $\phi_1 = 5.5 \times 10^6 \text{ cm}^{-2} \text{ s}^{-1}$  and  $P_1 = 1.5 \times 10^6 \text{ cm}^{-2} \text{ s}^{-1}$ .

Proposals for rather different scenarios have been made by Grinspoon (1987, 1993) and Grinspoon and Lewis (1988). These generally have involved comets or outgassing of the interior, as a consequence of volcanism or massive resurfacing events, as sources of hydrogen. Given the large fractionation factor that now appears to characterize escape of hydrogen and deuterium, it is not possible for planetary escape to approach a mature steady state in which  $R$  is as large as it is today if cometary sources of water are as poor in deuterium as Comet Halley or terrestrial water. The required value of  $R_0$  is too large. Grinspoon (1993) has proposed as



steady state candidates two examples of possible mantle sources. In one case, the outgassing water would be fractionated to within an order of magnitude of the present atmospheric value of  $R$ , the outgassing rates and hydrogen loss rates would be balanced and  $R$  close to its steady state value. Grinspoon proposed that the mantle of Venus may have attained its enhanced  $R$ , because of fractionation in the creation of a severely depleted mantle, or because of retention of the large  $D/H$  signature in water frozen into the mantle after the planet had undergone an early period of highly fractionating loss of hydrogen. Alternatively, Grinspoon suggests that a massive resurfacing event within the past billion years released water from the interior. The atmosphere was then supposed to have experienced rapid loss of hydrogen in which  $R$  was enhanced to a value even higher than it has today. Subsequent loss of hydrogen would then have caused  $R$  to decrease to its present value as it declines toward a steady state in both  $D$  and  $H$ . The suggested evolution of  $R$  for these examples is shown in Figure 10 (Grinspoon, 1993). Note that the  $D/H$  range in this figure is based on the measurement of deBergh, *et al.* (1991), which is centered at 120 times terrestrial, rather than 150 times terrestrial.

## 7. OUTSTANDING PROBLEMS

The present hydrogen inventory of Venus and the  $D/H$  ratio seem to be well understood, although there are some observations which make it out to be much wetter than it usually seems to be. Recalculation of charge exchange loss rates, which are based on our present understanding of the temporal history of Venus neutral and ionized hydrogen densities and their variation with solar activity, are needed. The type of calculation once performed by Kumar, *et al.* (1983) to determine the evolution of hydrogen and deuterium loss mechanisms over the 4.5 Gyr history of the planet but based on our present understanding of loss mechanisms, such as the electric field process, needs to be repeated. In view of the long time required for deuterium to reach a steady state, it would be instructive to investigate the effect on the present  $D/H$  ratio and water abundance of including the contribution of the remnants of a primitive "ocean" 10 meters deep on "steady state" degassing models, such as those proposed by Grinspoon (1993). Models of catastrophic mantle outgassing as sources of today's highly fractionated water vapor need to be bolstered with more robust and detailed foundations than those with which they are currently provided. It would be useful to have a study of the Venus thermosphere and mesosphere that continuously spans a complete solar cycle.



## REFERENCES

- Balsinger, H., Altwegg, K., and Geiss, J. 1995. D/H and  $^{18}\text{O}/^{16}\text{O}$  ratio in the hydronium ion and in neutral water from in situ ion measurements in comet Halley. *J. Geophys. Res.* 100:5827-5834.
- Bell, J.F., III, Crisp, D., Lucey, P.G., Ozorowski, T.A., Sinton, W.M., Willis, S.C., and Campbell, B.A. 1991. Spectroscopic observations of bright and dark emission features on the night side of Venus. *Science* 252:1293-1296.
- Bézard, B., de Bergh, C., Crisp, D., and Maillard, J.-P., 1990. The deep atmosphere of Venus revealed by high-resolution night-side spectra. *Nature* 345:508-511.
- Bézard, B., deBergh, C., Maillard, P., Crisp, D., Pollack, J., and Grinspoon, D. 1991. High resolution spectroscopy of Venus' nightside in the 2.3, 1.7, and 1.1-1.3 $\mu\text{m}$  windows. *Bull.Amer.Astron.Soc.*, 23:1192.
- Bougher, S., et al (this book)
- Bjoraker, G.L., Larson, H.P., Mumma, M.J., Timmerman, R., and Montani, J.L. 1992. Airborne observations of the gas composition of Venus above the cloud tops: measurements of  $\text{H}_2\text{O}$ , HDO, HF and the D/H and  $^{18}\text{O}/^{16}\text{O}$  isotopic ratios. *Bull. Am. Astronom. Soc.* 24:995.
- Brinton, H.C., Taylor, Jr., H.A., Niemann, H.B., Mayr, H.G., Nagy, A.G., Cravens, T.E., and Strobel, D.F. 1980. Venus Nighttime Hydrogen Bulge. *Geophys. Res. Letters* 7:865.
- Carlson, R.W., et al. 1991. Galileo infrared imaging spectroscopy measurements at Venus. *Science* 253:1541-1548.
- Crisp, D., Allen, D.A., Grinspoon, D.H., and Pollack, J.B. 1991a. The dark side of Venus: Near-infrared images and spectra from the Anglo-Australian Observatory. *Science* 253:1263-1266.
- Crisp, D., McMuldrock, S., Stephens, S.K., Sinton, W.M., Ragent, B., Hodapp, K.-W., Probst, R.G., Doyle, L.R., Allen, D.A., and Elias, J. 1991b. Ground based near-infrared observations of Venus during the Galileo encounter. *Science* 253:1538-1541.
- de Bergh, C., Bézard, D., Crisp, J., Maillard, P., Owen, T., Pollack, J., and Grinspoon, D. The  $\text{H}_2\text{O}$  abundance in the deep atmosphere of Venus from near-infrared spectroscopy of the night side. *World Space Congress*, Aug.28-Sept 5, 1992, Washington, D.C.
- de Bergh, C., Bézard, B., Owen, T., Crisp, D., Maillard, J.-P., and Lutz, B.L. 1991. Deuterium on Venus: Observations from Earth. *Science* 251:547-549.
- Donahue, T.M., and Hartle, R.E. 1992. Solar Cycle Variation in Venus  $\text{H}^+$  and  $\text{D}^+$  Densities in the Venus Ionosphere: Implications for Escape. *Geophys. Res. Lett.* 19:2449-2452.



- Donahue, T.M., and Hodges, Jr., R.R. 1993. Venus Methane and Water. *Geophys. Res. Lett.* 20:591-594.
- Donahue, T.M., and Hodges, Jr., R.R. 1992. Past and Present Water Budget of Venus. *J. Geophys. Res.* 97:6083-6091.
- Donahue, T.M., Hoffman, J.H., Hodges, Jr., R.R., and Watson, A.J. 1982. Venus was wet: A measurement of the ratio of deuterium to hydrogen. *Science* 216:630-633.
- Drossart, P., Bezard, B., Encrenaz, Th., Lellouch, E., Roos, M., Taylor, F.W., Collard, A.D., Pollack, J., Grinspoon, D.H., Carlson, R.W., Baines, K., and Kamp, L.W. 1993. Search for spatial variations in the H<sub>2</sub>O abundance in the lower atmosphere of Venus from NIMS-Galileo. *Planet. Space Sci.* 41:495-504.
- Eberhardt, P., Reber, M., Krankowsky, D., and Hodges, Jr., R.R. 1995. The D/H and <sup>18</sup>O/<sup>16</sup>O ratios in water from comet P/Halley. *Astron. and Astrophys.* ???-??.
- Esposito, L.W., et al. (this book)
- Grinspoon, D.H. 1987. Was Venus wet? Deuterium reconsidered. *Science* 238:1702-1704.
- Grinspoon, D.H. 1993. Evolutionary implications of a steady state water abundance on Venus. *Nature* 363:1702-1704.
- Grinspoon, D.H., and Lewis, J.S. 1988. Cometary water on Venus: Implication of stochastic impacts. *Icarus* 74:21-35.
- Gurwell, M.A. 1995. Evolution of deuterium on Venus. *Nature* 378:22-23.
- Gurwell, M.A., and Yung, Y.L. 1992. Fractionation of hydrogen and deuterium on Venus due to collisional ejection. *Planet. Space Sci.* 40:1620-1628.
- Hartle, R.E., Donahue, T.M., Grebowsky, J.M., and Mayr, H.G. 1995. Hydrogen and deuterium in the thermosphere of Venus: solar cycle variations and escape. *J. Geophys. Res.* 101:??-??.
- Hartle, R.E., and Grebowsky, J.M. 1995. Planetary loss from light ion escape on Venus. *Advances in Space Research* 15:4(117)-(4)122.
- Hartle, R.E., and Grebowsky, J.M. 1993. Light ion flow in the nightside ionosphere of Venus. *J. Geophys. Res.* 98:7437-7445.
- Hartle, R.E., and Taylor, Jr., H.A. 1983. Identification of deuterium ions in the ionosphere of Venus. *Geophys. Res. Lett.* 10:965-968.
- Hodges, R.R., Jr. 1993. Isotopic fractionation of hydrogen in planetary exospheres due to ionosphere-exosphere coupling: implications for Venus. *J. Geophys. Res.* 98:10833-10838.
- Hodges, R.R., Jr., Tinsley, B.A. 1986. The influence of charge escape on the velocity distribution of hydrogen in the Venus exosphere. *J. Geophys. Res.* 91: (13) 649-658.



- Hoffman, J.H., Hodges, R.R., Donahue, T.M., and McElroy, M.B. 1980. Composition of the Venus Lower Atmosphere From the Pioneer Venus Mass Spectrometer. *J. Geophys. Res.* 85:7882-7890.
- Hunten, D.M., Donahue, T.M., Walker, J.C.G., and Kasting, J.F. 1989. Escape of atmospheres and loss of water. In *Origin and Evolution of Planetary and Satellite Atmospheres*, eds. S.K. Atreya, et al. (Tucson: University of Arizona Press), pp. 386-422.
- Kar, J., Hartle, R.E., Grebowsky, J.M., Kasprzak, W.T., Donahue, T.M., and Cloutier, P.A. 1994. Evidence of electron impact ionization on the nightside of Venus from PVO/IMS measurements near solar minimum. *J. Geophys. Res.* 99: 11351-11355.
- Kasting, J.F. 1988. Runaway and moist greenhouse atmosphere and evolution of Earth and Venus. *Icarus* 74:472-494.
- Kasting, J.F., and Pollack, J.B. 1983. Loss of water from Venus, I, Hydrodynamic escape of hydrogen. *Icarus* 53:479-508.
- Kasting, J.F., Pollack, J.B., and Ackerman, T.P. 1984. Response of Earth's surface temperature to increases in solar flux and implications for loss of water from Venus. *Icarus* 57:335-355.
- Kasting, J.F., and Toon, O.B. 1989. Climate evolution on the terrestrial planets. In *Origin and Evolution of Planetary and Satellite Atmospheres*, eds. S.K. Atreya, et al. (Tucson: University of Arizona Press), pp. 423-449.
- Kaula, W. 1995. In *Volatiles in the Earth and Solar System*. ed. K. A. Farley (AIP Press), pp.139-142.
- Krasnopolsky, V.A. 1985. Total injection of water vapor into the Venus atmosphere. *Icarus* 62:221-229.
- Kumar, S., Hunten, D.M., and Pollack, J.B. 1983. Non-thermal escape of hydrogen and deuterium from Venus and implications for loss of water. *Icarus* 55:369-375.
- Kumar, S., and Taylor, Jr., H.A. 1984. Deuterium on Venus: model comparisons with Pioneer Venus observations of the predawn bulge ionosphere. *Icarus* 62:494-504.
- Lewis, J.S. 1972. Low temperature condensation from the solar nebula. *Icarus* 16:241-252.
- Lewis, J.S., and Grinspoon, D.H. 1990. Vertical distribution of water in the atmosphere of Venus: A simple thermochemical explanation. *Science* 249:1273-1275.
- McElroy, M.B., and Yung, Y.L. 1976. Oxygen isotopes in the Martian atmosphere: implications for the evolution of volatiles. *Planet. Space Sci.* 24: 1107-1113.
- Moroz, V.I., Moshkin, B.E., Ekonomov, A.P., Golovin, Y.M., Gnedykh, V.I., and Grigor'ev, A.V. 1982. Spectrophotometrical experiment on Venera 13 and Venera 14. *Pisma Astron. Zh.* 8:4044-4100.



- Owen, T., Bar-Nun, A., and Kleinfeld, I. 1992. Possible cometary origin of heavy noble gases in the atmospheres of Venus, Earth and Mars. *Nature* 358:43-45.
- Oyama, V.I., Carle, G.C., Woeller, F., Pollack, J.B., Reynolds, R.T., and Craig, R.A. 1980. Pioneer Venus gas chromatography of the lower atmosphere of Venus. *J. Geophys. Res.* 85:7891-7902.
- Paxton, L.J., Anderson, D.E., and Stewart, A.I.F. year? Analysis of Pioneer Venus Orbiter Ultraviolet Spectrometer Lyman- $\alpha$  Data from near the subsolar region. *J. Geophys. Res.* 93:1766-1772.
- Pepin, R.O. 1991. On the origin and early evolution of terrestrial planet atmospheres and meteoric volatiles. *Icarus* 114:15-27.
- Pepin, R.O. 1995. Evolution of Earth's noble gases: consequences of assuming hydrodynamic loss driven by giant impact. *Icarus*.
- Pollack, J.B., Dalton, J.B., Grinspoon, D., Wattson, R.B., Freedman, R., Crisp, D., Allen, D.A., Bézard, B., DeBergh, C., Giver, L.P., Ma, Q., and Tipping, R. 1993. Near-Infrared Light from Venus' Nightside: A Spectroscopic Analysis. *Icarus* 103:1-42.
- Prinn, R.G., Fegley, B., Jr. 1989. Solar Nebula Chemistry: Origin of Planetary, Satellite and Cometary Volatiles. In *Origin and Evolution of Planetary and Satellite Atmospheres*. Ed. S.K. Atreya, J.B. Pollack, and M.S. Matthews, (University of Arizona Press).
- Revercomb, H.E., Sromovsky, L.A., Suomi, V.E., and Boese, R.W. 1985. Net thermal radiation in the atmosphere of Venus. *Icarus* 61:521-538.
- Rodriguez, J.M., Prather, M.J., and McElroy, M.B. 1984. Hydrogen on Venus: exospheric distribution and escape. *Planet. Space Sci.* 32:1235-1355.
- Shoemaker, E., Weissman, P., Shoemaker, C. 1994. The Flux of Periodic Comets Near Earth. In *Hazards Due to Comets and Asteroids*. ed. T. Gehrels (University of Arizona Press), pp. 313-335.
- Shoemaker, E., Wolfe, R. 1982. Cratering Time Scales for the Gallilean Satellite of Jupiter. In *The Satellites of Jupiter*. ed. D. Morrison (University of Arizona Press), pp. 277-339.
- Shoemaker, E., Wolfe, R., Shoemaker, C. 1990. Asteroid and Comet Flux in Neighborhood of Earth. *Geol. Soc. of Amer. Special Publication* 247: 155-170.
- Watson, A.J., Donahue, T.M., and Walker, J.C.G. 1981. The dynamics of a rapidly escaping atmosphere: applications to the evolution of Earth and Venus. *Icarus* 48:150-166.
- Wetherill, G.W. 1991. Formation of the terrestrial planets from planetesimals. In *Planetary Sciences: American and Soviet Research*, ed. T.M. Donahue (Washington: National Academy Press), pp. 98-115.



# Hydrogen and deuterium in the thermosphere of Venus: Solar cycle variations and escape

R. E. Hartle

Laboratory for Atmospheres, Goddard Space Flight Center, Greenbelt, Maryland

T. M. Donahue

Space Physics Research Laboratory, Department of Atmospheric, Oceanic and Space Sciences, University of Michigan, Ann Arbor

J. M. Grebowsky and H. G. Mayr

Laboratory for Atmospheres, Goddard Space Flight Center, Greenbelt, Maryland

**Abstract.** A strong solar cycle variation in hydrogen and deuterium densities is observed in the nightside thermosphere of Venus when Pioneer Venus Orbiter (PVO) measurements made during the first three Venus years of the mission are compared with those made during the preentry phase of the mission. Solar maximum conditions prevailed during the former period, while near solar minimum conditions occurred during the latter. Pronounced density enhancements in H of 6.5 times and D of 4 times are observed in the nightside bulge region as solar activity decreased from maximum to near-minimum values. We attribute the buildup of H and D to a reduction in the escape fluxes as solar activity decreased, a behavior that is consistent with the known properties of the dominant escape processes due to the charge separation electric field (E) and charge exchange (CE). Application of this simple concept leads to expressions for the H and D escape fluxes which relate solar cycle variations of the respective bulge densities and escape fluxes to the dayside source fluxes. Planet averaged escape fluxes in the ranges  $1.23 \times 10^7 \text{ cm}^{-2} \text{ s}^{-1} \leq \Phi_e(\text{H}) \leq 1.45 \times 10^7 \text{ cm}^{-2} \text{ s}^{-1}$  and  $1.61 \times 10^5 \text{ cm}^{-2} \text{ s}^{-1} \leq \Phi_e(\text{D}) \leq 2.15 \times 10^5 \text{ cm}^{-2} \text{ s}^{-1}$  are obtained by this method without specifying any particular escape mechanism. Considering the uncertainties in the measured parameters, these flux ranges are in reasonable agreement with the escape fluxes derived from the specific processes, E and CE. When fractionation without or with an external source of water (e.g., comets) is applied to the range of possible escape fluxes, a fractionation factor  $f = 0.44$  is obtained and an ancient reservoir of water equivalent to the range 125 m to 570 m of liquid uniformly distributed on the surface or 3.7% to 17% of a full terrestrial ocean is derived. When the specific escape processes E and E + CE are considered, the  $f$  values are 0.15 and 0.1 and the magnitudes of the reservoirs are lower, having a range of equivalent depths of 4.1 m to 36.8 m, respectively.

## 1. Introduction

Knowledge of the density distribution of hydrogen and its isotope deuterium in the atmosphere of Venus is essential to understanding the evolution of these constituents and that of water. Measurement of H and D densities and determination of their escape rates as well as the D/H ratio were some of the primary objectives of the Pioneer Venus (PV) mission which began exploration of Venus in December 1978. The objectives of this paper are to determine the diurnal variation of H and D at high and low solar activity, evaluate the solar cycle variations of the respective escape fluxes, and apply them to an estimate of the size of an earlier water reservoir. A new approach is used here to evaluate the escape fluxes which requires little or no knowledge of the actual escape mechanisms.

Copyright 1996 by the American Geophysical Union.

Paper number 95JE02978.  
0148-0227/96/95JE-02978\$05.00

Early measurements of H were obtained from UV instruments on Mariner 5 [Barth *et al.*, 1967] and Veneras 10 and 11 [Bertaux *et al.*, 1982], while more detailed knowledge of its density and structure was obtained by several instruments on board the Pioneer Venus Orbiter (PVO). Using ion densities of  $\text{H}^+$  and  $\text{O}^+$  measured by the Orbiter ion mass spectrometer (OIMS) and neutral densities of O and  $\text{CO}_2$  observed by the Orbiter neutral mass spectrometer (ONMS), Brinton *et al.* [1980] obtained H densities in the chemical equilibrium region spanning the first diurnal cycle of the PVO mission. They discovered a large diurnal variation of H having a nighttime density bulge peaking near 0300 UT which was some 400 times more dense than that observed on the dayside. Taylor *et al.* [1985] extended the analysis of the H bulge region to include the first three Venus years of the PVO. An analysis by Paxton *et al.* [1988] of the Lyman  $\alpha$  fluxes measured by the Orbiter ultraviolet spectrometer (OVS) produced H concentrations similar to those of Brinton *et al.* [1980].

The first detection and measurement of D in the atmosphere of Venus was confirmed after considerable analysis of two sets

of measurements made during the PVO mission. For one set, a detailed study of mass spectra obtained from hydrated liquid cloud drops that fortuitously clogged the inlet leak system on the Pioneer Venus large probe neutral mass spectrometer (LNMS) led to the identification of D and an estimate of the D/H ratio of  $(1.6 \pm 0.2) \times 10^{-2}$  in the lower atmosphere [Donahue *et al.*, 1982]. At about the same time, McElroy *et al.* [1982] suggested that the mass 2 ion observed by the OIMS could be  $D^+$  instead of  $H_2^+$ . Subsequently, an analysis of the height distribution of the mass 2 ion measured in the chemical equilibrium region of the ionosphere by the OIMS led to the clear identification of  $D^+$ , from which a D/H ratio of  $(2.2 \pm 0.6) \times 10^{-2}$  was derived at the turbopause [Hartle and Taylor, 1983]. A recent analysis of the LNMS measurements by Donahue and Hodges [1992] revised the D/H ratio upward to  $(2.5 \pm 0.6) \times 10^{-2}$ .

In a recent study, Grebowsky *et al.* [1995] expanded the database used by Brinton *et al.* [1980] and Taylor *et al.* [1985] to derive the H distributions. The number of data points was increased by testing each derived H density to determine whether or not chemical equilibrium prevailed at each measurement point. In the previous studies, maximum altitudes of the chemical equilibrium region were preset, thereby eliminating valid H measurements when chemical equilibrium existed above such altitudes. The work of Grebowsky *et al.* [1995] included H densities from the first three Venus years as well as those from the preentry phase of the mission. The current study will extend this work by adding D to the H density database, which will then be used to evaluate their respective escape rates. In turn, these results are applied to an analysis of the evolution of H and D in the atmosphere of Venus to provide an estimate of the size of an early water reservoir on the planet.

## 2. Solar Activity and Escape Mechanisms

Periapsis of PVO was in the thermosphere during the first three Venus years of the mission before it ascended into the exosphere. During this period, between December 1978 and

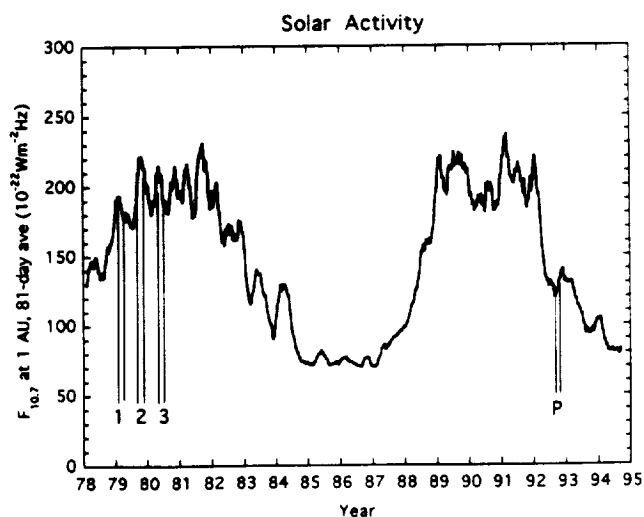


**Figure 1.** The 10.7 cm solar radio flux line spanning the calendar years of the PVO mission. The time intervals depicted by the vertical lines labeled 1, 2, 3, and P correspond to the periods when periapsis of PVO was in the midnight to dawn sector (only to 0430 UT for P) during Venus years 1, 2, and 3, and the preentry period, respectively.

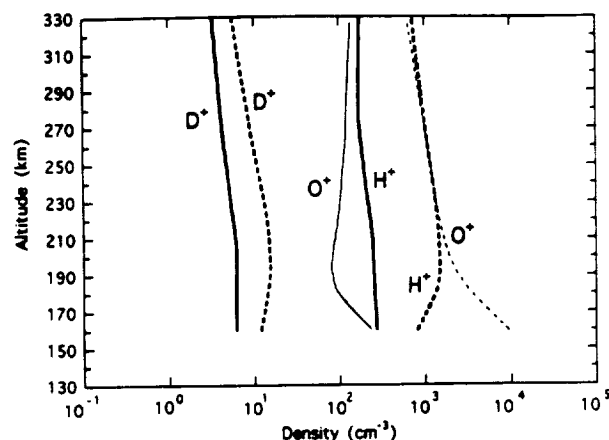


**Figure 2.** Height profiles of  $H^+$ ,  $D^+$ , and  $O^+$  for solar maximum (dashed lines) and near-solar minimum (solid lines).

July 1980, solar activity was at maximum levels, as indicated by the 10.7-cm solar flux line shown in Figure 1. In the preentry phase of the mission in 1992, almost 14 years after initial entry into the atmosphere, periapsis of PVO returned briefly to the thermosphere, where measurements were made in the predawn H bulge region, just before burnup of the orbiter on October 8, 1992. Solar activity was near a minimum during this phase of the mission, making it possible to study solar cycle effects on escape and evolution when this data set is considered together with that of 1978-1980.

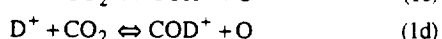
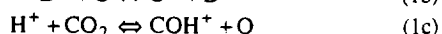
Immediately following the low solar activity measurements of 1992, the first study of this kind was done by Donahue and Hartle [1992], who noted a strong solar cycle variation in ion composition requiring changes in the known H and D escape fluxes. An example of ion composition dependence on solar activity is shown in Figure 2, where vertical profiles of average  $H^+$ ,  $D^+$ , and  $O^+$  densities in the 0200-0400 UT dawn sector are plotted. Two sets of ion densities are shown in the figure, one corresponding to averages taken over the first three Venus years and the other over the preentry phase, when solar maximum and near solar minimum conditions prevailed, respectively. The dawn sector is shown here because this is the bulge region where  $H^+$  and  $D^+$ , and H and D maximize, where most of these atoms and ions in the thermosphere reside, and consequently, where their respective escape fluxes maximize. In this sector,  $H^+$  and  $D^+$  densities near solar minimum are about 7 times and 3 times less, respectively, than those at solar maximum while the corresponding  $O^+$  densities are a factor of 20 times less at low altitudes (160-200 km) with the factor decreasing to 7 or 8 at higher altitudes. Similar solar cycle variations were described by Kar *et al.* [1994]. The reduction in ionospheric densities on the nightside is expected as solar activity declines. This is due to at least two major factors. (1) Fewer ions are produced on the dayside as solar activity decreases; therefore fewer ions are available to be transported to the nightside. (2) With a reduced ion population on the dayside, the ionopause altitude decreases, thereby reducing the area of the terminator annulus through which day to night ion flow takes place.

The discovery of the strong decrease in  $H^+$  and  $D^+$  densities as solar activity decreased led Donahue and Hartle [1992] to reevaluate the known escape mechanisms. Four basic mechanisms were known at the time, two of which are not considered to be important today. Thermal or Jeans escape was

shown to be insignificant due to the very low exospheric temperatures of 284°K at noon and 123°K in the nightside H bulge of Venus (note: the temperatures used throughout are from the Venus international reference atmosphere (VIRA) model [Keating *et al.*, 1985]). Collisions of H and D with energetic oxygen, O<sup>+</sup>, produced by dissociative recombination of O<sub>2</sub><sup>+</sup>, was considered to be an important escape mechanism for a number of years [Rodríguez *et al.*, 1984; Gurwell and Young, 1993]. However, Hodges [1993] has recently shown that when proper account is taken of the scattering down in energy of hot oxygen colliding with ambient thermal oxygen, the energy density of the hot oxygen population is reduced to the point that the resulting H and D escape fluxes are rendered unimportant. This leaves two escape mechanisms that are thought to remain important. One is due to charge exchange (CE) of "hot" ionospheric H<sup>+</sup> with H, which produces a population of "hot" H atoms possessing a significant number of escape trajectories. The most recent calculations of the loss rates due to CE were made by Rodríguez *et al.* [1984] and Hodges and Tinsley [1982], who obtained planet average escape rates of  $3.2 \times 10^6 \text{ cm}^2 \text{ s}^{-1}$  and of  $2.8 \times 10^7 \text{ cm}^2 \text{ s}^{-1}$ , respectively. Donahue and Hartle [1992] have shown that the large differences in these escape fluxes are due to the fact that both investigator groups used widely differing H<sup>+</sup> and H densities, none of which were representative of average conditions. When average H<sup>+</sup> and H densities derived from PVO data were used, Donahue and Hartle [1992] obtained an H escape flux due to CE of  $0.9 \times 10^7 \text{ cm}^2 \text{ s}^{-1}$  for the solar maximum conditions of the first three Venus years of the PVO mission. The CE escape process for D is very inefficient relative to that for H, and, consequently its fractionation factor is only 0.02 [Krasnopolsky, 1985]. The remaining escape mechanism of significance is a fluid-like upward flow of H<sup>+</sup> and D<sup>+</sup>, which is accelerated to escape speeds by the charge separation electric field in the ionosphere [Hartle and Grebowsky, 1995]. As the plasma flows to higher altitudes in the ion exosphere, the motional electric field of the solar wind impressed across the draped magnetic field lines of the ionotail of Venus eventually overtakes the polarization electric field and accelerates the ions up to solar wind speeds as the ionotail merges into the interplanetary medium. Essentially all escape of H<sup>+</sup> and D<sup>+</sup> by the electric field process (E) occurs in the light ion bulge, where most of these ions reside. When the escape fluxes derived by Hartle and Grebowsky [1993, 1995] are averaged over the planet, we obtain values of  $1.5 \times 10^7 \text{ cm}^2 \text{ s}^{-1}$  and  $5.6 \times 10^4 \text{ cm}^2 \text{ s}^{-1}$  for H<sup>+</sup> and D<sup>+</sup>, respectively, for solar maximum conditions.

### 3. H and D Density Distributions

Apart from minuscule differences due to their nuclear masses, the atomic properties of H and D are the same. Consequently, H and D atoms and ions obey the same principal chemical reactions



which determine the H and D densities

$$n(\text{H}) = \frac{n(\text{H}^+)}{n(\text{O}^+)} \left[ K_1 n(\text{O}) \left( \frac{T_i}{T} \right)^{1/2} + K_2 n(\text{CO}_2) \right] \quad (2a)$$

$$n(\text{D}) = \frac{n(\text{D}^+)}{n(\text{O}^+)} \left[ K_1' n(\text{O}) \left( \frac{T_i}{T} \right)^{1/2} + K_2' n(\text{CO}_2) \right] \quad (2b)$$

at all altitudes in the ionosphere of Venus where chemical equilibrium holds. The ion densities  $n(\text{H}^+)$ ,  $n(\text{D}^+)$ , and  $n(\text{O}^+)$  were measured by the OIMS, the neutral densities  $n(\text{O})$  and  $n(\text{CO}_2)$  and their temperature  $T$  were measured by the ONMS, and the ion temperature  $T_i$  was measured by the Orbiter retarding potential analyzer (ORPA). The coefficient  $K_1$  for reaction (1a) is that used by Brinton *et al.* [1980]. For reaction (1b) we take  $K_1' = K_1$ . This can be seen to be a valid approximation upon first considering that  $K_1(T_i/T)^{1/2}$  can be expressed as the ratio of the forward rate factor  $\sigma_f(8kT_i/\pi\mu_{1,16})^{1/2}$  to the reverse rate factor  $\sigma_r(8kT/\pi\mu_{1,16})^{1/2}$  near thermal equilibrium (as is the case here), where the cross sections  $\sigma_f$  and  $\sigma_r$  are energy averaged and  $\mu_{1,16} = m_H m_O / (m_H + m_O)$  is the reduced mass of the reactants [e.g., Holzer and Banks, 1969]. In this form,  $K_1 = \sigma_f/\sigma_r$  is independent of mass. Therefore, since  $K_1'$  has the same form as  $K_1$  and the ratio  $\sigma_f/\sigma_r$  is essentially the same for hydrogen and deuterium collisions, then  $K_1' = K_1$ . The coefficient  $K_2$  is the ratio of the rate  $3.8 \times 10^{-9} \text{ cm}^3 \text{ s}^{-1}$  [Anicich, 1993] of the reaction  $\text{H}^+ + \text{CO}_2$  divided by the rate of the reaction  $\text{O}^+ + \text{H}$ , which is  $2.5 \times 10^{-11} T^{1/2} \text{ cm}^3 \text{ s}^{-1}$  [Nagy *et al.*, 1980]. Similarly, the coefficient  $K_2'$  is the ratio of the rate of the  $\text{D}^+ + \text{CO}_2$  reaction,  $3.5 \times 10^{-9} \text{ cm}^3 \text{ s}^{-1}$  [Anicich, 1993], divided by the rate of the  $\text{O}^+ + \text{D}$  reaction, which has not been measured yet. However, considering the simple expressions above for the rate factors, the later rate can be estimated by multiplying the rate for  $\text{O}^+ + \text{H}$  by  $(\mu_{1,16}/\mu_{2,16})^{1/2} = 0.73$ .

The principal database used in the analysis is the Pioneer Venus unified abstract data system (UADS) consisting of 12-s averages of the measurements. When measurements of some of the parameters are missing in UADS, empirical models are used to fill in the gaps; i.e., the Hedin *et al.* [1983] model is used for the O and CO<sub>2</sub> densities and the neutral temperature, while the VIRA model is used for the ion temperature. In contrast, models are not used for the ion densities because they cannot properly account for the high spatial and temporal variations required by (2). Consequently, when ion densities are missing from the database, no H or D densities are derived.

The chemical equilibrium region where (2a) and (2b) are valid is determined by an algorithm developed previously to derive H densities [Grebowsky *et al.*, 1995]. In this case, values of  $n(\text{H})$  and  $n(\text{D})$  are only retained when the chemical

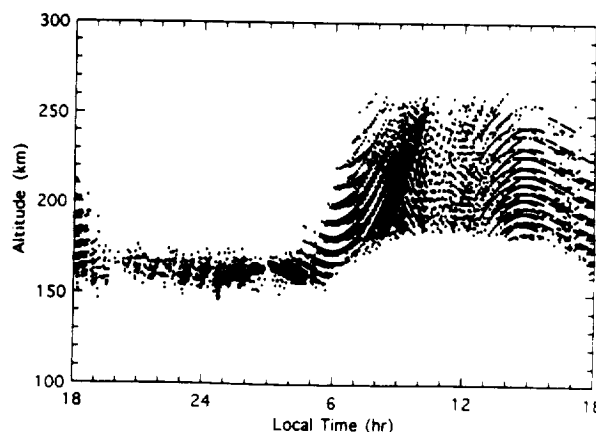


Figure 3. Altitude versus local time of each point where both chemical equilibrium and a value of  $n(\text{H})$  exist.

timescale  $1/k_1 n(O)$  is less than the  $H^+$  diffusion timescale  $h^2/d$ , where  $h$  is the O scale height and  $d$  is the diffusion coefficient for  $H^+$  ions [Banks and Kockarts, 1973]. This approach is conservative for evaluating  $n(D)$  because the diffusion time constant for  $D^+$  is greater than that for  $H^+$ , and consequently, chemical equilibrium for D is valid to somewhat higher altitudes than it is for H. Collisions with all major ion and neutral species are accounted for in the calculation of the diffusion coefficient. The scale height for  $CO_2$  is not used in the diffusion time because it is only important at low altitudes, where  $H^+$  is not detected. Applying these guidelines, we find that the altitudes where both chemical equilibrium exists and enough data exist to allow  $n(H)$  to be derived are distributed in a distinct diurnal pattern as indicated in Figure 3. In particular, chemical equilibrium extends up to about 250–260 km on the dayside and only to 170–175 km on the nightside, a diurnal variation which is largely a reflection of the variation of the major ion  $O^+$  at these altitudes. The lower limits of the altitude distribution in Figure 3 are not the lower limits of the chemical equilibrium region, but simply the lowest altitudes where  $H^+$  remained detectable.

The H and D densities derived from (2a) and (2b) in the chemical equilibrium region are shown in Figure 4, where the large H density bulge discovered by Brinton *et al.* [1980] is displayed. Helium densities [e.g., Kasprzak *et al.*, 1993; Grebowsky *et al.*, 1995] at 170 km are also shown for comparison in Figure 5. An absence of telemetry caused the postdusk data gap in Venus year 2, while a special OIMS operational mode resulted in a similar gap in Venus year 3. After about 1000 UT in Venus year 3, periapsis of PVO rose above the chemical equilibrium region and did not return until the preentry phase, where measurements were fortunately made in the bulge, just before burnup. Since the latitude of periapsis of PVO was about  $16^\circ$  during the first three Venus years and about  $-10^\circ$  at preentry, the diurnal variations shown in Figure 4

are considered essentially equatorial for the purposes of this paper. The variance in the densities at a fixed local time is due to atmospheric waves and structures; some structures have been shown by Taylor *et al.* [1985] to be related to solar wind ram pressure changes. Average values of the H and D densities are shown in Figure 6, which are convenient for making comparisons and carrying out quantitative analysis.

Apart from the large nightside H and D density bulges, perhaps the most striking features in Figure 6 are the enhancements of the preentry bulges over those observed during the first three Venus years. In particular, we find that the density of the preentry H bulge is about 6.5 times greater than the average density found in the bulge during the first three Venus years. A similar comparison made with D reveals a density enhancement of 4 times. Referring to Figure 1, we see that solar activity levels during the first three Venus years, 1978–1980, are similar to the solar maximum levels just preceding preentry. In the ensuing analysis, we make the reasonable assumption that the H and D densities in 1991 were similar to those in the 1978–1980 period. In this scenario, density enhancements developed when solar activity dropped from its high level in early 1992 to the low level of the last 4 months of the mission. It is fortunate that solar activity was relatively steady during this latter period, when all the preentry bulge densities were measured, as will be clear in the steady state analysis that follows.

The major gas densities and temperatures in the H and D bulge region were observed to be similar during both solar maximum and near solar minimum conditions [Kasprzak *et al.*, 1993]. Keating and Hsu [1993] have observed that the thermospheric temperatures and densities on the dayside decrease somewhat as solar activity decreases from maximum to minimum conditions. These observations are consistent with the solar cycle variations predicted by Bougher *et al.* [1986], whose circulation model also suggests that thermospheric winds vary

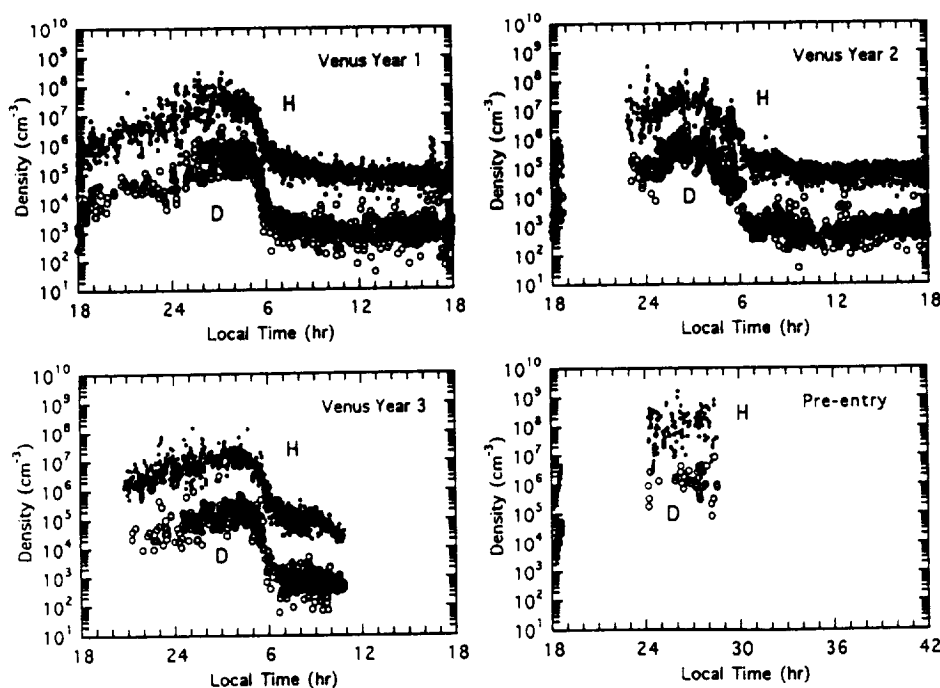
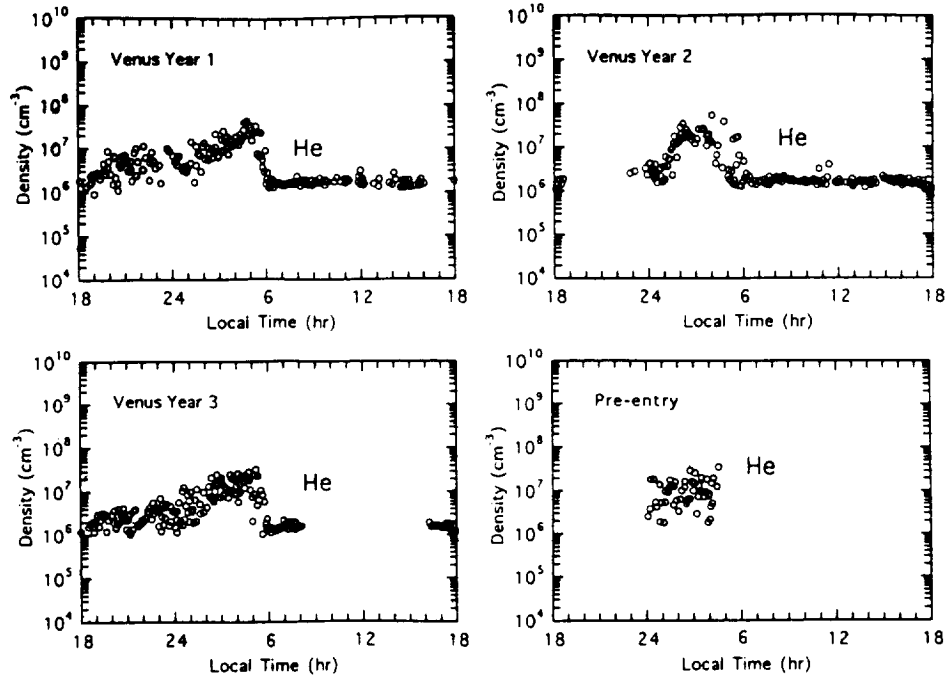


Figure 4. Diurnal variations of H and D densities derived from (2) for each Venus year and the preentry period at altitudes shown in Figure 3.



**Figure 5.** Diurnal variations of He densities for each Venus year and the pre-entry period as measured by ONMS in the altitude range 170–180 km.

only slightly over a solar cycle. The weak solar cycle variation in thermospheric circulation, which transports H and D into the nightside, can not account for the large solar cycle variations of these constituents. However, the weak solar cycle variation in thermospheric circulation is consistent with the He density observations shown in Figure 5, indicating no noticeable solar cycle variation, because the density buildup of this species on the nightside is primarily driven by thermospheric circulation and not at all by escape [Mengel *et al.*, 1989].

#### 4. Escape Rates From Solar Cycle Variations

We suggest that a likely cause of the H and D enhancements occurring in the bulge region as solar activity decreased is a

consequence of the known decrease in the escape rates of these constituents [Donahue and Hartle, 1992] as solar activity declines. Thus we examine this concept here and show how such solar cycle variations can be used to estimate the escape fluxes of H and D. We note that this scenario for H and D is fundamentally different from and consistent with that for He, which does not exhibit a solar cycle variation and whose density variation is not affected by escape, but primarily by thermospheric circulation.

Considering the variation in H first, which can be described in terms of the rate of change of the number of H atoms in the thermosphere,  $\psi$ , by

$$\frac{d\psi}{dt} = \phi_S A_d - (\phi_e + \phi_d) A_b \quad (3)$$

where  $\phi_S$  is the source flux of atomic H which flows up into the thermosphere from the mesosphere after being formed there by photolysis of  $\text{H}_2\text{O}$  and  $\text{H}_2$ . Since the source is confined to the dayside, its flux is multiplied by  $A_d$ , the area of the dayside. As H flows from day to night, a fraction escapes from the top of the nighttime atmosphere with a flux  $\phi_e$ , while the remainder recirculates in the mixing region after flowing downward through the lower thermosphere with a flux  $\phi_d$ . Essentially all of the hydrogen in the thermosphere resides in the nighttime bulge region; therefore the downward flow and escape flux are multiplied by the area of the bulge,  $A_b$ , which is about 20% of the total area  $A$ . We have varying degrees of knowledge of  $\psi$ ,  $\phi_S$ , and  $\phi_d$  which can be used to estimate the escape flux  $\phi_e$  as will be shown below.

##### 4.1 Steady State Analysis

Since solar maximum conditions prevailed just before the final entry of PVO's periaapsis into the thermosphere and since the corresponding levels of the 10.7-cm solar flux were similar to those of the first three Venus years of the mission, the

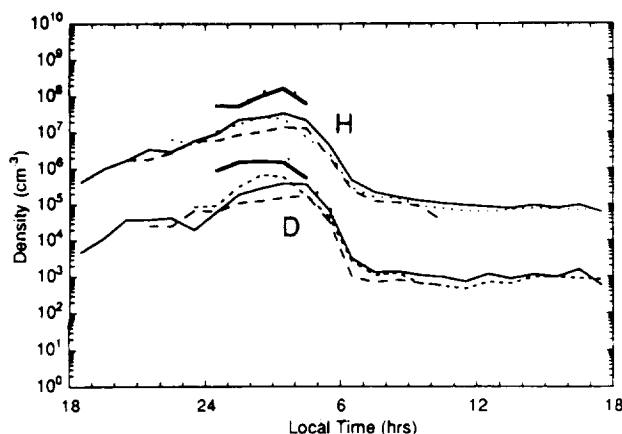


**Figure 6.** Diurnal variations of average values of H and D densities derived from data in Figure 4 for Venus year 1 (light solid line), year 2 (long-dashed line), year 3 (short-dashed line), and preentry period (heavy solid line).

**Table 1.** Escape Fluxes ( $10^7 \text{ cm}^2 \text{ s}^{-1}$ )

Process	$\Phi_e$	$\bar{\Phi}_e$	$\phi_e$	$\bar{\phi}_e$	$\langle \Phi_e \rangle$	$\langle \bar{\Phi}_e \rangle$
E	7.5	1.5	1.1	0.23	4.3	0.86
CE	4.5	0.9	3.3	0.64	3.9	0.77
E+CE	12	2.4	4.4	0.85	8.2	1.60

conditions in the thermosphere during the latter period are assumed to approximate those of the former period. Consequently, when solar maximum occurred during the preentry phase,  $d\psi/dt \equiv 0$ , and (3) becomes

$$\Phi_S A_d = (\Phi_d + \Phi_e) A_b \quad (4)$$

where  $\Phi$  refers to solar maximum conditions. Time independence also applies to the period when the preentry measurements of H were made in 1992 because, as noted previously, the solar flux remained steady during that interval. Therefore

$$\phi_S A_d = (\phi_d + \phi_e) A_b \quad (5)$$

where  $\phi$  refers to conditions near solar minimum. The steady state approximation should be valid over most of the solar cycle and not just during the maximum and minimum periods considered here. For example, the diffusion timescale  $h^2/k$ , in terms of the scale height  $h$  for  $\text{CO}_2$  and the eddy diffusion coefficient  $k$ , is only about 0.7 days at 110 km and 4 days at 100 km, periods much shorter than that of a solar cycle. Furthermore, the residence time,  $\psi/\phi_S$ , for thermospheric H is only about 10 to 20 days.

A parameter that will be useful in the analysis is the escape flux ratio

$$\varepsilon = \phi_e / \Phi_e \quad (6)$$

As will be clear below, the relation between  $\phi_d$  and  $\Phi_d$  is known,  $\Phi_S$  is known as are upper and lower bounds on  $\Phi_S$ . When these relationships and equations (4) and (5) are combined, an expression relating  $\Phi_e$  to  $\phi_e$  results. However, the magnitudes of  $\Phi_e$  and  $\phi_e$  can be evaluated using current knowledge of the dominant escape fluxes [Donahue and Hartle, 1992] due to charge exchange (CE) and the charge separation electric field mechanism (E) to constrain  $\varepsilon$ . Values of the

escape fluxes obtained by Donahue and Hartle [1992] are shown in Table 1. The overbar used throughout corresponds to a global average (e.g.,  $\bar{\Phi}_e = \Phi_e A_b / A = \Phi_e / 5$ ), and the quantity  $\langle \Phi_e \rangle = (\Phi_e + \phi_e) / 2$  is the average flux over a solar cycle. The low solar activity escape fluxes were taken to be negligible by Donahue and Hartle [1992], whereas they have been scaled here by multiplying the solar maximum fluxes by  $n^*/N^*$  for E and  $n^*n/(N^*N)$  for CE. When flux ratios are derived from Table 1,  $\varepsilon$  values of 0.15, 0.73, and 0.37 are obtained for the processes E, CE, and E + CE, respectively.

The most recent work pertaining to the source flux has been done by Paxton *et al.* [1988], who derived the upward flux of H from Lyman  $\alpha$  intensities observed by the OUVS on PVO. They obtained an upward flux of  $7.5 \times 10^7 \text{ cm}^2 \text{ s}^{-1}$  in the subsolar region using data from the first three years of the PVO mission, when solar maximum conditions prevailed. We have reevaluated this flux in the appendix and obtain an upward flux  $\Phi_S$  of  $2.3 \times 10^7 \text{ cm}^2 \text{ s}^{-1}$ , which does not exceed the limiting flux of  $\Phi_e = 3.5 \times 10^7 \text{ cm}^2 \text{ s}^{-1}$ , as required. Furthermore, the observed H densities described in section 3 are 1.25 times greater than the values used by Paxton *et al.* [1988]; therefore adjusting the upward flux by this factor leads to  $\Phi_S = 2.9 \times 10^7 \text{ cm}^2 \text{ s}^{-1}$ . At this time we do not know the value of the source flux  $\Phi_S$ ; however, it is probably larger than  $\Phi_S$ , as more H is circulated through the upper atmosphere. An upper bound is fixed by the fact that the source rate  $\Phi_S A_d$  cannot exceed the maximum rate  $\Phi_e A_d$ . Thus there is an upper bound for  $\phi_S = 1.5 \times \Phi_S$ . The bounds on the source flux near solar minimum are expressed by the flux ratio

$$1 \leq \varepsilon_S \equiv \phi_S / \Phi_S \leq 1.5. \quad (7)$$

A downward flux of H in the nightside bulge region has been shown to be significant in a number of global circulation models [Mayr *et al.*, 1978; Hartle *et al.*, 1978; Mayr *et al.*, 1980]. To a first approximation, it is proportional to the density in the bulge region as expected from the diffusion equation. Thus, we define the flux ratio

$$\varepsilon_n \equiv \Phi_d / \phi_d = N / n \quad (8)$$

in terms of the average H densities  $N$  and  $n$  observed in the H bulge during solar maximum and near-solar minimum, respectively. When the average densities in Figure 6 are scaled,  $\varepsilon_n = 0.21$ , 0.17, and 0.09 for Venus years 1, 2 and 3, respectively, and an average  $\varepsilon_n = 0.15$ . These ratios reflect density variations in the height range of about 150 km to 170 km, the limited region where H and D densities could be evaluated on the nightside. Consequently, the analysis here is restricted to a lower boundary of about 160 km through which the source flux and the downward flux flow. The upper boundary through which the escape flux flows is taken to be at an altitude high enough to include all the significant processes contributing to E and CE while avoiding the complicating

**Table 2.** Escape Efficiencies and Globally Averaged Escape Fluxes ( $10^7 \text{ cm}^2 \text{ s}^{-1}$ )

Process	$\varepsilon$	$\eta$	$\bar{\Phi}_e$ (From (9))	$\bar{\Phi}_e$ (Table 1)
	0.00	0.85	1.23	
E	0.15	0.87	1.26	1.50
E + CE	0.37	0.90	1.31	2.40
CE	0.73	0.95	1.38	0.90
	1.00	1.00	1.45	

**Table 3.** Escape Fluxes ( $10^7 \text{ cm}^2 \text{ s}^{-1}$ ) From (9)

Process	$\Phi_e$	$\bar{\Phi}_e$	$\phi_e$	$\bar{\phi}_e$	$\langle \phi_e \rangle$	$\langle \bar{\phi}_e \rangle$
E	6.31	1.26	0.95	0.19	3.63	0.73
CE	6.89	1.38	5.03	1.01	5.96	1.20
E+CE	6.53	1.31	2.41	0.48	4.47	0.90

effects of lateral transport; in particular, we choose an upper boundary of 500 km, the approximate altitude of the ion exobase which is well above the neutral exobase.

When values for  $\epsilon$ ,  $\epsilon_n$ , and  $\epsilon_S$  are used in (4) and (5), the escape flux and its time average can be evaluated. The analysis is simplified by combining these equations to obtain the following convenient forms:

$$\bar{\Phi}_e = \eta(\epsilon, \epsilon_n, \epsilon_S) \bar{\Phi}_S \quad (9)$$

where

$$\eta = \frac{1 - \epsilon_n \epsilon_S}{1 - \epsilon \epsilon_n} \quad (10)$$

is the efficiency for escape. Considering the estimated values of  $\epsilon_n$  and  $\epsilon_S$ , physical limits can be placed on  $\eta$  as  $\epsilon$  is varied. An upper bound  $\eta \leq 1$  results from the physical limit  $\bar{\Phi}_e \leq \bar{\Phi}_S$ , which also requires  $\epsilon \leq 1$ . In the other extreme, when  $\epsilon = 0$ ,  $\epsilon_n = 0.15$  (average value)  $\eta = 0.85$  and  $\bar{\Phi}_e = 0.85 \bar{\Phi}_S$ . Altogether, the following range of variables apply:  $0 \leq \epsilon \leq 1$ ;  $0 \leq \eta \leq 1$ ;  $0.85 \bar{\Phi}_S \leq \bar{\Phi}_e \leq \bar{\Phi}_S$  or  $1.23 \times 10^7 \text{ cm}^2 \text{ s}^{-1} \leq \bar{\Phi}_e \leq 1.45 \times 10^7 \text{ cm}^2 \text{ s}^{-1}$ . These limits are applicable when  $\epsilon_S = 1$ ; however, considering the upper limit  $\epsilon_S = 1.5$ , the ratio  $\eta(\epsilon, \epsilon_n, 1.5)/\eta(\epsilon, \epsilon_n, 1.0) = 0.91$  indicates that an ignorable change in the fluxes occurs as  $\epsilon_S$  spans its limits. Escape efficiencies and globally averaged escape fluxes from (9) are shown in Table 2 for the limiting values of  $\epsilon$  and those of the three processes E, CE, and E + CE, when  $\epsilon_S = 1$ . Also shown in Table 2, for comparison, are escape fluxes from Table 1.

Shown in Table 3 are all types of escape fluxes obtained from (9) for the processes E, CE, and E + CE, for completeness.

A few things are immediately apparent from the range of parameters discussed above and in Tables 2 and 3. (1) The escape flux in Table 1 which combines the electric field and charge exchange processes  $\bar{\Phi}_e(\text{E} + \text{CE}) = 2.4 \times 10^7 \text{ cm}^2 \text{ s}^{-1}$  is considerably larger than the upper limit for the escape fluxes inferred from the solar cycle variations in the bulge. (2) Separately, the escape fluxes due to the charge separation electric field,  $\bar{\Phi}_e(\text{E})$ , and charge exchange,  $\bar{\Phi}_e(\text{CE})$ , are also

outside, but very close to the upper and lower bounds, respectively, allowed by (9). (3) The escape efficiencies and the escape fluxes are constrained to vary a maximum of only 18% when  $0 \leq \epsilon \leq 1$ , and no more than 9% when the processes E, CE, and E + CE are considered. It is fortunate that the escape flux is so tightly bound to the range  $1.23 \times 10^7 \text{ cm}^2 \text{ s}^{-1} \leq \bar{\Phi}_e \leq 1.45 \times 10^7 \text{ cm}^2 \text{ s}^{-1}$ , making it possible to study the evolution of H in this flux range without identifying any particular escape mechanism.

Equations (6) through (10) can be applied directly to evaluate escape parameters for D. Density ratios  $\epsilon_n(\text{D}) = 0.25$ , 0.4, and 0.1 are obtained by scaling the average D densities in Figure 6 for Venus years 1, 2, and 3, respectively, yielding an average  $\epsilon_n(\text{D}) = 0.25$ . The physically derived escape flux due to electric field acceleration at solar maximum [Hartle and Grebowsky, 1995] (hereinafter referred to as HG) is  $\Phi_e(\text{E}; \text{D}^*) = 2.8 \times 10^5 \text{ cm}^2 \text{ s}^{-1}$  when averaged over the D\* bulge. This flux was derived at 500 km. Because the D\* densities at low solar activity are below the detection range of the OIMS at this altitude, we do not have adequate statistics for D\* densities to determine  $\phi_e(\text{E}; \text{D}^*)$  directly. Instead, we make the reasonable assumption that the ratio of the average D\* density at low solar activity to the one at solar maximum is the same as the ratio for H\*, in which case  $\epsilon(\text{E}; \text{D}^*) = 0.15$  for both H\* and D\*. For the D charge exchange escape flux we use the fractionation factor  $f = 0.02$  [Krasnopolsky, 1985] to obtain  $\Phi_e(\text{CE}; \text{D}) = R/\Phi_e(\text{CE}; \text{H}) = 2.5 \times 10^{-2} \times 0.02 \times 0.9 \text{ cm}^2 \text{ s}^{-1} = 4.5 \times 10^3 \text{ cm}^2 \text{ s}^{-1}$ , where  $R$  is the D/H ratio. Using the scaling relation defined above,  $n^*(\text{D})n(\text{D})/[N^*(\text{D})N(\text{D})] = 0.54$ , we obtain  $\phi_e(\text{CE}; \text{D}) = 2.4 \times 10^3 \text{ cm}^2 \text{ s}^{-1}$  and  $\epsilon(\text{CE}; \text{D}) = 0.54$ . Clearly, only  $\Phi_e(\text{E}; \text{D}^*)$  and  $\phi_e(\text{E}; \text{D}^*)$  need be considered in the escape of D because the respective escape fluxes due to charge exchange are 2 orders of magnitude less. Following a similar procedure to that used to derive the source flux for H, a D source flux  $\Phi_S(\text{D}) = 4.3 \times 10^5 \text{ cm}^2 \text{ s}^{-1}$  is obtained in the appendix. Using these values, escape efficiencies and globally averaged escape fluxes from (9) are shown in Table 4 and compared with the flux due to electric field acceleration (HG). Two values of

**Table 4.** Escape Efficiencies and Globally Averaged Escape Fluxes ( $10^5 \text{ cm}^2 \text{ s}^{-1}$ )

Process	$\epsilon$	$\eta$ ( $\epsilon_n = 0.25$ )	$\bar{\Phi}_e$ (From (8))	$\eta$ ( $\epsilon_n = 0.4$ )	$\bar{\Phi}_e$ (From (8))	$\bar{\Phi}_e$ (From HG)
E	0.00	0.75	1.61	0.60	1.29	0.56
	0.15	0.78	1.68	0.64	1.38	
	1.00	1.00	2.15	1.00	2.15	

the density ratio have been used for comparison; namely,  $\epsilon_n = 0.25$  and  $\epsilon_n = 0.4$ , the average value and the one for Venus year 2, respectively.

To produce agreement between the observed HG flux and the calculated value,  $\Phi_S(D)$  would have to be reduced by a factor between one third and one half. This could be done by reducing the deuterium density at the homopause by about the same factor in order to maintain the same density at 220 km with the reduced flux. The D/H ratio in the mixed atmosphere would be between  $0.8 \times 10^{-2}$  and  $1.3 \times 10^{-2}$  instead of  $2.5 \times 10^{-2}$ , as deduced by *Donahue and Hodges* [1992]. A ratio as small as  $1.5 \times 10^{-2}$  is compatible with one measurement of [HDO]/[H<sub>2</sub>O] by near-infrared spectroscopic sounding [*deBergh et al.*, 1991]. Two other measurements [*Donahue and Hodges*, 1993; *Bjoraker et al.*, 1992] set the lower limit at  $2 \times 10^{-2}$ . So an adjustment of the D/H ratio can at best bring  $\Phi_e$  down to about  $1.1 \times 10^5 \text{ cm}^{-2} \text{ s}^{-1}$  or  $0.83 \times 10^5 \text{ cm}^{-2} \text{ s}^{-1}$  for  $\epsilon_n = 0.25$  or 0.4, respectively. Furthermore, the value of  $\Phi_S(D)$  used may be somewhat larger than the actual one because a fraction of the upward flow in the lower thermosphere will be diverted by horizontal winds and never flow across the lower boundary of the region where the flux balance is calculated. An estimate of this effect could be made with a yet to be developed three-dimensional circulation model which includes the light constituents H and D. The foregoing discussion was prompted by the differences in average quantities; however, it should be

kept in mind that when the scatter in the measurements is taken into account, the observed HG flux and the calculated flux are then within the variances of one another.

#### 4.2. Time-Dependent Considerations

In early 1982 the 10.7-cm solar flux decreased rapidly during 4 months from about  $220 \times 10^{-22} \text{ W m}^{-2} \text{ Hz}$  to about  $120 \times 10^{-22} \text{ W m}^{-2} \text{ Hz}$  (Figure 1). By the time hydrogen and deuterium were being observed in the bulge region in mid-1992, their densities, as we have seen, were higher than they had been during the first three Venus years by a factor of about 6.5 in the case of hydrogen and a factor of 4 in the case of deuterium. Considering only the region of the bulge, the time-dependent expression (3) can be used to evaluate the time average vertical flux

$$\langle \phi_e + \phi_d \rangle = 2.5 \langle \phi_s \rangle - \Delta \mathcal{N} / \Delta t \quad (11)$$

where  $\mathcal{N}$  is the column density of H above the turbopause and the ratio  $A_d/A_h = 2.5$  has been applied. Because the hydrogen and deuterium densities were measured for only a small range of altitudes near 160 km, it is not possible to evaluate  $\Delta \mathcal{N} / \Delta t$  precisely, nor  $\phi_e(t)$  and  $\phi_d(t)$  separately. Therefore several extreme cases will be considered. These demonstrate the degree of uncertainty that exists with regard to the establishment of the steady state below 160 km. It is possible that the densities at and above 160 km are approximately

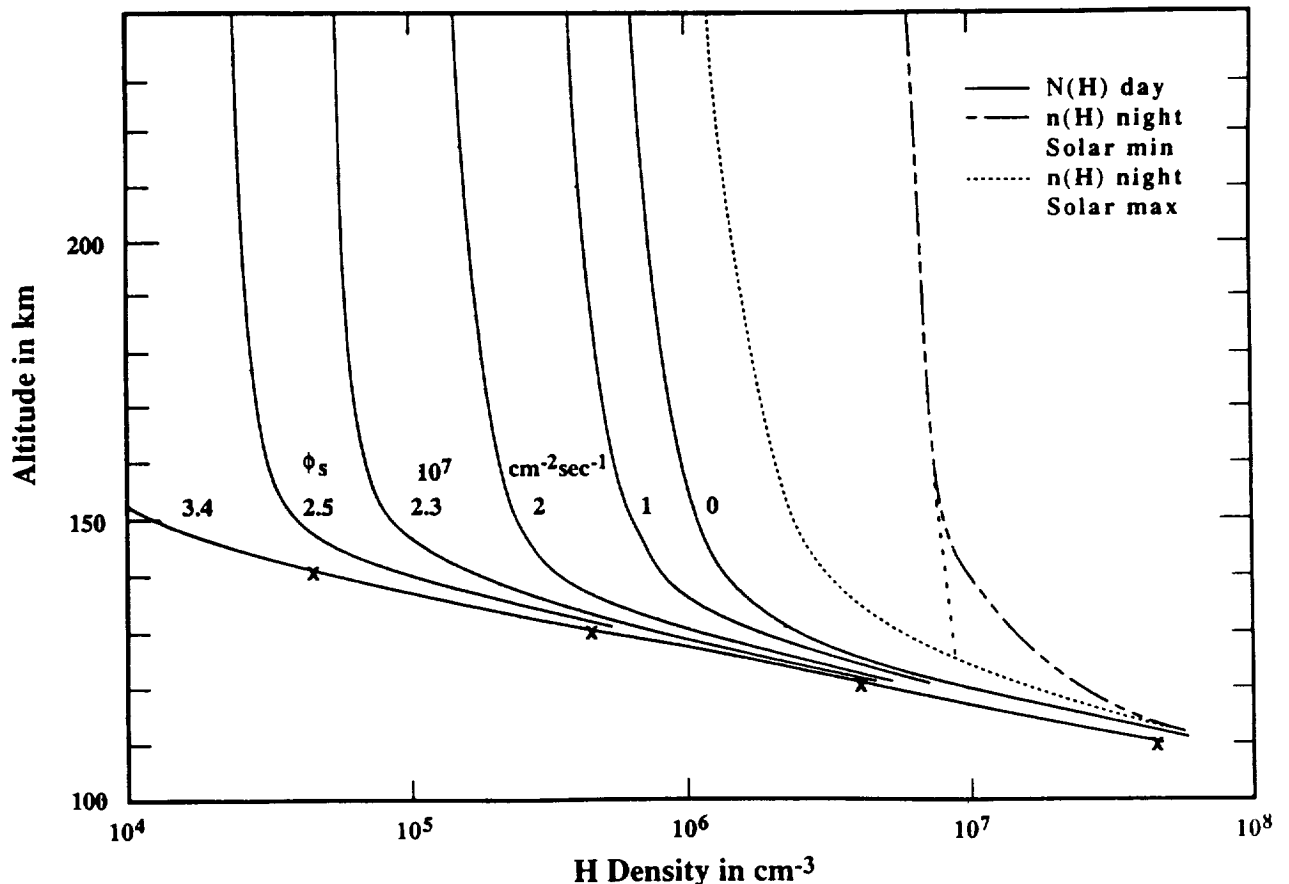


**Figure 7.** Altitude profiles of H densities at the subsolar point for various upward fluxes (solid lines). Altitude profiles of H densities in the bulge region at solar maximum (short-dashed line) and solar minimum (long-short-dashed line).

**Table 5.** Rate of Change of Hydrogen Column Density ( $10^7 \text{ cm}^{-2} \text{ s}^{-1}$ )

Case( $\Delta t$ )	$\Delta\mathcal{H}/\Delta t$
a(0.8)	5.6
b(0.8)	7.9
c(0.8)	10

\*time in years

those of the steady state and can be used to calculate the eventual steady state fluxes, even though the steady state downward flux and density below 160 km may not have been reached. Thus, the time required for the hydrogen content of the bulge to change to its observed value will be taken to be either (1) 0.4 year, the time interval during which solar activity decreased from its high to low value, or (2) 0.8 year, the time from the end of solar maximum to the end of observations in 1992. Three possibilities for  $\Delta\mathcal{H}$  will be considered. The assumed steady state H bulge profiles are shown in Figure 7. These were obtained by extrapolating the H densities deduced from measurements at 160 km to 110 km, where the density is assumed to be the same as in the daytime. Above 160 km, diffusive equilibrium is assumed. An extreme lower limit to  $\Delta\mathcal{H}$  is obtained for the first possibility, case a, by assuming that the change with time occurs only above 160 km. Case b approximates the effective density in 1992 below 160 km by extending the H profile above 160 km back to 120 km, where it meets the solar maximum profile (dotted line), and case c assumes that as  $\Delta t \rightarrow 0.8$  year, a steady state had been reached and that  $\Delta\mathcal{H}$  is the difference between the two steady state curves at all altitudes. The results for  $\Delta t = 0.8$  year are shown in Table 5. The values for a(0.4), b(0.4), and c(0.4) are all twice as large as the rates in Table 5. As for  $\langle\phi_S\rangle$ , it can be assumed that  $\phi_S$  increases from  $\Phi_S$  to the limiting flux  $\Phi_{Smax} = 4.4 \times 10^7 \text{ cm}^{-2} \text{ s}^{-1}$  as soon as solar activity decreased, or that it remains fixed at its solar maximum value.

The value for  $\langle\phi_e + \phi_d\rangle$  obtained by subtracting  $\Delta\mathcal{H}/\Delta t$  from  $2.5\langle\phi_S\rangle$  should be larger than the least value that  $\langle\phi_e + \phi_d\rangle$  can reasonably be expected to have. This can be obtained by assuming that  $\phi_e$  decreases from  $\Phi_e$  to  $0.15\Phi_e$  in 0.4 year and then remains at the lower level while  $\phi_d$  remains fixed at its steady state level:

$$\langle\phi_d\rangle = 2.5\Phi_S - \Phi_e. \quad (12)$$

Thus

$$\langle\phi_e + \phi_d\rangle_{min} = 2.5\Phi_S - 0.425[1 + 1/(p+1)] \quad (13)$$

where  $p$ , the power of time in the integrand of the time average integral, is taken to be 1. Eventually  $\phi_d$  will become 6.5 times larger, but as we shall see, such large values in 1992 cannot be tolerated. In order to maintain consistency in the steady state and time-dependent analyses,  $\Phi_e$  is taken to be the calculated flux in Table 3, not the observed flux in Table 1. These assumptions are consistent with the steady state analysis in which  $\Phi_e$  was compatible only with the electric field escape process for which  $\epsilon = 0.15$ . Thus it is necessary that

$$2.5\Phi_{Smax} - \Delta\mathcal{H}/\Delta t \geq 2.5\Phi_S - 0.638\Phi_e. \quad (14)$$

On the right-hand side of (14), the choice of  $\epsilon_S$  makes very little difference. The terms in (14) are compared in Table 6. This table shows that to meet condition (14) it is necessary that steady state conditions for solar minimum were not yet established in the lower thermosphere during preentry. Thus hydrogen densities below 160 km and  $\phi_d$  must have remained close to their 1991 levels throughout the preentry period to allow  $\Delta\mathcal{H}$  on the left-hand side of (14) and  $\langle\phi_e\rangle$  on the right hand side to be sufficiently small as to satisfy condition (14).

In the case of deuterium a similar analysis gives the results in Table 7, where  $\mathcal{D}$  is the column density of D above the turbopause. When  $\Delta t = 0.4$  year, case values are twice as large as those in Table 7.  $\Phi_{Smax}$  is  $6.5 \times 10^5 \text{ cm}^{-2} \text{ s}^{-1}$ . Table 8 compares terms in the analog of conditions in (14).

The criterion (14) is easily satisfied for deuterium under a wide range of conditions. Thus the results of the time-dependent analysis, while not quite as rewarding as those for the steady state, are reasonably close to those expected if indeed the escape fluxes from Venus, especially for hydrogen, are quite small. They can exceed those shown in Table 3 for the electric field process E by very little, just as in the case of the steady state.

## 5. Discussion and Summary

In this paper, a strong solar cycle variation in the H and D densities in the nightside thermosphere of Venus is reported. Prominent density enhancements in H of 6.5 times and D of 4 times are found in the nighttime bulge region as solar activity decreases from maximum to near minimum values. Knowing

**Table 6.** Comparison of Terms in (14) for Hydrogen ( $10^7 \text{ cm}^{-2} \text{ s}^{-1}$ )

Case	$2.5\Phi_{Smax} - \Delta\mathcal{H}/\Delta t$		$2.5\Phi_S - 0.638\Phi_e$	
	$\Delta t = 0.8 \text{ yr}$	$\Delta t = 0.4 \text{ yr}$	Year	Value
a	5.4	0.0	1	3.5
b	3.1	-4.8	2	3.3
c	1.0	-9.0	3	3.0
Average				3.3

**Table 7.** Rate of Change of Deuterium Column Density ( $10^5 \text{ cm}^{-2} \text{ s}^{-1}$ )

Case( $\Delta t^*$ )	$\Delta \mathcal{D}/\Delta t$
a(0.8)	2.5
b(0.8)	5.0
c(0.8)	8.8

\*time in years

that the dominant escape fluxes due to the charge separation electric field (E) and charge exchange (CE) decrease as solar activity declines [Donahue and Hartle, 1992], we propose that the observed buildup of H and D is a direct consequence of this decrease.

Making use of the observed H and D densities for both the high and low solar activity conditions, the respective flow budgets are evaluated with only minimal knowledge about the escape processes involved. The H and D escape fluxes so derived serve as an independent test of the escape scenario described by Donahue and Hartle [1992]. In the following, the concept behind the derivation of these escape fluxes is briefly summarized and is illustrated in Figure 8.

Given the observed H and D densities on the dayside, the upward fluxes of these constituents,  $\Phi_S$  (solar maximum conditions) or  $\phi_S$  (solar minimum conditions) from the mesospheric source region can be derived from standard diffusion equations. As illustrated in Figure 8, these fluxes feed the net horizontal transport (due to winds and exospheric return flow) that effectively carries H and D into the nightside, where they pile up and attain values that are 2 orders of magnitude higher than those on the dayside. Such large density enhancements naturally lead to increased downward transport having flux magnitudes,  $\Phi_d$  or  $\phi_d$ , taken to be proportional to the densities with proportionality factors that are the same for both high and low solar activity conditions. Essentially all escape of H and D is expected to occur from the bulge region with flux magnitudes,  $\Phi_e$  or  $\phi_e$ , that are considered unknown quantities to be derived. The expected inverse relations between the H and D bulge densities and escape fluxes are indicated in Figure 8. Finally, the H and D escape fluxes are uniquely defined when conservation of flow is applied simultaneously to both high and low solar activity conditions.

Applying this concept, we developed a simple relationship (9) between the planet averaged escape and source fluxes at solar maximum; i.e.,  $\Phi_e = \eta \Phi_S$ , where the escape efficiency  $\eta$  provides the connecting link between parameters at high and low solar activity. With knowledge of the source fluxes and the solar cycle dependence of the bulge densities, expression (9) was used to evaluate the H and D escape fluxes. Source fluxes  $\Phi_S(\text{H}) = 1.45 \times 10^7 \text{ cm}^{-2} \text{ s}^{-1}$  and  $\Phi_S(\text{D}) = 2.15 \times 10^5 \text{ cm}^{-2} \text{ s}^{-1}$  were derived, where the former is a reevaluation of a previous derivation by Paxton *et al.* [1988]. By spanning the range of possible parameters in the escape efficiencies, the escape fluxes were found to be in the range  $1.23 \times 10^7 \text{ cm}^{-2} \text{ s}^{-1} \leq \Phi_e(\text{H}) \leq 1.45 \times 10^7 \text{ cm}^{-2} \text{ s}^{-1}$  and  $1.61 \times 10^5 \text{ cm}^{-2} \text{ s}^{-1} \leq \Phi_e(\text{D}) \leq 2.15 \times 10^5 \text{ cm}^{-2} \text{ s}^{-1}$ , where H and D densities in the respective bulges, averaged over the first three Venus years (solar maximum), were used.

It is fortunate that the ranges of escape fluxes obtained by analysis of the solar cycle induced bulge changes were found to be so narrow that they can be used to analyze the evolution of H and D without specifying any particular escape mechanisms. Alternatively, these fluxes also provide valuable constraints for the study of escape mechanisms. For example, the H escape fluxes derived directly from the charge exchange mechanism,  $\Phi_e(\text{CE}; \text{H}) = 0.9 \times 10^7 \text{ cm}^{-2} \text{ s}^{-1}$ , and the electric field mechanism,  $\Phi_e(\text{E}; \text{H}) = 1.5 \times 10^7 \text{ cm}^{-2} \text{ s}^{-1}$ , are just outside the bounds derived from analysis of the solar cycle induced bulge changes. Thus, considering the variance of the measured densities and other possible uncertainties such as the effective areas of the bulges where escape takes place, these fluxes and their sum  $\Phi_e(\text{E} + \text{CE}; \text{H}) = 2.4 \times 10^7 \text{ cm}^{-2} \text{ s}^{-1}$  appear to be reasonable estimates. In contrast, the D escape flux due to the electric field process,  $\Phi_e(\text{E}; \text{D}) = 0.56 \times 10^5 \text{ cm}^{-2} \text{ s}^{-1}$ , is outside the experimental range derived from solar cycle variations by about a factor of 3 (escape due to CE is not important here because the fractionation factor is 0.02). This gap can be reduced by a factor of 2 if the experimentally possible D/H ratio of  $1.5 \times 10^{-2}$  instead of  $2.5 \times 10^{-2}$  is used in the derivation of  $\Phi_S(\text{D})$ . When the other uncertainties mentioned in section 4 are taken into account, the gap should be reduced even further. The analysis presented here thus provides independent estimates of the H and D escape fluxes that are in reasonable agreement with values derived earlier [Donahue and Hartle, 1992; Hartle and Grebowsky, 1995].

The above analysis assumed that steady state conditions applied at the high and low solar activity periods when the measurements were made. We have examined the validity of this assumption by applying the time-dependent variation

**Table 8.** Comparison of Terms in the Analog of (14) for Deuterium ( $10^6 \text{ cm}^{-2} \text{ s}^{-1}$ )

Case	$2.5\Phi_{S_{\max}} - \Delta \mathcal{D}/\Delta t$		$2.5\Phi_S - 0.638\Phi_e$	
	$\Delta t = 0.8 \text{ yr}$	$\Delta t = 0.4 \text{ yr}$	Year	Value
a	1.3	1.04	1	0.70
b	1.1	0.60	2	0.89
c	0.7	-0.16	3	0.65
			Average	0.64

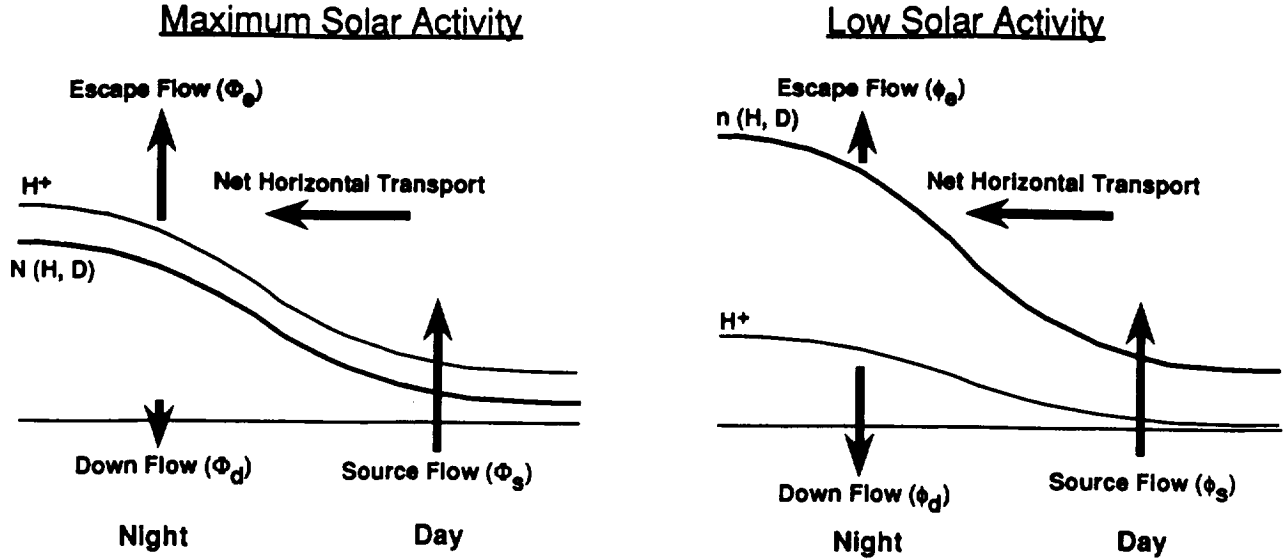


**Figure 8.** Schematic of flow balances in thermosphere of Venus during solar maximum and minimum periods.

described in (3) to the period when solar activity changed from its maximum value to the low value at the end of the PVO mission. We found that steady state conditions were established for H above about 160 km but not yet in the lower thermosphere during the preentry period, while they appear to be for D throughout the thermosphere. Therefore we conclude that the steady state analysis is a valid approximation because it dealt with only the observed density variations in the upper thermosphere above about 160 km. Consequently, these results can be used in an evaluation of the evolution of H and D.

The fractionation factor

$$f = \frac{1/\langle\phi_e(D)\rangle}{R/\langle\phi_e(H)\rangle} \quad (15)$$

is about 0.44, using the results listed in Tables 2 and 4 and  $R$ , the current D/H ratio of  $2.5 \times 10^{-2}$ . This large value is incompatible with charge exchange for which  $f$  is 0.02 [Krasnopolsky, 1985]. Hence the combined results suggest that virtually all of the escape flux determined by this procedure is due to the charge separation electric field. In any case, taking the H and D fluxes obtained in this way without specifying the physical mechanism, we arrive at the solar cycle average rates

$$\begin{aligned} \langle\phi_e(H)\rangle &= 3.6 \times 10^7 \text{ cm}^{-2} \text{ s}^{-1} \\ \langle\phi_e(D)\rangle &= 4 \times 10^5 \text{ cm}^{-2} \text{ s}^{-1} \\ f &= 0.44 \end{aligned}$$

when  $\epsilon_n(D) = 0.4$ . The fluxes averaged over the entire planet and the solar cycle are  $\langle\phi_e(H)\rangle = 7.2 \times 10^6 \text{ cm}^{-2} \text{ s}^{-1}$  and  $\langle\phi_e(D)\rangle = 8 \times 10^4 \text{ cm}^{-2} \text{ s}^{-1}$ .

The present water vapor mixing ratio is 30 ppm (0.015 m of liquid or  $8.3 \times 10^{22}$  H atoms  $\text{cm}^{-2}$ ). If this is the remnant of simple Rayleigh fractionation of an early water reservoir where the D/H ratio  $R_0$  was terrestrial or  $1.6 \times 10^{-4}$  and there are no hydrogen sources comparable to  $\langle\phi_e(H)\rangle$  the size of the early reservoir was a factor

$$r = (R/R_0)^{1/(1-f)} = (157)^{1/(1-0.44)} = 8.34 \times 10^3 \quad (16)$$

times as large as the present one. This is enough water to cover the planet with 125 m of liquid and is 3.8% of a full terrestrial ocean.

If, on the other hand, hydrogen is in a steady state currently with some source (e.g., cometary water and/or outgassed interior water) whose D/H ratio is  $R_i = 1.6 \times 10^{-4}$  the ratio of the primitive reservoir to the present one [Gurwell, 1995; Donahue et al., 1996] is given by

$$r = \rho e^{ft/\tau_H} - (e^{ft/\tau_H} - 1) \frac{1}{f} \quad (17)$$

Here  $\rho$  is  $R/R_0$  or 157 and

$$\tau_H = \mathcal{S}/\langle\phi_e(H)\rangle \quad (18)$$

with  $\mathcal{S}$  being the column abundance of hydrogen in the entire atmosphere. We note that (17) results when  $t/\tau_H \gg 1$  in Gurwell's [1995] full equation, which implies that H reaches a steady state long before D does. Here,  $\tau_H$  is 365 m.y.,  $t/\tau_H$  is 12.3, and  $r$  is  $3.8 \times 10^4$ . The consequence would be 570 m of water or 17% of a full terrestrial ocean 4.5 Gyr ago on Venus.

With such a large fractionation factor, the relaxation time for deuterium,  $\tau_D$ , is very small and the time required to establish a steady state

$$\tau_{SS} = \tau_H/f \quad (19)$$

is only 830 m.y.. However, the D/H ratio in a source with which the present-day hydrogen is in a steady state would have to be very large

$$R_S = R_{SS}f = 1.1 \times 10^{-2} \quad (20)$$

If instead the fluxes in Table 1 with the corresponding deuterium fluxes are used, we can consider two cases, one in which process CE is added to E, the other in which it is not. In the first case,  $f = 0.1$ , and in the second  $f$  is 0.15. Then

$$\begin{aligned} \tau_H &= (160 - 306) \text{ m.y.}, \\ r &= 275 \text{ or } 383, \end{aligned}$$

calling for an original reservoir 4.1 or 5.7 m deep when there is no external source of water. Considering  $t = 4.5$  Gyr, then  $t/\tau_H$  would be either 14.7 or 28.1, which calls for a ratio  $r$  of

Table 9. Three Approaches Used to Determine Escape Fluxes

Key Parameters	Solar Cycle Bulge Density Changes		Electric Field		Electric Field and Charge Exchange	
	$f = 0.44$		$f = 0.15$		$f = 0.1$	
	No Source	Source	No Source	Source	No Source	Source
$\tau_H$ (m.y.)	365	365	306	306	160	160
$t/\tau_H$	-	12.3	-	14.7	-	28.1
$\langle \phi_e \rangle^*$	3.6	3.6	4.3	4.3	8.2	8.2
$r \times 10^{-3}$	8.3	38	0.28	1.37	0.38	2.45
$d$ (m)	125	570	4.13	20.6	5.75	36.8

\*units of  $10^7 \text{ cm}^{-2} \text{ s}^{-1}$ 

1370 to 2450 between the original and present water abundance if hydrogen is in a steady state with a source having an Earth-like D/H ratio. This amounts to 20.6 or 36.8 m of water uniformly distributed on the surface.

The various scenarios described above for the decay of an ancient reservoir of water are conveniently summarized in Table 9 in terms of the three approaches used to determine escape fluxes; namely, those derived from solar cycle changes in the H and D bulges, those obtained from measurements related to electric field acceleration, and those produced by combining escape fluxes due to charge exchange and electric field processes. The table identifies key parameters used in describing the decay of an early water reservoir on Venus, where time  $t$  is 4.5 Gyr,  $\langle \phi_e \rangle$  is the global average hydrogen escape flux,  $r$  is the ratio of the initial column of water in the atmosphere to the current one, and  $d$  is its depth in liquid form uniformly distributed over the surface. For each method, the size of an ancient water reservoir is determined for two possibilities, one with no external source of water and the other in which the D/H ratio of the source  $R_S$  is  $1.6 \times 10^{-4}$ . In all cases, the D/H enrichment  $p$  is 157. For each method, the amount of water required in an initial reservoir when the hydrogen escape flux is in equilibrium with an external source is about 5 to 6 times greater than is required for simple decay (no source) of the reservoir. This result is expected because the primordial water reservoir must be larger in the steady state case to overwhelm the low D/H water brought in by an external (e.g., cometary) source. Although the hydrogen escape fluxes only differ by about a factor of 2, the sizes of the ancient water reservoirs differ widely to attain the deuterium enrichment observed in Venus' atmosphere today. This is due to the fact that while the fractionation factors  $f$  differ by 3 to 4 times, these differences are magnified by the exponential dependence of an initial water reservoir on  $f$ . The differences in the fractionation factors are primarily attributed to the differences in the respective deuterium escape fluxes. At this time we have no way of determining which  $\phi_e(D)$  is most likely. However, future work aimed at minimizing some of the uncertainties mentioned above could narrow this gap. For example, since the source fluxes and downward fluxes are dependent on global circulation, improved estimates of these fluxes and their effective areas could be obtained by a three-dimensional, global circulation model for the major constituents and H and

D (e.g., similar to the one developed by Mengel *et al.* [1989] for He). This approach would require inclusion of lateral transport and escape of H and D, because these processes are expected to have important effects on their circulation. Of course, experiments to measure the structure and dynamics of H and D throughout the thermosphere on a future mission to Venus could greatly improve our understanding of escape and evolution of the atmosphere.

## Appendix

Paxton *et al.* [1988] compared daytime Lyman- $\alpha$  obtained in nadir to horizon scans by the Pioneer Venus Orbiter Ultraviolet spectrometer (OUVS) during the first three Venus years with that predicted from model hydrogen density profiles. These profiles were the result of calculating the density with a specified upward hydrogen flow  $\phi$  from the expression

$$n(z) = n_c(z) \left[ 1 - \phi \int_{z_c}^z \frac{dz'}{n_c(z') [K(z') + D(z')]} \right] \quad (\text{A1})$$

where  $K(z)$  and  $D(z)$  are the eddy and molecular diffusion coefficients

$$n_c(z) = n_c(z_c) \frac{T(z)}{T_c} \times \exp \left\{ - \int_{z_c}^z \left[ \frac{D(z')}{H_1(z')} + \frac{K(z')}{H_a(z')} \right] \frac{dz'}{K(z') + D(z')} \right\} \quad (\text{A2})$$

Here,  $H_1$  and  $H_a$  are the scale heights for hydrogen and the bulk atmosphere. Paxton *et al.* set the reference altitude  $z_c$  at 200 km. The emission rates near the horizon are sensitive mainly to the density at high altitude, while the emission rates from directly below the spacecraft are essentially determined by the integrated vertical column density. This, in turn, is set by  $\phi$  and the hydrogen density below the hydrogen homopause. The best fit to their data came from a profile with a flux of  $7.5 \times 10^7 \text{ cm}^{-2} \text{ s}^{-1}$  and a density of  $6 \times 10^4 \text{ cm}^{-3}$  at 200 km.

This profile calls for a density of  $6 \times 10^7 \text{ cm}^{-3}$  at 110 km. There is a problem associating a flux as large as  $7.5 \times 10^7 \text{ cm}^{-2} \text{ s}^{-1}$  with such a profile because that flux exceeds the limiting

flux of hydrogen under the conditions specified. The limiting flux  $\phi_e$  is  $D(100) n_i / H_a$ . With VIRA

$$D(z) = 8.4 \times 10^{17} T^{0.6} / n_a(z). \quad (A3)$$

Here,  $\phi_e$  is  $3.3 \times 10^7 \text{ cm}^2 \text{ s}^{-1}$ , when  $T = 178^\circ\text{K}$ ,  $n_a = 8.3 \times 10^{13} \text{ cm}^{-3}$  at 110 km. We have recalculated the hydrogen densities, with  $n = 6 \times 10^7 \text{ cm}^{-3}$  at 110 km and  $K = 1.4 \times 10^{13} / \sqrt{n_a} \leq 3 \times 10^7 \text{ cm}^2 \text{ s}^{-1}$ . The results for a range of  $\phi$  from 0 to  $\phi_e$  are shown in Figure 7. A density of  $6 \times 10^4 \text{ cm}^{-3}$  at 200 km results for the profile with  $\phi = 2.3 \times 10^7 \text{ cm}^2 \text{ s}^{-1}$ . That is a profile very similar to that of Paxton et al. with  $\phi = 7.5 \times 10^7 \text{ cm}^2 \text{ s}^{-1}$ . In this paper we assume that the PVOUVS results for 1978-1981 are best represented by this profile. Because the average hydrogen densities for Venus years 1, 2, and 3 were  $7.5 \times 10^4 \text{ cm}^{-3}$  at 200 km, the densities and fluxes in Figure (7) should be multiplied by a factor 1.25 to apply to the analysis in this paper.

The noontime deuterium densities at 220 km during solar maximum average  $730 \text{ cm}^{-3}$ . If the D/H ratio is  $2.5 \times 10^{-2}$  for Venus hydrogen, the deuterium density at 110 km will be  $1.9 \times 10^6 \text{ cm}^{-3}$  when the hydrogen density is  $7.5 \times 10^7 \text{ cm}^{-3}$ . We have calculated  $n_a$  for deuterium from (A2) with the molecular diffusion coefficient

$$D(z) = 2.3 \times 10^{17} T^{0.75} / n_a(z) \quad (A4)$$

the same as that for  $\text{H}_2$  in  $\text{CO}_2$  [Hunten, 1973]. The diffusive equilibrium density at 220 km according to (A1) is  $1.3 \times 10^4 \text{ cm}^{-3}$ . It follows from (A2) that the observed deuterium density of  $730 \text{ cm}^{-3}$  at 220 km calls for an upward deuterium flux of  $4.3 \times 10^5 \text{ cm}^2 \text{ s}^{-1}$  near the subsolar point. To reduce that flux sufficiently to bring the calculated  $\Phi_e$  into agreement with the HG flux,  $n_e$  would have to be reduced by a factor between 0.3 ( $\epsilon = 1$ , year 3) and 0.5 ( $\epsilon = 1.3$ , year 2). This would call for the D/H ratio to be correspondingly reduced.

**Acknowledgment.** The authors thank Joel Seleko of Hughes STX for his data analysis support.

## References

- Anicich, V. G., Evaluated bimolecular ion-molecule gas phase kinetics of positive ions for use in modeling planetary atmospheres, cometary comae, and interstellar clouds, *J. Phys. Chem. Ref. Data*, 22, 1469, 1993.
- Banks, P. M., and G. Kockarts, *Aeronomy*, Academic, San Diego, Calif., 1973.
- Barth, C. A., J. B. Pearce, K. K. Kelly, L. Wallace, and W. G. Fastie, Ultraviolet emissions observed near Venus from Mariner V, *Science*, 158, 1675, 1967.
- Bertaux, J. L., V. M. Lepine, V. G. Kurt, and A. S. Smirnov, Altitude profile of H in the atmosphere of Venus from Lyman- $\alpha$  observations of Venera 11 and Venera 12 and origin of the hot exospheric component, *Icarus*, 52, 221, 1982.
- Bjoraker, G. L., H. P. Larson, M. J. Mumma, R. Timmerman, and J. L. Montani, Airborne observations of the gas composition of Venus above the cloud tops: measurements of  $\text{H}_2\text{O}$ , HDO, HF and the D/H and  $^{18}\text{O}/^{16}\text{O}$  isotopic ratios, *Bull. Am. Astron. Soc.*, 24, 995, 1992.
- Bougher, S. W., R. E. Dickinson, E. C. Ridley, R. G. Roble, A. F. Nagy, and T. E. Cravens, Venus mesosphere and thermosphere: II. Global circulation, temperature, and density variations, *Icarus*, 68, 284, 1986.
- Brinton, H. C., H. A. Taylor Jr., H. B. Niemann, H. G. Mayr, A. F. Nagy, T. E. Cravens, and D. F. Strobel, Venus nighttime hydrogen bulge, *Geophys. Res. Lett.*, 7, 865, 1980.
- deBergh, C., B. Bezard, T. Owen, D. Crisp, J.-P. Maillard, and B. L. Lutz, Deuterium on Venus: Observations from Earth, *Science*, 251, 547, 1991.
- Donahue, T. M., and R. E. Hartle, Solar cycle variation in Venus  $\text{H}^+$  and  $\text{D}^+$  densities in the Venus ionosphere: Implications for escape, *Geophys. Res. Lett.*, 19, 2449, 1992.
- Donahue, T. M., and R. R. Hodges Jr., Past and present water budget of Venus, *J. Geophys. Res.*, 97, 6083, 1992.
- Donahue, T. M., and R. R. Hodges Jr., Venus methane and water, *Geophys. Res. Lett.*, 20, 591, 1993.
- Donahue, T. M., J. H. Hoffman, R. R. Hodges Jr., and A. J. Watson, Venus was wet: A measurement of the ratio of deuterium to hydrogen, *Science*, 216, 630, 1982.
- Donahue, T. M., D. Grinspoon, R. E. Hartle, and R. R. Hodges Jr., Ion neutral escape of hydrogen and deuterium: Evolution of water, in *Venus II*, edited by S. W. Bougher et al., Univ. of Ariz. Press, Tucson, in press, 1996.
- Grebowsky, J. M., W. T. Kasprzak, R. E. Hartle, and T. M. Donahue, A new look at Venus' thermosphere H distribution, *Adv. Space Res.*, in press, 1995.
- Gurwell, M. A., Venus deuterium: Evolution and implications for primordial water, *Nature*, 378, 22, 1995.
- Gurwell, M. A., and Y. L. Yung, Fractionation of hydrogen and deuterium on Venus due to collisional ejection, *Planet. Space Sci.*, 41, 91, 1993.
- Hartle, R. E., and J. M. Grebowsky, Light ion flow in the nightside ionosphere of Venus, *J. Geophys. Res.*, 98, 7437, 1993.
- Hartle, R. E., and J. M. Grebowsky, Planetary loss from light ion escape on Venus, *Adv. Space Res.*, 15 (4), 117, 1995.
- Hartle, R. E., and H. A. Taylor Jr., Identification of deuterium ions in the ionosphere of Venus, *Geophys. Res. Lett.*, 10, 965, 1983.
- Hartle, R. E., H. G. Mayr, and S. J. Bauer, Global circulation and distribution of hydrogen in thermosphere of Venus, *Geophys. Res. Lett.*, 5, 719, 1978.
- Hedin, A. E., H. B. Niemann, W. T. Kasprzak, and A. Seiff, Global empirical model of the Venus thermosphere, *J. Geophys. Res.*, 88, 73, 1983.
- Hodges, R. R., Jr., Isotopic fractionation of hydrogen in planetary exospheres due to ionosphere-exosphere coupling: Implications for Venus, *J. Geophys. Res.*, 98, 10,833, 1993.
- Hodges, R. R., Jr., and B. A. Tinsley, The influence of thermospheric winds on exospheric hydrogen on Venus, *Icarus*, 51, 440, 1982.
- Holzer, T. E., and P. M. Banks, Accidentally resonant charge exchange and ion momentum transfer, *Planet. Space Sci.*, 17, 1074, 1969.
- Hunten, D. M., The escape of light gases from planetary atmospheres, *J. Atmos. Sci.*, 30, 1481, 1973.
- Kar, J. R. E. Hartle, J. M. Grebowsky, W. T. Kasprzak, T. M. Donahue, and P. A. Cloutier, Evidence of electron impact ionization on the nightside of Venus from PVO/IMS measurements near solar minimum, *J. Geophys. Res.*, 99, 11,351, 1994.
- Kasprzak, W. T., H. B. Niemann, A. E. Hedin, S. W. Bougher, and D. M. Hunten, Neutral composition measurements by the Pioneer Venus neutral mass spectrometer during orbiter re-entry, *Geophys. Res. Lett.*, 20, 2747, 1993.
- Keating, G. M., and N. C. Hsu, The Venus atmospheric response to solar cycle variations, *Geophys. Res. Lett.*, 20, 2751, 1993.
- Keating, G. M., J. L. Bertaux, S. W. Bougher, T. E. Cravens, R. E. Dickinson, A. E. Hedin, V. A. Krasnopolsky, A. F. Nagy, J. Y. Nicholson III, L. J. Paxton, and U. von Zahn, Models of Venus neutral upper atmosphere: Structure and composition, *Adv. Space Res.*, 5, 117, 1985.
- Krasnopolsky, V. A., Total injection of water vapor into the Venus atmosphere, *Icarus*, 62, 221, 1985.
- Mayr, H. G., I. Harris, R. E. Hartle, and W. R. Hoegy, A diffusion model for the upper atmosphere of Venus, *J. Geophys. Res.*, 83, 4411, 1978.
- Mayr, H. G., I. Harris, H. B. Niemann, H. C. Brinton, N. W. Spencer, H. A. Taylor Jr., R. E. Hartle, W. R. Hoegy, and D. M. Hunten, Dynamic properties of the thermosphere inferred from Pioneer Venus mass spectrometer measurements, *J. Geophys. Res.*, 85, 7841, 1980.
- McElroy, M. B., M. J. Prather, and J. M. Rodriguez, Escape of hydrogen from Venus, *Science*, 215, 1614, 1982.
- Mengel, J. G., H. G. Mayr, I. Harris, and D. R. Stevens-Rayburn, Non-linear three dimensional spectral model of the Venusian thermosphere with superrotation; II. Temperature, composition, and winds, *Planet. Space Sci.*, 37, 707, 1989.
- Nagy, A. F., T. E. Cravens, S. G. Smith, H. A. Taylor Jr., and H. C. Brinton, Model calculations of the dayside ionosphere of Venus: ionic composition, *J. Geophys. Res.*, 85, 7795, 1980.

- Paxton, L. J., D. E. Anderson, and A. I. F. Stewart, Analysis of Pioneer Venus orbiter ultraviolet spectrometer Lyman- $\alpha$  data from near the subsolar region, *J. Geophys. Res.*, 93, 1766, 1988.
- Rodriguez, J. M., M. J. Prather, and M. B. McElroy, Hydrogen on Venus: Exospheric distribution and escape, *Planet. Space. Sci.*, 32, 1235, 1984.
- Taylor, H. A., Jr., H. Brinton, H. B. Niemann, H. G. Mayr, R. E. Hartle, A. Barnes, and J. Larson, In situ results on the variation of neutral atmospheric hydrogen at Venus, *Adv. Space Res.*, 5(9), 125, 1985.
- T. M. Donahue, Space Physics Research Laboratory, Department of Atmospheric, Oceanic and Space Sciences, University of Michigan, Ann Arbor, MI 48104.
- J. M. Grebowsky, R. E. Hartle, and H. G. Mayr, Laboratory for Atmospheres, Goddard Space Flight Center, Greenbelt, MD 20771.

(Received July 17, 1995; revised September 20, 1995; accepted September, 22, 1995.)

SOLAR CYCLE VARIATIONS IN H<sup>+</sup> AND D<sup>+</sup> DENSITIES IN THE VENUS IONOSPHERE:  
IMPLICATIONS FOR ESCAPE

Thomas M. Donahue

Space Physics Research Lab, Department of Atmospheric, Oceanic and Space Sciences, University of Michigan

Richard E. Hartle

Laboratory for Atmospheres, Goddard Space Flight Center

**Abstract.** The hydrogen ion concentrations recently observed on Venus, near solar minimum, by the Ion Mass Spectrometer on the Pioneer Venus Orbiter in the anti-solar sector (22:00-02:00 LST) of the ionosphere are more than an order of magnitude less than those previously observed at solar maximum. This strong solar cycle variation has a profound effect on the escape of hydrogen (and deuterium) from Venus; almost all escape occurs during solar maximum. After adjustment for solar cycle variation, a planet-averaged hydrogen escape flux of  $0.6\text{--}1.4 \times 10^7 \text{ cm}^{-2} \text{ s}^{-1}$  is obtained along with a large deuterium fractionation factor of 0.1-0.14. These results suggest at least two plausible scenarios for the evolution of water on Venus: (1) Water vapor on Venus may be approaching a steady state if the escape flux is balanced by endogenous or exogenous sources of water. The source of water must be highly fractionated, with a D/H ratio differing by less than an order of magnitude from the present ratio of  $2.4 \times 10^{-2}$ , thus precluding low D/H water from comets, asteroids or a mantle reservoir. (2) The present day D/H ratio of  $2.4 \times 10^{-2}$  could be established by Rayleigh fractionation of an early low D/H water reservoir if the escape flux was sufficiently large in earlier times. An early water endowment at least 340 times today's abundance, equivalent to 4.2 to 14 m of liquid water on the surface, would be needed.

### 1. Introduction

The Pioneer Venus Orbiter (PVO) spacecraft, which explored the thermosphere of Venus between December, 1978 and July, 1980, has recently revisited that region. During the late summer and fall of 1992 the spacecraft was exploring the nighttime atmosphere at altitudes as low as 132 km. 1978-80 was a time of maximum solar activity. In September, 1992, activity was declining toward a minimum. Hence the Venus thermosphere and ionosphere was examined with the same instruments during times of high and low activity. The present paper will contrast the hydrogen ion population of the ionosphere between 150 km and 700 km in the anti-solar sector (22:00 - 02:00 LST) under these very different conditions.

### 2. Hydrogen Ion Densities at High and Low Solar Activity

Figure 1 shows examples of hydrogen ion densities obtained by the PV Orbiter Ion Mass Spectrometer (OIMS)

on orbits 5021 and 5032 (LST 00:47 - 01:57). Ions of mass 2 are also plotted. These are characteristic of conditions during the present epoch. These profiles provide a vivid contrast with conditions in 1978-80 when the densities observed under similar conditions were about 10 times larger at 200 km and 30 times larger at 600 km [Bauer et al., 1985]. Even though some of these data points will need further scrutiny, no fine tuning can change the essential element on which this analysis depends. The general level of the densities will not change. It is very low. Figure 2 shows average profiles for H<sup>+</sup> in filled and depleted ionospheres between 22:00 and 02:00 LST (orbits 4995-5033, 31 cases in all). Averages for the two hours before and after midnight are shown separately. In Figure 3 the VIRA model H<sup>+</sup> densities [Bauer et al., 1985] for 150° - 170° SZA are shown along with the current results.

### 3. Implications for Hydrogen Escape

We wish to draw attention to the significance of such large variations in H<sup>+</sup> for escape of hydrogen and deuterium from Venus. Until recently four processes have been recognized as contributing currently to escape: classical "Jeans" escape (J), charge exchange between low temperature atoms and high temperature ions (CE), collisions of hydrogen atoms with high speed oxygen atoms produced by dissociative recombination of O<sub>2</sub><sup>+</sup> (O\*), and outflow in the plasma tail (T). The first process is virtually inactive in the cold upper atmosphere of Venus. Calculations of CE by Hodges and Tinsley [1986] and by Rodriguez et al. [1984] give disparate results --  $2.4 \times 10^7 \text{ cm}^{-2} \text{ s}^{-1}$  in the first case and  $0.4 - 1 \times 10^7 \text{ cm}^{-2} \text{ s}^{-1}$  in the second. The latter authors also model a loss by O\* amounting to  $1.2 \times 10^6 \text{ cm}^{-2} \text{ s}^{-1}$  that contrasts with a recent result of  $3.5 \times 10^6 \text{ cm}^{-2} \text{ s}^{-1}$  obtained by Gurwell and Yung [1992]. (T) has been discussed by Brace et al. [1987] who produced evidence for O<sup>+</sup> escape in 1984 and argued for an accompanying -- but unobserved -- planet wide average H<sup>+</sup> flux of  $5 \times 10^6 \text{ ions/cm}^{-2} \text{ s}^{-1}$ . Two remarks need to be made concerning the calculations. First, the ionospheric models on which they were based were constructed with data obtained by the PV orbiter during the solar maximum of 1978-80 (or the solar minimum of 1984 for T). Second, the ionospheric models adapted by the two groups who have calculated CE differ strikingly from each other, and neither corresponds closely to the VIRA empirical model, which is no more than an average of (OIMS and OETP) data obtained during three successive passages of periapsis over the night hemisphere (Figure 3). Obviously, these calculations need to be repeated using H<sup>+</sup> densities obtained from PVO observations. Allowance should be made for changes with solar activity which will reduce the average CE flux by a factor of 2 unless compensating changes in the neutral

Copyright 1992 by the American Geophysical Union.

Paper number 92GL02927  
0094-8534/92/92GL-02927\$03.00



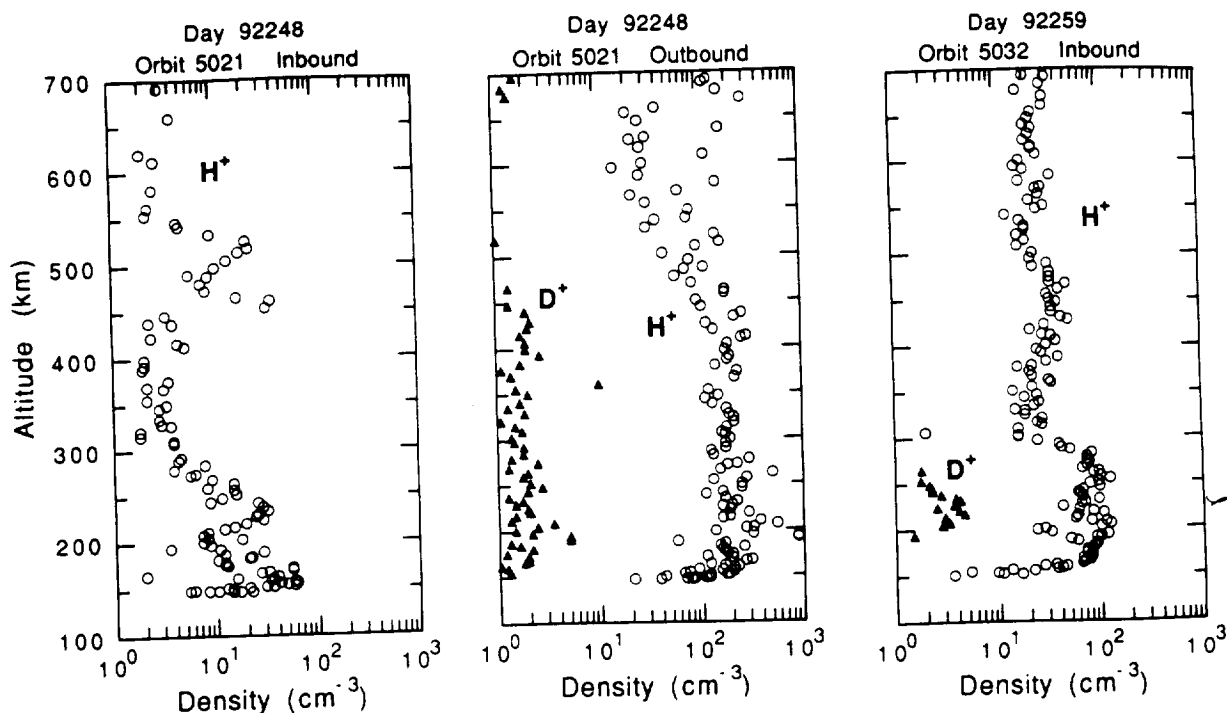


Fig. 1 Mass 1 and Mass 2 ions observed on three orbits in 1992 by the PV OIMS.

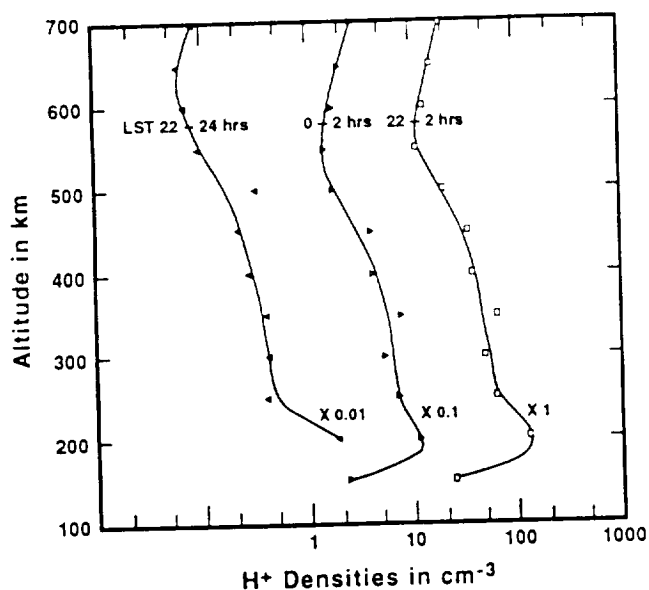


Fig. 2 Average  $H^+$  densities in the midnight sector of Venus, 31 cases from Orbits 4995-5032, 9 August - 14 September, 1992.

density occur. We note that  $O^+$  will also vary, because radio occultation data [Kliore and Mullen, 1988] clearly show that there is a large solar cycle modulation in  $O_2^+$  density.

While awaiting the results of these exercises, it may be possible to reconcile the results already published and to adjust them for solar variability by recourse to the PV OIMS results. From Figure 3 it is clear that the Tinsley and Hodges [1986] ion densities above 250 km are too high by a factor of 3 for SZA  $150^\circ$ - $180^\circ$ . A similar comparison at other zenith

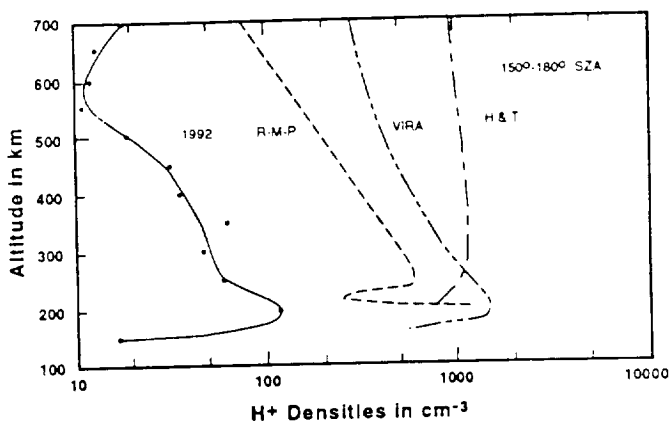


Fig. 3  $H^+$  densities Solar Zenith Angle  $150^\circ$  -  $180^\circ$ , OIMS and OETP, 1978-80 (VIRA), OIMS 1992 and models used by Hodges and Tinsley (H.T.), [1986] and Rodriguez et al. (R-P-M), [1984].

angles shows that, overall, they are effectively high by a factor of about 2.7 for the entire nightside. Thus their CE probably should be reduced from  $2.8$  to  $1 \times 10^7 \text{ cm}^{-2} \text{ s}^{-1}$ . Likewise the Rodriguez et al. [1984] fluxes are too low by a factor of 2.3 and 1.9 for the SZA zones  $150^\circ$ - $180^\circ$  and  $120^\circ$ - $150^\circ$ , in which almost all CE is generated. For their Case 3 this changes their CE flux from  $3.2 \times 10^6 \text{ cm}^{-2} \text{ s}^{-1}$  to  $9 \times 10^6 \text{ cm}^{-2} \text{ s}^{-1}$  during solar maximum. Thus, the results of the two calculations may converge at about  $10^7 \text{ cm}^{-2} \text{ s}^{-1}$  if they are performed using the same (observed)  $H^+$  densities.

It is interesting to compare these theoretical fluxes with the recent determination of the upward flux of  $H^+$  in the nightside thermosphere of Venus by Hartle and Grebowsky



[1992]. Data obtained in the dawn (hydrogen bulge) sector between midnight and 2 a.m., 150°-180° SZA show that H<sup>+</sup> (and D<sup>+</sup>) ions in this region flow upward between 300 km and the ion exobase at 500 km, accelerated by the charge separation electric field. This occurs in filled ionospheres under quiet solar conditions -- as well as in ionospheric holes. The H<sup>+</sup> flux reaches a local value of  $8 \times 10^7 \text{ cm}^{-2} \text{ s}^{-1}$  and the D<sup>+</sup> flux  $3 \times 10^5 \text{ cm}^{-2} \text{ s}^{-1}$  at 500 km, with values larger by a factor of 2 -- especially for D<sup>+</sup> -- possible. The midnight region was selected because the lateral flow of ions from the dayside stagnates there, and the vertical flow is not complicated by the effects of day to night transport. There is reason to expect that the outward flow detected here will also be a component of the vertical flow everywhere on the nightside, and be particularly strong in the region of the bulge. Allowing for variation in H<sup>+</sup> density with SZA in the bulge leads to the estimate that this flux would attain a value of about  $14 \times 10^7 \text{ cm}^{-2} \text{ s}^{-1}$  between 150° and 120° and drop to about  $2.9 \times 10^7 \text{ cm}^{-2}$  between 120° and 90°. The average bulge flux would be  $7.5 \times 10^7 \text{ cm}^{-2} \text{ s}^{-1}$ . This would correspond to a globally averaged flux of  $1.5 \times 10^7 \text{ cm}^{-2} \text{ s}^{-1}$  if it assumed that almost all of the flow occurs in the bulge which covers 20% of the planet's surface.

These upward flowing ions have two possible destinations. One of these is the plasma flow of H<sup>+</sup> and D<sup>+</sup> accompanying the tail ray O<sup>+</sup> flow described by Brace et al. [1987] which we have called T. The other is an analog of the telluric polar wind in which the upward flowing ions are accelerated to escape speed and escape into the solar wind with a flux P. Thus a new process (P) would be added to the four already identified in contributing to escape. We proceed now to estimate the contribution of these five processes to obtain the hydrogen escape flux averaged over the planet and over the solar cycle. We shall also estimate the fractionation factor for each process and for the aggregate of the five.

#### 4. Escape Fluxes and Fractionation Factors

The fractionation factor for D escape relative to H is given by

$$f = \frac{\phi_D}{\alpha \phi_H}, \quad (1)$$

where  $\alpha$  is the D/H ratio in the mixed atmosphere [Krasnopolsky, 1985]. With  $\alpha = 2.4 \times 10^{-2}$  [Donahue et al., 1982; de Bergh et al., 1991; T.M. Donahue and R.R. Hodges, Jr., unpublished 1992]  $f$  is 0.17 (and perhaps considerably larger) for the thermospheric D<sup>+</sup> and H<sup>+</sup> flows obtained by Hartle and Grebowsky [1992]. If the tail ray flow is really a plasma flow, the fractionation factor  $f_t$  is merely the ratio of the D<sup>+</sup> and H<sup>+</sup> densities divided by  $\alpha$ . Since the density ratio obtained by Hartle and Grebowsky [1992] is  $6.2 \times 10^{-3}$ , it follows that  $f_t = 0.26$ . If the D<sup>+</sup> and H<sup>+</sup> ions in the Venus wind flow (P) have equal kinetic energies, as they should if they are accelerated by an electric field,  $f_p$  will be  $f_t/\sqrt{2}$  or 0.15. (We note that the ratio of H<sup>+</sup> and D<sup>+</sup> velocities obtained by Hartle and Grebowsky is, in fact, 1.4.) It follows then, that P is  $1.2 \times 10^7 \text{ cm}^{-2} \text{ s}^{-1}$  and T is  $0.3 \times 10^7 \text{ cm}^{-2} \text{ s}^{-1}$ .

Combining these flux values with the estimate of  $0.9 \times 10^7 \text{ cm}^{-2} \text{ s}^{-1}$ , arrived at in Section 3 for CE, and  $0.35 \times 10^7 \text{ cm}^{-2}$

Table 1. Escape Fluxes and Fractionation Factors

Process	$\phi$ $\text{cm}^{-2} \text{ s}^{-1}$	$f$	$\phi$ $\text{cm}^{-2} \text{ s}^{-1}$	$f$	$f$
CE	0.9(1)	0.02(3)	0.9	0.02	0.02
O <sup>+</sup>	0.35(2)	0.31(2)	0.35	0(4)	0.31
t	0.3(1)	0.26			
P	1.2(1)	0.15(1)			
total	2.75	0.14	1.25	0.013(5)	0.1
average	1.4		0.6		

(1)This paper; (2)Gurwell and Yung, [1992];

(3)Krasnopolsky, [1985]; (4)McElroy et al., [1982];

(5)Hunten et al., [1982].

$\text{s}^{-1}$  for O<sup>+</sup> calculated by Gurwell and Yung [1992] gives a total flux of  $2.75 \times 10^7 \text{ cm}^{-2} \text{ s}^{-1}$  at solar maximum, or a solar cycled averaged flux  $\bar{\phi}$  of  $1.4 \times 10^7 \text{ cm}^{-2} \text{ s}^{-1}$ . Taking the values derived for  $f_p$  and  $f_t$  together with 0.02 for  $f_{ce}$  and 0.31 for  $f_{o^+}$  [Gurwell and Yung, 1992] yields a total fractionation factor of  $\bar{f} = 0.14$ . Here we have always taken  $\alpha$  to be  $2.4 \times 10^{-2}$  or 150 times terrestrial.

In Table 1 we display the contributions of various mechanisms to the escape flux and fractionation factors that have been associated with these processes. The first two columns give the values suggested in this paper. The next three columns show the effect of neglecting tail ray and Venus wind losses but allowing for the large increase in  $f_{o^+}$  proposed by Gurwell and Yung [1992]. From this table it is apparent that only charge exchange, and Jeans escape now seem to discriminate severely against deuterium escape. No matter what combination of processes is considered the fractionation factor is 0.1 or larger, and the effective hydrogen escape flux is severely reduced by solar cycle effects. We shall now discuss the implications of these changes for the evolution of water on Venus.

#### 5. Evolution of Venus Water

Recently there has been a convergence of some measurements of the water vapor mixing ratio in the lower atmosphere toward 30 ppm [Pollack et al., 1992; Donahue and Hodges, unpublished results 1992]. However, some older credible analyses that call for much higher mixing ratios -- up to 200 ppm -- remain unexplained. Thus there is a possibility that the water vapor concentration is variable in space and time and that possibility should still be allowed for in a discussion of the water vapor budget of Venus -- present and past. The rest of the hydrogen inventory is virtually unbounded except by aeronomic constraints. Here we shall consider a possible range of 30 to 100 ppm H<sub>2</sub>O equivalent. The time required to exhaust such reservoirs by the escape flux discussed here is given by

$$\tau = H/\bar{\phi}, \quad (2)$$

where  $H$  is  $8.3 \times 10^{22}$  atoms  $\text{cm}^{-2}$  if the water vapor mixing ratio is 30 ppm. For a flux of  $1.4 \times 10^7 \text{ cm}^{-2} \text{ s}^{-1}$   $\tau$  lies



between 190 and 630 My. The characteristic time for decay of the D/H signature as D/H approaches a steady state value in the presence of sources and sinks of water, is

$$\tau_{ss} = \tau/\bar{f} \quad (3)$$

[Krasnopolsky, 1985]. This is between 1.4 and 4.5 Gy. The order of magnitude increase in  $\bar{f}$  resulting from the reevaluation of  $f_0^*$  and the large values of  $f_t$  and  $f_p$ , therefore, means that it is plausible that the present day water vapor is well on its way toward a steady state if sufficiently strong sources -- endogenous or exogenous -- exist. However, the same high efficiency for deuterium escape which, on the one hand, makes  $\tau_{ss}$  short, on the other hand, makes the ultimate D/H ratio, given by

$$(D/H)_{ss} = \alpha_s/\bar{f}, \quad (4)$$

[Krasnopolsky, 1985] only 7 times the source value,  $\alpha_s$ . Because water in comets very likely has a D/H ratio in the neighborhood of a few times  $10^{-4}$ , this would appear to preclude comets [Grinspoon and Lewis, 1988] as important sources and to require mechanisms for producing a highly fractionated source of water from a mantle reservoir, given the present very high D/H ratio of  $2.4 \times 10^{-2}$ .

On the other hand it would be possible for the presently large value of D/H to be established by simple Rayleigh fractionation of an early water reservoir with a terrestrial like D/H ratio if  $\bar{\phi}$  should increase adequately with H. If  $\alpha/\alpha_0$  is 150 and  $\bar{f}$  is 0.14 an ancient water supply 340 times larger than the present atmospheric inventory would be required. This is equivalent to 0.14 to 0.47 percent of a full terrestrial ocean. To exhaust the associated hydrogen,  $\bar{\phi}$  would have to increase appropriately with increasing water abundance [Kumar et al., 1985].

## 6. Conclusions

Solar activity has a profound effect on hydrogen escape from Venus; the fractionation factor for deuterium and hydrogen escape is very large and our understanding of the history of water on Venus is very confused. Virtually the only scenario that appears to be excluded by our present understanding of hydrogen and deuterium escape processes is one that involves a steady state in which H and D outflow are balanced by an input of low D/H water from comets, asteroids or a mantle reservoir. However, it would be difficult to underestimate the quality of our present understanding either of the processes or the present hydrogen inventory. Developments are occurring, it remains to be seen whether or not they represent progress.

Conclusions, similar to those reached here regarding the significance of the large fractionation factor generated by process O\* and T, were reached, prior to the preparation of this paper, by D. H. Grinspoon [Unpublished manuscript; International Colloquium on Venus, Aug. 10-12, Pasadena, CA.]

**Acknowledgments.** The authors wish to acknowledge the contributions of Paul Cloutier and Leonard Cramer of Rice University for supplying OIMS data so efficiently and of Larry Brace for discussion of electron densities. S. Bougher

and D.M. Hunten made useful suggestions for improving this presentation. This work was supported by NASA under grant NAG 2-488 and letter of agreement PPO 4880.

## References

- Bauer, S.J., L.M. Brace, H.A. Taylor, Jr., T.K. Breus, A.J. Kliore, W.C. Knudsen, A.F. Nagy, C.T. Russell, and N.A. Savich, The Venus Ionosphere, *Adv. Space Res.*, **5**, 11, 233-267, 1985.
- Brace, L.H., W.T. Kasprzak, H.A. Taylor, R.F. Theis, C.T. Russell, A. Barnes, J.D. Mihalov, and D.M. Hunten, The ionotail of Venus: its configuration and evidence for ion escape, *J. Geophys. Res.*, **92**, 15-26, 1987.
- de Bergh, C., B. Bézard, T. Owen, D. Crisp, J.-P. Maillard, and B.L. Lutz, Deuterium on Venus: Observations from Earth, *Science*, **251**, 547-549, 1991.
- Donahue, T.M., J.H. Hoffman, R.R. Hodges, Jr., and A.J. Watson, Venus was wet: A measurement of the ratio of deuterium to hydrogen, *Science*, **216**, 630-633, 1982.
- Donahue, T.M. and R.R. Hodges, Jr., The past and present water budget of Venus, *J. Geophys. Res.*, **97**, 6083-6091, 1992.
- Grinspoon, D.H. and J.S. Lewis, Cometary water on Venus: implications of stochastic impacts, *Icarus*, **74**, 21-35, 1988.
- Gurwell, M.A. and Y.L. Yung, Fractionation of hydrogen and deuterium on Venus due to collisional ejection, *Planet. Space Sci.*, in press, 1992.
- Hartle, R.E. and J.M. Grebowsky, Planetary loss from light ion escape on Venus, *Adv. Space Res.*, in press, 1992.
- Hodges, R.R., Jr., and B.A. Tinsley, The influence of charge escape on the velocity distribution of hydrogen in the Venus exosphere, *J. Geophys. Res.*, **91**, 13, 649-658, 1986.
- Hunten, D.M., T.M. Donahue, J.C.G. Walker, and J.F. Kasting, Escape of atmospheres and loss of water, in *Origin and Evolution of Planetary and Satellite Atmospheres*, edited by S.K. Atreya et al., pp. 386-422, University of Arizona Press, Tucson, 1989.
- Kliore, A.J. and L. Mullen, The long-term behavior in the main peak of the dayside ionosphere of Venus during Solar Cycle 21, *J. Geophys. Res.*, **94**, 13339-13347, 1988.
- Krasnopolsky, V.A., Total injection of water vapor into the Venus atmosphere, *Icarus*, **62**, 221-229, 1985.
- Kumar, S., D.M. Hunten, J.B. Pollack, Nonthermal escape of hydrogen and deuterium from Venus and implications for loss of water, *Icarus*, **55**, 369-373, 1985.
- McElroy, M.B., M.J. Prather and J.M. Rodriguez, Escape of hydrogen from Venus, *Science*, **215**, 1614-1615, 1982.
- Pollack, J.B., J.B. Dalton, D. Grinspoon, R.B. Wattson, R. Freedman, D. Crisp, D.A. Allen, B. Bézard, C. de Bergh, L.P. Giver, Q. Ma, R. Tipping, Near-Infrared light from Venus' nightside: a spectroscopic analysis, *Icarus*, 1992.
- Rodriguez, J.M., M.J. Prather, and M.B. McElroy, Hydrogen on Venus: exospheric distribution and escape, *Planet. Space Sci.*, **32**, 1235-1355, 1984.

T.M. Donahue, University of Michigan, Space Physics Research Lab, Department of Atmospheric, Oceanic and Space Sciences, Ann Arbor, MI 48109-2143.

Richard E. Hartle, Laboratory for Atmospheres, Goddard Space Flight Center, Greenbelt, MD 20771.

(Received October 13, 1992;

Accepted November 16, 1992.)

